AD_____

Award Number: DAMD17-99-1-9503

TITLE: Genetic Definition and Phenotypic Determinants of Human Ovarian Carcinomas

PRINCIPAL INVESTIGATOR: Beth Y. Karlan, M.D.

CONTRACTING ORGANIZATION: University of California
Los Angeles, California 90095-1406

REPORT DATE: October 2002

TYPE OF REPORT: Final

PREPARED FOR: U.S. Army Medical Research and Materiel Command
Fort Detrick, Maryland 21702-5012

REPORT DOCUMENTATION PAGE

Form Approved
OMB No. 074-0188

1. AGENCY USE ONLY (Leave blank)	2. REPORT DATE	3. REPORT TYPE AND DATES COVERED
	October 2002	Final (1 Oct 99 - 30 Sep 02)

4. TITLE AND SUBTITLE
Genetic Definition and Phenotypic Determinants of Human Ovarian Carcinomas

5. FUNDING NUMBERS
DAMD17-99-1-9503

6. AUTHOR(S) :
Beth Y. Karlan, M.D.

7. PERFORMING ORGANIZATION NAME(S) AND ADDRESS(ES)
University of California
Los Angeles, California 90095-1406

E-Mail: karlanb@cshs.org

8. PERFORMING ORGANIZATION REPORT NUMBER

9. SPONSORING / MONITORING AGENCY NAME(S) AND ADDRESS(ES)
U.S. Army Medical Research and Materiel Command
Fort Detrick, Maryland 21702-5012

10. SPONSORING / MONITORING AGENCY REPORT NUMBER

11. SUPPLEMENTARY NOTES

12a. DISTRIBUTION / AVAILABILITY STATEMENT
Approved for Public Release; Distribution Unlimited

12b. DISTRIBUTION CODE

13. Abstract *(Maximum 200 Words)* *(abstract should contain no proprietary or confidential information)*

Ovarian cancer is the fourth leading cause of cancer-related death in U.S. women. This program project approaches the ovarian cancer problem by 1) establishing a human ovarian tissue and clinical data base core facility to support the proposed projects and future investigations, 2) identifying genes which are differentially expressed in ovarian cancers and thereby discovering biomarkers for early detection, 3) studying ovarian tumorigenesis in ovarian tissues obtained from germline *BRCA1* mutation carrier to better understand the interaction between mutational inactivation of *BRCA1*, the cellular caretaker gene and *p53*, the cellular gatekeeper gene, and 4) developing a genetically defined mouse model of epithelial ovarian cancer.

To date, the ovarian tissue core has banked over 260 surgical specimens and provided sufficient resources for the ongoing projects and other collaborative research on ovarian cancer etiology. Representational difference analysis was used to identify 160 genes specific for normal ovarian epithelium and 95 genes specific for ovarian cancer. The *BRCA1*-mutation associated ovarian tissues required to understand the functional interaction between of *p53* and *BRCA1* have been identified. And, a new viral construct carrying the cre recombinase under the control of the K18 promoter has been tested to establish its ability to mediate recombination in mouse ovarian epithelial cells.

14. SUBJECT TERMS
ovarian cancer

15. NUMBER OF PAGES
68

16. PRICE CODE

17. SECURITY CLASSIFICATION OF REPORT	18. SECURITY CLASSIFICATION OF THIS PAGE	19. SECURITY CLASSIFICATION OF ABSTRACT	20. LIMITATION OF ABSTRACT
Unclassified	Unclassified	Unclassified	Unlimited

TABLE OF CONTENTS

Genetic Definition and Phenotypic Determinants of Human Ovarian Carcinomas

Beth Y. Karlan, MD, Principal Investigator

INTRODUCTION:

It is estimated that 23,300 women will be diagnosed with ovarian cancer in the year 2002, and 13,900 women will succumb to this disease. In recent years, we have seen a slight decline in the number of new cases of ovarian cancer, and survival from ovarian cancer has been prolonged by improvements in surgery and chemotherapy. However, substantial progress towards ultimately eliminating ovarian cancer as a threat to women has been undermined by our ignorance about its etiology. Without additional insight into the genetic alterations that result in the clinical entity of ovarian carcinoma, we are left with empiric approaches to prevention, early detection and therapy. This program project is aimed at approaching the ovarian cancer problem by 1) establishing a human ovarian tissue and clinical data base core facility to allow the successful completion of the proposed projects and future studies aimed at understanding and eradicating ovarian cancer, 2) identifying genes which are differentially expressed in ovarian cancers and using this information to discover biomarkers for early detection, 3) studying ovarian tumorigenesis in "high risk" ovarian tissues obtained from carriers of germline *BRCA1* mutations to better understand the interaction between mutational inactivation of *BRCA1*, the cellular caretaker gene and *p53*, the cellular gatekeeper gene, and 4) developing a genetically defined mouse model of epithelial ovarian cancer which would be a vital tool for further studies of ovarian cancer etiology, prevention and therapy. This annual report prepared for the USAMRMC describes our progress towards achieving these goals during our three years of funding.

BODY:

Ovarian Tissue and Clinical Database Core Facility
Beth Y. Karlan, MD, Principal Investigator

The late stage of clinical presentation characteristic of human ovarian carcinoma is responsible for the tragically high mortality rates associated with the disease. To address this problem, we will draw on the rich human ovarian tissue resources we have available. The Ovarian Tissue and Clinical Database Core Facility is the cornerstone of this program project designed to define the genetic alterations and phenotypic determinants of human ovarian carcinoma. It provides a rich resource of clinical specimen from patients with ovarian and peritoneal adenocarcinoma and from patients at high risk of ovarian cancer due to a genetic predisposition. Additionally, the core establishes, characterizes and maintains *in vitro* models to facilitate research aimed at understanding genetic mechanisms involved in ovarian carcinogenesis and preclinical investigations of molecular-based therapeutics. The core facility has also built resources to support future studies on ovarian cancer etiology, prevention and treatment.

One of the important strengths of the Core facility is its state-of-the-art relational database system that links all patient demographic, epidemiologic, medical and clinical information with each banked specimen and resource. This link facilitates translational research that will allow us to make clinical correlations with basic research findings and makes it possible to transfer basic laboratory findings to the clinical arena. In addition, the database was designed to facilitate a multidisciplinary approach to ovarian cancer research and therefore includes additional fields for data entry that will support future studies including behavioral, and environmental influences and prevention studies.

TASK 1: Provide a continuing resource of normal and carcinomatous ovarian tissues from patients with benign gynecologic conditions and sporadic and familial ovarian cancer, respectively (months 1-36):

We have continued to provide all ovarian tissues requested by project principal investigators for the proposed projects. These include: 16 snap frozen tumor specimens to Project 1 (D. Chang, PI) of variable histologies (12 papillary serous, 1 clear cell, 3 endometrioid) as well as 5 snap frozen normal ovarian tissue specimens.

As in year 2, the third year of funding for the Ovarian Tissue and Clinical Database Core Facility has been very productive. This funding year, we banked 95 surgical specimens: 56 ovarian carcinomas and 39 benign ovaries. Of the 39 benign ovaries, 13 were donated from patients with a known *BRCA1* or *BRCA2* germline mutation or a family history of breast and/or ovarian cancer. We also

obtained matching blood DNA, serum and plasma samples from 90% of patients donating surgical specimens and consented patients without surgical specimens available for donation. Non-donating consented patients include those patients who were discovered to have insufficient tissue for donation during their surgical procedure. These accrual numbers are significantly increased from the previous year and meet our target projection for accrual.

Very strict Institutional Review Boards regulations for protecting the rights of human subjects involved in research continue to impede the banking of otherwise discarded surgical specimen from outside institutions. Nevertheless, we have IRB approval from UCLA and Olive View Medical Centers for the banking of surgical specimens and blood samples and we have accrued a limited number of patients from these institutions. All contacts and procedures have been established and we expect to continue patient accrual from these external sites.

- Determine *BRCA* mutation status on consenting ovarian cancer patients and screening program participants. Store and highlight these DNA and ovarian samples (when available) (months 1-36).

Genomic DNA samples have been isolated from blood specimens from patients with ovarian cancer and/or a family history of ovarian and/or breast cancers. These specimens have been or will be sent to our collaborators in Canada for *BRCA* mutation screening. When known, *BRCA1* and *BRCA2* mutation status has been recorded in the Core's Clinical Database.

- Disseminate announcement of the Core Facility's services to the scientific community in Southern California and provide ovarian tissues to approved projects (months 24-46)

The availability of services and resources from the Ovarian Tissue and Clinical Database Core Facility has been disseminated to investigators nationally and in Southern California via oral communication and through recognition of the Core Facility and DOD funding at scientific meetings and on research publications. After reviewing requests, we have provided resources to the two following investigators: Michel Schummer, Institute for Systems Biology, Seattle Washington who received 100 mg RNA isolated from 5 HOSE cultures to use for microarray analysis; Kurt Gish, Ph.D., EOS Biotechnology Inc., South San Francisco, in collaboration with Rae Lynn Baldwin, Ph.D. and Beth Karlan, M.D (Core Co-Investigator and PI, respectively) received snap frozen tissue specimens from 44 ovarian adenocarcinoma and 10 benign ovaries for use in microarray analysis and one ascites specimen for monoclonal antibody screening.

TASK 2: Establish, characterize and maintain monolayer cultures of human ovarian epithelial cells, human ovarian stromal cells and human ovarian carcinomas according to established procedures (months 1-36)

We have provided the requisite ovarian epithelial cell cultures for the projects, including 29 CSOC cultures and 13 HOSE cultures to Project 1 during the first 24 months. In addition, of the 45 CSOC cultures established during this time, we have frozen cultures on 21. Last year we had a higher than usual attrition rate due to fungal infections. These infections were due to construction in and around our tissue culture facility which had resulted in water leaks and other damage. The construction was completed and we did not suffer any additional infections. Likewise we have not been exposed to any adverse conditions in our new location in the Davis Research Building which verifies that our procedures to limit and eliminate infections are. We have also established 30 HOSE cultures of which 19 have been cryopreserved and 28 ovarian stromal cultures of which 17 have been frozen.

Of the 10 CSOC cultures established this past year, we have frozen cultures on 9, reflecting a 90% success rate. This rate is exceptionally higher that the expected limits. We are happy to again report that we were free of fungal infections during the previous 12-month reporting period making this a 24 month fungal free duration. We have also established 5 HOSE and HOST cultures and 5 have been cryopreserved.

TASK 3: Expand and maintain the clinical database to serve as an ongoing resource for translational studies (months 1-36)

Clinical, epidemiologic and demographic data as well as specimen inventory information is now being entered as samples are collected and banked. We are actively formatting historical data on previously banked specimen for downloading and enhancing our reporting capabilities. The major accomplishments for of downloading historical data during this funding period include:

- Inventory and growth records of all primary cultures
- Characterization IHC data from all cultures
- Inventory of viably frozen primary cell cultures
- Linkage of culture data to patient and patient cancer histopathology data.

The compilation of this historical data into the Oracle-based database has been a major undertaking that is already giving productive results for research design and data acquisition and analysis.

We have also made many major and minor enhancements to improve and expand the utility of the database. Some of the enhancements made to the Database during this funding period include:

- new screen to store records and inventory of archival pathology slides.
- new column to record date that patient informed consent was signed that is linked to the IRB number.
- new report to tract patient who sign informed consent but for which surgical specimen were not collected due to unavailability

We continue to use the web-based version of BrioQuery Explorer for free form data query design and formatting. Dr. Baldwin gave an oral presentation describing the design and functionality of the Gynecologic Oncology Database to investigators at the Pacific Ovarian Cancer Research Consortium, Fred Hutchinson Cancer Center, Seattle Washington who are recipients of an NIH SPORE in ovarian cancer (Nicole, Urban, ScD, PI). These investigators are developing a similar database and are interesting in our data model and system design.

Project #1, Molecular Biomarkers in Ovarian Cancer
David D. Chang, MD, PhD Principal Investigator

Cancer diagnosis is based on the detection of features that are unique to transformed cells. Each unique phenotype displayed in cancer cells must be accompanied by changes in gene expression. The genes that are differentially expressed in ovarian cancers compared to their normal counterparts therefore constitute logical candidates for molecular biomarkers for cancer detection. In Project 1, we proposed to conduct a detailed analysis of gene expression differences underlying human ovarian carcinogenesis and use the information to develop biomarkers for ovarian cancer.

TASK 1: To clone genes that are differentially expressed in ovarian cancer and determine their expression profile (months 1-12).

The main objective of our project is to study the gene expression differences underlying human ovarian carcinogenesis. As proposed in Task 1 of the original application, we have conducted a representational difference analysis (RDA) using primary cultures of normal human ovarian surface epithelium (HOSE) and Cedars-Sinai ovarian carcinoma (CSOC). The rational for using cultured ovarian epithelial cells for gene expression analysis was based on the fact that the epithelial cells, which give rise to ~90% of ovarian cancer, constitute a very small fraction (<1%) of the total ovarian

mass. We hypothesized that using primary cultures of normal and malignant ovarian epithelium for differential gene expression analysis would preferentially identify epithelial cell-specific genes. We have successfully identified 160 HOSE-specific and 95 CSOC-specific genes from our initial analysis, which employed HOSE and CSOC cultures obtained from two different patients. The expression of these cloned genes were surveyed in 5 additional HOSE and 10 additional CSOC cultures to identify 46 HOSE-specific and 14 CSOC-specific genes that exhibited at least 2.5-fold difference in expression level. Based on this encouraging result, we expanded our differential gene expression analysis into a gene expression profiling study. Using oligonucleotide-based microarray chips capable of assessing expression of >12,000 genes, we examined the gene expression patterns in 10 HOSE and 22 CSOC samples.

The gene expression profiling studies revealed several promising targets that could be further pursued in biomarker studies. Included in the list of genes we are further characterizing are periostin (PN), transglutaminase-2, several protease inhibitors, and PDGF receptor. We have further investigated the expression of PN and found it to have a strong oncofetal pattern of expression and be abundantly present in ascites of ovarian cancer patients. Purified PN supported integrin dependent cell adhesion, prompting us to initiate additional studies directed at testing a hypothesis that PN is involved in peritoneal spread of ovarian cancer.

TASK 2: To characterize the protein coding information and subcellular localization of the differentially expressed genes (month 9-24)

In parallel to the above gene expression studies, we have started biochemical studies on selected genes as proposed in Task 2. In particular we have characterized a gene known as periostin (or osteoblast specific factor 2). Pertinent findings from this analysis include: (i) periostin is a secreted protein; (ii) malignant ascitic fluid contains high amount of periotin; (iii) periostin mediates avb3 and avb5 integrin dependent cell adhesion and migration of ovarian epithelial cells. We plan to extend this line of analysis by examining whether periostin promotes intraperitoneal spread of ovarian cancer cells in year 2.

TASK 3: To study the utility of differentially expressed genes as molecular biomarkers for ovarian cancer (months 21-36)

Using a subtractive cloning and a chip-based gene expression profiling approach, we have successfully identified target genes that could be developed into biomarkers for ovarian cancer. In addition, the newly established immortalized ovarian epithelial cell lines will be used to study the functions of the genes that are differentially expressed in cancer-derived ovarian epithelial cells.

Project #2, Interactions Between *BRCA1* and *P53* Mutations in Human Epithelial Ovarian Carcinogenesis

Mark D. Pegram, MD, Principal Investigator

The molecular/genetic alterations responsible for the genesis of epithelial ovarian cancer are poorly understood. Recent molecular epidemiologic studies have defined a role for the *BRCA1* tumor suppressor gene in familial breast and ovarian cancer syndromes. Using a full-length sequencing strategy, we have recently identified a high incidence (62/108) of *p53* tumor suppressor gene mutations in sporadic epithelial ovarian cancers. This finding has recently been confirmed in our screen for research subjects in a prospective randomized trial of *p53* adenovirus gene therapy for newly diagnosed ovarian cancers in which ~70% of screened subjects had sequence confirmed *p53* mutations (which was an eligibility criteria for this clinical trial).

Several lines of experimental evidence suggest that *BRCA1* and *p53* may act in concert in DNA damage response and repair pathways: 1) both *p53* and *BRCA1* are physically altered in response to DNA damage; *p53* by stabilization and *BRCA1* by hyperphosphorylation and nuclear relocalization; 2) *p53* and *BRCA1* molecules have a direct physical interaction; 3) both *p53* and *BRCA1* activate P21/WAF-1/cip1 as a common target gene; 4) *BRCA1* is a transcriptional co-activator of *p53*, and; 5) early embryonic lethality in *BRCA1* knock-out mice is partially rescued by mutation of *p53*. Furthermore a very high percentage of breast cancers with *BRCA1* mutations exhibit *p53* mutation. We hypothesize that familial ovarian cancer tumorigenesis caused by mutational inactivation and allelic loss of the cellular caretaker gene *BRCA1* requires the mutational or functional inactivation of the cellular gatekeeper gene *p53* which controls cell cycle checkpoints and/or directs cells to undergo apoptosis. If our hypothesis is correct then we expect to find mutational or functional inactivation of *p53* in 100% of ovarian cancers from *BRCA1*-affected individuals. To test this hypothesis we are collecting and characterizing *p53* expression levels and mutational status in ovarian cancers from a large cohort of known *BRCA1* mutation carriers. This project is relevant to understanding the etiology of familial ovarian cancer which accounts for 10% of all ovarian cancers and as such represents a significant public health problem. Moreover, greater understanding of the biology of familial ovarian cancer will lead to improved diagnostic techniques which may have the potential to be exploited clinically in the management of patients with this disease. For example, a patient with known germline *BRCA* mutation and evidence of *p53* mutation in preneoplastic ovarian tissue may be at especially high risk for malignancy and prophylactic intervention either with surgery or with participation in biochemical prevention trials may be appropriate. The hypothesis that *p53* tumor suppressor function is required for *BRCA1*-linked ovarian tumorigenesis is testable using the human tissue resources available in our laboratory and the Ovarian Tissue Core Facility. We have made considerable progress on the aims and objectives which we originally proposed for this project.

The objectives for Project #2 are outlined as follows:

TASK 1: Identification and histologic analysis of ovarian cancer specimens with sequence-verified germ line *BRCA1* mutations (months 1-36)

This task is relevant to Aim I of the proposal: to assess the frequency of *p53* gene mutations in epithelial ovarian cancers with known mutations of the *BRCA1* gene. During the initial year of funding we identified ~71 malignant ovarian tumors in the Core's ovarian tumor bank for which peripheral blood lymphocyte DNA is available and will be tested for *BRCA1* and *BRCA2* mutations. Since that time we have continued to add to this number at the anticipated rate of 10 - 15 cases per year via the ongoing Core Project effort at UCLA and Cedars Sinai Medical Centers. We have been unable to obtain more samples through our originally proposed collaborative efforts because of new IRB restrictions on identification of human subjects with known germ line molecular genetic alterations. We are thus not allowed to identify potential participants for this study based on tumor bank data registry of known *BRCA* mutational carriers. Therefore we will continue our ongoing effort to collect specimens at our institutions prospectively.

TASK 2: Assessment of frequency of *P53* gene mutations in *BRCA1*-linked ovarian tumors identified in Task 1 above (months 6-36)

Task 2 is also relevant to Aim I of the proposal. In order to assess the frequency of *p53* mutations in *BRCA*-linked ovarian cancer, we first developed DNA sequence reactions to study mutational frequency. Conditions have been optimized for each of the PCR reactions required for sequencing runs using genomic DNA extracted from tumor tissues obtained from the Core Ovarian Tumor Facility. We anticipate being able to complete the proposed sequence analysis in the coming months; however, pilot studies (and previously published studies) indicate that for increased accuracy in the analysis of *p53* DNA sequence, it will be necessary to microdissect tumor cells from each of the banked ovarian tumor samples in order to avoid missing *p53* mutations due to stromal cell contamination of tumor tissues which would contain wild-type *p53* and could confound results from PCR amplification from genomic DNA extracted from ovarian tumor tissue. Strategically, because of the relatively high frequency of *p53* mutation in this disease, it may be possible in select cases to complete sequence analysis of available tumor samples without microdissection, with microdissection being reserved for those cases which are found to be wild-type on the original sequence analysis. Using this strategy, false negative results may be avoided by confirming *p53* mutational status on microdissected tumor cells. Another group has recently reported analysis of *p53* mutational status on *BRCA*-linked ovarian cancers (Buller, et al., Clin Cancer Res. 2001 Apr;7(4):831-8.). These investigators have reported as very high frequency of mutations as we have

hypothesized in this proposal. No unique types of *p53* mutations were identified as being specifically associated with a mutant *BRCA* genotype in this study. Further data are needed to confirm these findings and it is hoped that our data will complement the observations already reported by Buller and colleagues on this issue.

TASK 3: Assessment of MDM2 expression in *BRCA1*-linked and sporadic ovarian cancers using immunostaining techniques and compilation of *BRCA1* genotype data from all subjects (months 1-24)

Analysis of MDM2 expression in the available Core Facility Tumor Bank is currently ongoing. In addition we have access to a new large tumor bank from Munich with long-term clinical follow-up. We have recently utilized this cohort to measure expression of UPA and PAI-1 to demonstrate the prognostic significance of these markers in ovarian cancers of different clinical stages (Konecny, et al., Clin Cancer Res. 2001 Jun;7(6):1743-9). We aim to develop an ELISA format assay suitable for measurement of MDM2 expression using these same samples. Such analysis would expand the number of available samples for analysis significantly. Development of a suitable assay for retrospective analysis of large tumor banks is ongoing at this time.

TASK 4: To determine whether expression of wild-type *P53* in *P53*-mutant, *BRCA1*-mutant CSOC is sufficient to induce cell cycle arrest, induction of *P21* expression, and/or apoptosis (months 6-20)

This task addresses Aim III of the proposed research: to determine whether overexpression of wild-type *p53* is sufficient to induce cell cycle arrest/apoptosis in *BRCA1*-mutant ovarian cells. In this aim, we compare the biological effects of *p53* in *BRCA*-linked ovarian cancer cells to those which are wild-type for *BRCA* genes. Our preliminary data indicate that one of the most important determinant for response to adenoviral vector containing *p53* cDNA is in fact expression of the adenovirus receptor p46 hCAR. However, cells which are *p53* mutant and express hCAR all respond to *p53* transfection in terms of induction of apoptosis, including CSOC lines which are known to harbor *BRCA1* mutations. We have now cloned the cDNA for human 46kD hCAR and have developed expression vectors for this cDNA. Transfection of hCAR into hCAR-negative ovarian cancer cells allows further ability to transduce these lines with our *p53* adenoviral vector so that we can now evaluate response to *p53* adenovirus in most all of the available CSOC lines. This finding also may have implications for Project #3 in which adenoviral vectors had been proposed for transfection studies of ovarian surface epithelium *in vivo*.

TASK 5: To determine the frequency of *P53* alterations in "normal" ovaries from *BRCA1*-linked individuals who have undergone prophylactic oophorectomy (months 12-24)

This task addresses Aim II of the proposal: to determine the frequency of *p53* mutations in "normal" ovarian surface epithelium from *BRCA1*-affected individuals undergoing prophylactic oophorectomy. This aim was cited by reviewers as the most difficult to complete. We have recently identified and evaluated normal ovarian tissues from several samples from the Ovarian Tissue Core Facility which met criteria for this study. Using an immunohistochemical screen for aberrant accumulation of mutant *p53* protein, we have sought evidence of *p53* mutation in these otherwise normal tissues. Thus far we have not identified cases of *p53* alteration in the tissues so far evaluated with this methodology. There are at least two limitations to this approach however. One is that ovarian surface epithelium is frequently denuded from the ovarian samples during tissue procurement and processing in the pathology laboratory so it may be difficult to find the cells of interest on the slides following *p53* immunostaining. Moreover, we know from study of malignant ovarian tissue that there can be false negative results from *p53* immunostaining resulting from truncation mutations of *p53* due to point- or frameshift-mutations resulting in premature stop codons. Therefore it is anticipated that further study of these tissues may be required using microdissection followed by DNA extraction, PCR amplification, and sequence analysis for *p53*.

Project #3, Manipulation of Genes in the Ovarian Epithelium of Mice
Timothy F. Lane, PhD, Principal Investigator

Without models to test ideas about the initial stages of ovarian cancer, the task of identifying relevant markers and relevant targets for therapy becomes a daunting search for a needle in a haystack. One problem is the lack of a genetically defined animal model of epithelial ovarian cancer that can be used to test genes and gene pathways for their involvement during disease development. Techniques have now been developed for introducing genes into mice and expressing them in virtually any tissue type. Such an approach has led to major advances in our understanding of genes involved in a large number of other cancers. Successful demonstration of the utility of such an approach will make it possible to test the involvement of virtually any gene in ovarian cancer progression, and would be a major advance to the field. The strategy we proposed was to test the ability of wild type and modified adenovirus to deliver genes to normal ovarian epithelial cells *in vivo* with the idea that we could then use the *cre*-lox system to activate or delete genes of interest in a tissue specific fashion.

TASK 1: To establish the efficacy of Ad5-*cre* delivery to the ovarian epithelium (months 1-24)

The experiments specified in Task 1 of our Statement of work have progressed nicely. As specified in Task 1, we used a recombinationally activated gene cassette that would allow the production of a β-galactosidase gene only in cells expressing *cre* recombinase; this cassette is referred to as RABE. Several experiments have been carried out *in vitro* showing that the components of the system work well in cultured primary epithelial cells, and this allowed us to move into work on RABE transgenic mice. To date, we have injected Ad-*cre* into the ovarian capsule of 4 RABE female mice. We have looked for expression of β-galactosidase at 8 hrs (2 mice) and 24 hrs (2 mice). β-galactosidase positive cells were identified only in the 24 hr time point and transduction appeared to be rather inefficient. We are currently producing more concentrated viral stocks in the hopes that poor infection rates can also be overcome with higher titers.

A complication was also quite evident from these experiments. Adenoviral injections resulted in recruitment of a lymphoid infiltrate into sites of injection. We may request additional funds to document the cell types involved, but will likely switch to our proposed alternative strategy of transplanting the ovaries to avoid the need for exposure of animals to large amounts of virus.

We are also generating more mice to try the alternative strategy proposed for infecting the cells (ovarian transplants). This has been delayed because some of the mice became contaminated with a murine virus (MPV) and had to be destroyed. In year 2, we reestablished a clean colony of RABE mice, but continued too have problems with the RABE transgenic line due to MPV infection and eventually decided to discontinue the line. In order to replace the line we have obtained a ROSA26 (129s-gtrosa 26) from Jackson Labs which should be suitable. These mice are obtained in July and the colony has now been expanded to a useable size for our experiments. This has been a setback, but we hope to rapidly progress through the studies that were started in year one. Specifically, we have learned that direct injection of Ad5 particles is impractical due to immune infiltrate into the peritoneal cavity. Thus, we will be focusing our efforts on the more time consuming alternative strategy of infecting ovaries dissected from transgenic donors and then reimplanting them into host females. We have tried several pilots of this strategy and have encountered the following difficulties: 1) it is very difficult to manipulate mouse ovaries without removing the ovarian epithelium. 2) we were not able to use our standard FVB or 129vEv mice as recipients of ROSA ovarian transplants due to tissue rejection. These difficulties were not unexpected and will be overcome through use of syngeneic ROSA 129 hosts and improved skill in transplantation. Establishment of RA-DN*p53* animals are scheduled to start at the end of November and the RA-herB2 will be injected in January 2003. Constructs for the *p53* were delayed because of theMPV infection in our colony. This infection has now been eliminated and we are scheduling all transgenic injections to proceed very rapidly.

TASK 2: To establish the ability of Ad5-*cre* delivery to delete genes from the ovarian epithelium (months 1-28)

The experiments specified in Task 2 are currently behind schedule due to a backlog in the availability of floxPTEN mice from Dr. Wu. As with our RAGE mice, the floxPTEN colony was dealt a setback from MPV infection. Thus we will be focusing our efforts on the more time consuming alternative strategy of infecting ovaries dissected from transgenic donors and then re-implanting them into host females. We have tried several pilots of this strategy and have encountered the following difficulties: i) it is very difficult to manipulate mouse ovaries without removing the ovarian epithelium. ii). we were not able to use our standard FVB or 129SvEv mice as recipients of ROSA ovarian transplants due to tissue rejection. These difficulties were not unexpected and will be overcome through use of syngeneic ROSA129 hosts and improved skill in transplantation.

We have learned that direct injection of Ad5 particles into immunocompetant mice is impractical due to immune infiltrate into the peritoneal cavity. We proposed to focus our efforts on isolating mouse ovarian epithelial cells and infecting them *in vitro* in preparation for transfer. Because of the issues with infection *in vivo*, we have chose to pursue development of *in vitro* systems as proposed as an alternative strategy in our original application. We have developed a method of isolating mouse ovarian surface epithelial cells (MOSE) and find that they are efficiently infected by our retroviral constructs. Since it appears that transplantation will be required to carry out the proposed experiments, we believe it is impractical to pursue Ad delivery of *cre* and have instead established a collaboration with Thomas Hamilton, PhD, (Fox Chase Cancer Center, PA) who had recently established a transgenic system that is based on keratin 19 promoter. We have will transfer our remaining effort into placing our inducible *cre* recombinase construct into this promoter and establishing a transgenic line.

TASK 3: To establish the ability of Ad5-*cre* delivery to activate over-expression of transforming oncogenes in the ovarian epithelium (months 12-36)

TASK 4: To establish the ability of Ad5-*cre* delivery to activate over-expression of dominant negative anti-oncogenes in the ovarian epithelium (months 24-36)

The experiments specified in Tasks 3-4 rely on development of plasmid vectors and transgenic mice in Task 3. The RA-her2 vector is currently near completion and will be tested *in vitro* ahead of schedule. Establishment of RA-DN*p53* animals are scheduled to start at the end of November, 2001, and the RA-herB2 will be injected in January 2002. Constructs for the *p53* were delayed

because of the MPV infection in our colony. This infection has now been eliminated and we are scheduling all transgenic injections to proceed very rapidly.

KEY RESEARCH ACCOMPLISHMENTS:

Ovarian Tissue and Clinical Database Core Facility

- Collected and snap froze surgical specimen from 152 Ovarian cancer patients
- Collected and snap froze surgical specimen from 110 patients with benign ovarian of which 29 were from patients with family history of ovarian cancer or *BRCA1* or *BRCA2* heterozygotes
- Collected blood and isolated serum and genomic DNA from all patients that donated surgical tissues
- Established primary cultures from 55 malignant ovarian tumors and 40 normal ovaries
- Cryopreserved primary cultures from 30 malignant ovarian tumors and 24 normal ovaries
- Provided all material requested to the 3 projects outlined in the Genetic Definition and Phenotypic Determinants of Human Ovarian Carcinomas Project
- Provided resources to the ovarian cancer scientific community
- Expanded and enhanced the Ovarian Tissue and Clinical Database Core Facility electronic database

Project #1, Molecular Biomarkers in Ovarian Cancer

- Cloned genes that are differentially expressed in ovarian cancer cells using cDNA-RDA.
- Sequenced cloned DNA fragments to identify 160 HOSE and 95 CSOC specific genes
- The cloned DNA fragments were used to fabricate a high density DNA arrays. These arrays were interrogated with cDNA probes from 15 different HOSE and CSOC cells to identify 46 HOSE-specific and 14 CSOC-specific genes that exhibited at least 2.5-fold difference in expression level
- Constructed an ovarian epithelial cell cDNA library
- We carried out a gene-expression profiling study using 10 HOSE and 22 CSOC samples
- We have generated a high quality anti-periostin antisera to study the expression of periostin in ascites and sera
- We have established immortalized ovarian epithelial cell lines by transducing the catalytic subunit of telomerase (hTERT) and/or HPV-16 E7

Project #2, Interactions Between *BRCA1* and *P53* Mutations in Human Epithelial Ovarian Carcinogenesis

- Identified *BRCA1*-linked ovarian cancers in the Ovarian Tissue Core Facility
- Established optimal conditions for each of 10 PCR reactions required for amplification of genomic *p53* sequence. We have confirmed the validity of this approach by sequencing *p53* from MDA-MB-231 cells which are known to harbor a specific *p53* mutation

Project #2, Interactions Between *BRCA1* and *P53* Mutations in Human Epithelial Ovarian Carcinogenesis (cont.)

- Identified a large cohort of both sporadic and *BRCA*-linked ovarian tumors suitable for MDM2 expression analysis
- Discovered an association between expression of the human coxsackie and adenovirus receptor and adenoviral vector transduction efficiency in ovarian cell cultures
- Elucidated anti-adenovirus antibodies as an inhibitor of adenoviral vector transduction in human malignant ovarian cancer ascites specimens
- Procured the first 8 samples of "normal ovaries" from known *BRCA1* mutation carriers. We will seek evidence of *p53* gene mutation in these premalignant specimens

Project #3, Manipulation of Genes in the Ovarian Epithelium of Mice

- Created a new construct that carries the *cre* recombinase under the control of the k18 promoter
- Tested the ability of this construct to mediate recombination in mouse ovarian epithelial cells in culture
- Generated Ad5-*cre* under the control of standard adenoviral promoter elements for pilot work *in vitro* and *in vivo*

REPORTABLE OUTCOMES:

Ovarian Tissue and Clinical Database Core Facility

1. A well endowed human tissue and serum repository for normal and malignant ovarian tissues and corresponding serum and germline DNA.

2. The development and preservation of primary cultures of normal and malignant human ovarian epithelial and stromal cells.

3. The Ovarian Cancer Laboratory and Clinical Database, linking laboratory specimens and results with patient demographic, epidemiologic and clinical data.

Project #1, Molecular Biomarkers in Ovarian Cancer

1. Matei D, Graeber T, Karlan BY, and Chang DD: Gene-expression profiling in normal and malignant ovarian epithelia. Oncogene 21:6289-6298; 2002.

2. Gillian L, Matei D, Fishman DA, Gerbin CS, Karlan BY and Chang DD: Periostin secreted by epithelial ovarian carcinoma is a ligand for avb3 and avb5 integrins and promotes cell motility. Cancer Research 62:5358-5364; 2002.

Project #2, Interactions Between *BRCA1* and *P53* Mutations in Human Epithelial Ovarian Carcinogenesis

1. Buller RE, Runnebaum IB, Karlan BY, Horowitz JA, Shahin M, Buekers T, Petrauskas S, Kreienberg R, Slamon D and Pegram M: A phase I/II trial of rAD/*p53* (SCH 58500) gene replacement in recurrent ovarian cancer. Cancer Gene Therapy 9:553-566; 2002.

2. Buller RE, Shahin MS, Horowitz JA, Runnebaum IB, Mahavni V, Petrauskas S, Kreienberg R, Karlan B, Slamon D and Pegram M: Long term follow-up of patients with recurrent ovarian cancer after Ad p53 gene replacement with SCH 58500. Cancer Gene Therapy 9:567-572; 2002.

3. Konecny G, Untch M, Pihan A, Kimmig R, Gropp M, Stieber P, Hepp H, Slamon D, Pegram M: Association of urokinase-type plasminogen activator and its inhibitor with disease progression and prognosis in ovarian cancer. Clin Cancer Res 7(6):1743-1749; 2001.

4. Elkas JC, Pegram MD, Nielsen L, Tseng Y, Baldwin RL, Slamon DJ and Karlan BY: Immunoglobulins in malignant ascites inhibit adenoviral infection of tumor cells: Implications for adenoviral gene therapy. Submitted: Human Gene Therapy.

Project #3, Manipulation of Genes in the Ovarian Epithelium of Mice

1. Developed an adenoviral vector expression *cre* recombinase and a variant with the K18 promoter.

2. Determined that adenoviral delivery of *cre* in immunocompentant mouse peritoneal cavity is impractical due to immune reactions at the site of injection.

CONCLUSIONS:

This program project is a multidisciplinary collaboration aimed at elucidating genetic alterations that contribute to human ovarian carcinoma with an eye towards identifying useful targets for early ovarian cancer detection and prevention. Towards these ends, the **ovarian tissue core facility** has banked over 160 surgical specimens, including 96 ovarian carcinomas and 71 benign ovaries, of which approximately one third are from women with a family history of ovarian cancer of or a known *BRCA* mutation. Furthermore, the Core's tissue resources are linked to clinical, demographic, and epidemiologic data that allows us to make clinical correlations with our laboratory findings. The Core together with the Clinical Database will support all avenues of ovarian cancer research including those directed toward understanding the basic biology, etiology, genetic influences, prevention and therapeutic developments. In **Project 1**, representational difference analysis was used to identify 46 genes significantly overexpressed in normal ovarian epithelium and 14 specific genes overexpressed in ovarian cancer cells. Using these subtractive cloning techniques as well as a chip based expression profiling approach, we have successfully identified target genes that could be developed into biomarkers for ovarian cancer. In addition, the newly established immortalized ovarian epithelial cell lines will be used to study the functions of the genes that are differentially expressed in cancer-derived ovarian epithelial cells. **Project 2** has established the necessary techniques and identified the *BRCA1* mutation associated ovarian tissues required to understand the functional interaction and contribution of *p53* and *BRCA1* to ovarian epithelial transformation. In addition, as a byproduct of these studies, we discovered that adenoviral gene transfer may only be efficiently accomplished in ovarian cells which express a gene called hCAR (human coxsackie and adenovirus receptor). This observation may have far reaching implications for patients undergoing gene therapy for ovarian cancer using adenoviral vectors. **Project 3** has focused efforts at creating the necessary viral constructs for the proposed experiments aimed at establishing a murine human ovarian cancer model. A new construct carrying the *cre* recombinase under the control of the K18 promoter has been tested to establish its ability to mediate recombination in mouse ovarian epithelial cells. Work on general application of adenovirus into various mouse tissues has demonstrated complications. We will focus future efforts on using our ability to transplant ovaries to overcome this problem. We have determined that adenoviral delivery of *cre* in immunocompentent mice peritoneal cavity is impractical due to immune reactions at the site of injection. Recent development of a viable surface epithelial promoter for standard transgenics has made the adenoviral approach less appealing. We thus plan to switch over to the K19 promoter in collaboration with the lab that developed it as a viable alternative.

"So what?" In order to reduce the unacceptably high mortality rate associated with ovarian cancer, diagnostic modalities which can reliably detect early stage ovarian cancer and preventative strategies to diminish the number of new cases must be discovered. This Program Project has undertaken a multi-faceted approach to the ovarian cancer problem. Using the human ovarian specimens and clinical correlates provided by the core facility, new genes will be identified in Project 1 to serve as targets for detection, prevention, and/or therapy; functional interactions between important known

genes, *BRCA1* and *p53*, will be elucidated in Project 2 and shed light on the molecular etiology of ovarian cancer; and a murine animal model to test these findings and others *in vivo* will be established in Project 3. At the conclusion of this program project, we will be closer to our goal of rationale rather than empiric approaches to ovarian cancer prevention, early detection, and therapy.

REFERENCES:

1. Matei D, Graeber T, Karlan BY, and Chang DD: Gene-expression profiling in normal and malignant ovarian epithelia. Oncogene 21:6289-6298; 2002.

2. Gillan L, Matei D, Fishman DA, Gerbin CS, Karlan BY and Chang DD: Periostin secreted by epithelial ovarian carcinoma is a ligand for $\alpha_v\beta_3$ and $\alpha_v\beta_5$ integrins and promotes cell motility. Cancer Research 62: 5358-5364; 2002.

3. Buller RE, Runnebaum IB, Karlan BY, Horowitz JA, Shahin M, Buekers T, Petrauskas S, Kreienberg R, Slamon D and Pegram M: A phase I/II trial of rAD/*p53* (SCH 58500) gene replacement in recurrent ovarian cancer. Cancer Gene Therapy 9:553-566; 2002.

4. Buller RE, Shahin MS, Horowitz JA, Runnebaum IB, Mahavni V, Petrauskas S, Kreienberg R, Karlan B, Slamon D and Pegram M: Long term follow-up of patients with recurrent ovarian cancer after Ad p53 gene replacement with SCH 58500. Cancer Gene Therapy 9:567-572; 2002.

5. Konecny G, Untch M, Pihan A, Kimmig R, Gropp M, Stieber P, Hepp H, Slamon D, Pegram M: Association of urokinase-type plasminogen activator and its inhibitor with disease progression and prognosis in ovarian cancer. Clin Cancer Res 7(6):1743-1749; 2001.

6. Elkas JC, Pegram MD, Nielsen L, Tseng Y, Baldwin RL, Slamon DJ and Karlan BY: Immunoglobulins in malignant ascites inhibit adenoviral infection of tumor cells: Implications for adenoviral gene therapy. Submitted: Human Gene Therapy.

APPENDICES

1. Matei D, Graeber T, Karlan BY, and Chang DD: Gene-expression profiling in normal and malignant ovarian epithelia. Oncogene 21:6289-6298; 2002.

2. Gillan L, Matei D, Fishman DA, Gerbin CS, Karlan BY and Chang DD: Periostin secreted by epithelial ovarian carcinoma is a ligand for $\alpha_v\beta_3$ and $\alpha_v\beta_5$ integrins and promotes cell motility. Cancer Research 62: 5358-5364; 2002.

3. Buller RE, Runnebaum IB, Karlan BY, Horowitz JA, Shahin M, Buekers T, Petrauskas S, Kreienberg R, Slamon D and Pegram M: A phase I/II trial of rAD/*p53* (SCH 58500) gene replacement in recurrent ovarian cancer. Cancer Gene Therapy 9:553-566; 2002.

4. Buller RE, Runnebaum IB, Karlan BY, Horowitz JA, Shahin M, Buekers T, Petrauskas S, Kreienberg R, Slamon D and Pegram M: A phase I/II trial of rAD/*p53* (SCH 58500) gene replacement in recurrent ovarian cancer. Cancer Gene Therapy 9:553-566; 2002.

5. Konecny G, Untch M, Pihan A, Kimmig R, Gropp M, Stieber P, Hepp H, Slamon D, Pegram M: Association of urokinase-type plasminogen activator and its inhibitor with disease progression and prognosis in ovarian cancer. Clin Cancer Res 7(6):1743-1749; 2001.

6. Elkas JC, Pegram MD, Nielsen L, Tseng Y, Baldwin RL, Slamon DJ and Karlan BY: Immunoglobulins in malignant ascites inhibit adenoviral infection of tumor cells: Implications for adenoviral gene therapy. Submitted: Human Gene Therapy.

Oncogene (2002) 21, 6289–6298

www.nature.com/onc

Gene expression in epithelial ovarian carcinoma

Daniela Matei[1,2], Thomas G Graeber[3], Rae Lynn Baldwin[4,6], Beth Y Karlan[4,6], Jianyu Rao[5] and David D Chang*[1,2]

[1]*Department of Medicine, UCLA School of Medicine, 10833 Le Conte Avenue, Los Angeles, California, CA 90095, USA;* [2]*Department of Microbiology, Immunology and Molecular Genetics, UCLA School of Medicine, 10833 Le Conte Avenue, Los Angeles, California, CA 90095, USA;* [3]*UCLA-Department of Energy Laboratory of Structural Biology and Molecular Medicine, UCLA School of Medicine, 10833 Le Conte Avenue, Los Angeles, California, CA 90095, USA;* [4]*Department of Obstetrics and Gynecology, UCLA School of Medicine, 10833 Le Conte Avenue, Los Angeles, California, CA 90095, USA;* [5]*Department of Pathology and Laboratory Medicine, UCLA School of Medicine, 10833 Le Conte Avenue, Los Angeles, California, CA 90095, USA;* [6]*Division of Gynecologic Oncology, Cedars-Sinai Medical Center, Los Angeles, California, CA 90048, USA*

We analysed the mRNA levels corresponding to 12 600 transcripts in primary cultures of ovarian epithelial cells derived from nine normal ovaries and 21 epithelial ovarian carcinoma. The class distinction and hierarchical clustering of expression data revealed a clear distinction in gene expression between normal and carcinoma-derived ovarian epithelial cells. Comparison of expression levels revealed 111 genes with mean expression values of > 2.5-fold higher in carcinoma cells. Similarly, 62 genes were expressed at > 2.5-fold higher levels in normal ovarian epithelial cells. For a few selected genes, we demonstrate that the pattern of differential expression observed in cultured epithelial cells is present in the normal ovaries and epithelial ovarian carcinoma. Use of cultured epithelial cells represents a novel strategy to study gene expression in a cell-type specific manner.
Oncogene (2002) **21**, 6289–6298. doi:10.1038/sj.onc.1205785

Keywords: ovarian epithelial cells; oligonucleotide arrays; RT–PCR; periostin

Introduction

Approximately 23 000 women will be diagnosed with epithelial ovarian carcinoma (EOC) each year, and less than half of them will be alive at 5 years (Greenlee *et al.*, 2000). If diagnosed early, the disease is curable with surgical resection and adjuvant chemotherapy. However, because of absence of specific symptoms in early stages of the disease, two-thirds of patients are diagnosed with advanced disease (Young *et al.*, 2001). The only serologic marker in use for EOC is CA125, which is helpful for monitoring disease progression, but lacks the specificity to be useful in screening (Jacobs and Bast, 1989). Recent studies have shown that the patterns of proteins in serum can provide a discriminatory power to correctly diagnose early stage EOC (Petricoin *et al.*, 2002). These proteomics assays, either alone or in conjunction with other screening tests, may improve early detection of EOC.

EOC originates from the single layer of epithelial cells covering the surface of the ovaries (Bell and Scully, 1994). Different histological patterns can be identified, sometimes intermixed within the same tumor. The serous papillary subtype is the most common, while mucinous, endometroid, and clear cell subtypes represent less commonly encountered variants (Young *et al.*, 2001). A related entity, primary peritoneal carcinomatosis, arises from extraovarian sites in the peritoneum and has a clinical behavior that mirrors advanced stage ovarian cancer. It often has Müllerian features, reflecting a common embryological origin in the celomic epithelium that gives rise to both peritoneal lining and ovarian surface epithelium. It has been hypothesized that EOC and primary peritoneal carcinomatosis arise from either the mesothelial lining of the ovarian surface or components of the secondary Müllerian system, which include paratubal cysts, rete ovarii, endosalpingiosis, endometriosis, and endomucinosis (Dubeau, 1999).

The molecular changes associated with EOC include mutations in the *BRCA 1* and *2* genes, alterations of *p53*, and amplification of *HER2/neu*, *PIK3CA*, *AKT2*, and *myc* (Cheng *et al.*, 1992; Foster *et al.*, 1996; Marks *et al.*, 1991; Shayesteh *et al.*, 1999; Slamon *et al.*, 1989; Takahashi *et al.*, 1995). In addition, a number of genes have been reported to be either up- or down-regulated in EOC (Hough *et al.*, 2000; Ismail *et al.*, 2000; Mok *et al.*, 1994; Ono *et al.*, 2000; Schummer *et al.*, 1999; Welsh *et al.*, 2001). Gene expression comparison of EOC to the normal ovarian epithelial counterpart has been difficult to perform, as the epithelial layer of the ovaries comprises < 1% of the mass of the organ. This problem is further confounded by the lack of premalignant changes in the ovaries and the heterogeneity of the disease. To focus on cancer cell specific molecule changes, an

*Correspondence: DD Chang, UCLA School of Medicine, Division of Hematology-Oncology, Factor 11-934, 10833 Le Conte Avenue, Los Angeles, California, CA 90095-1678, USA;
E-mail: ddchang@mednet.ucla.edu
Received 7 March 2002; revised 12 June 2002; accepted 18 June 2002

ovarian cancer model based on primary cells cultured from the normal ovaries and EOC, which eliminates signals from non-malignant cells intermixed within tumors (e.g., stromal cells, endothelial cells, immune cells), has been used (Ismail *et al.*, 2000; Mok *et al.*, 1994).

We characterize gene expression in EOC-derived epithelial cells (CSOC, Cedar Sinai Ovarian Cancer) and normal ovarian epithelial cells (HOSE, Human Ovarian Surface Epithelia) using Affymetrix U95Av2 Genechips. The analysis of expression data revealed a clear distinction between CSOC and HOSE. For a limited number of selected genes, the differential expression was also demonstrated in EOC. We suggest that primary epithelial cells cultured from tumors can be used to study gene expression in a cell-type specific manner to complement gene expression analysis based on tumors.

Results

Primary cell cultures of HOSE and CSOC

Nine HOSE and 21 CSOC cultures were used for analysis. These primary cells display a limited life span of 5–12 passages for HOSE and a slightly extended 10–15 passages for CSOC. The characteristics of the CSOC cultures and the EOC they were derived from are detailed in Tables 1 and 2. While cultures of varying passage numbers were used, no apparent correlation between the passage number and the proximity of samples based on the gene expression pattern was observed in the hierarchical clustering analysis (Figure 2).

Gene expression-based distinction of HOSE and CSOC

RNA from primary ovarian epithelial cultures was used to determine expression levels for 12 600 transcripts using the Affymetrix U95Av2 Genechips and gene expression differences between the HOSE and CSOC samples were compared to differences between randomly generated groups of equivalent sizes. This 'neighborhood analysis' (Golub *et al.*, 1999) allows one to establish whether the correlation of observed gene expression in HOSE and CSOC samples to the normal/malignant classification is stronger than would be expected by chance (see Materials and methods). Based on this analysis, $<0.1\%$ of the random classifications had more genes with significant expression differences than the normal/malignant classification (Figure 1). Thus, the differences between HOSE and CSOC are reflected in their overall gene expression patterns.

Genes differentially expressed in HOSE and CSOC

When the two groups (HOSE and CSOC) were compared, 2176 genes had levels of difference in expression that reach statistical significance, based on the two-tailed Student's *t*-test ($P<0.05$). Within this group, there were 111 genes (0.9% of 12 600) with >2.5-fold higher levels of expression in the cancer cells and 62 genes (0.5% of 12 600) with >2.5-fold higher levels of expression in the normal cells. Tables 3 and 4 list the top 30 genes in each category with their mean expression levels and *P*-values.

Genes previously reported to be up-regulated in ovarian cancer (e.g. *PAI2*, *ALP*, *COL11A1*, *OSF2*, *PDGFRα*) and novel genes not previously associated with EOC (e.g., *TGM2*, *ACLP*, *RAGE3*, *TSG14*,

Table 1 Characteristics of the cancer-derived CSOC cultures

CSOC	*Passage*	*Cytokeratin*	*Factor VIII*	*Vimentin*	*Tumor histology*	*Nuclear grade*	*LVI*[a]	*Tumor stage*[b]
C798	11	+	–	+ +	Papillary serous	High grade	+	IIIC
C815	2	+	–	+ +	Papillary serous	High grade	–	IIIC
C817	15	+ +	–	+ +	PD adenocarcinoma	High grade	–	IIIC
C823	9	+ +	–	+ +	PD adenocarcinoma	High grade	+	IIIC
C824	11	+	–	+ +	Papillary serous	High grade	+	IIIC
C834	7	+ +	–	+ +	PD[c] adenocarcinoma	High grade	–	IIIC
C839	9	+	–	+ +	Papillary serous	High grade	–	IV
C843	11	+ +	–	+ +	Papillary serous	Moderate	+	IIIC
C844	6	+	–	+ +	Papillary serous	High grade	+	IIIC
C846	5	+ +	–	+ +	Papillary serous	High grade	+	IV
C848	8	+	–	+ +	Papillary serous	High grade	–	IIIC
C857	8	+	–	+ +	Papillary serous	High grade	–	IIIC
C858	8	+ + +	–	+ +	Mullerian adenocarcinoma	High grade	+	IV
C866	7	+ +	–	+ +	Mullerian adenocarcinoma	High grade	+	IIIC
C874	8	+	–	+ +	Papillary serous	High grade	–	III
C881	8	+ +	–	+ +	Papillary serous	Moderate	–	IIIC
C886	9	+ +	–	+ +	Papillary serous	High grade	+	IIIC
C889	8	+	–	+ +	Papillary serous	High grade	+	IIIC
C908	5	+ +	–	+ +	Papillary serous	High grade	+	IIIC
C917	9	+	–	+ +	Serous carcinoma	High grade	–	IV
C918	5	+ + +	–	+ +	Papillary serous	High grade	+	IV

IHC staining for cytokeratin, vimentin and factor VIII is graded from '+' to '+ + +'. Histological characteristics of the tumours from which the CSOC cells are derived and the stages of the tumors based on the pathological reports. [a]LVI, lymphovascular invasion; [b]tumor staging according to FIGO is provided; [c]PD, poorly differentiated

Table 2 Characteristics of HOSE cultures

HOSE	*Passage*	*Cytokeratin*	*Vimentin*	*Factor VIII*	*Pathology*	*Indication for hysterectomy*
H224	12	+	+ +	0	Benign	Uterine fibroids
H246	5	+	+ +	0	Benign	Uterine fibroids
H253	11	+	+ +	0	Benign	Uterine fibroids
H254	8	+	+ +	0	Benign, serosal adhesions	Endometriosis
H259	9	+	+ +	0	Benign cyst	Pelvic mass
H263	10	+ + +	+ +	0	Benign cyst, stromal hyperplasia	Ovarian cyst
H274	8	+	+ +	0	Benign	Prophylactic BSO; Family history
H281	8	+	+ +	0	Benign	Prophylactic BSO[a]; BRCA1 carrier
H293	8	+	+ +	0	Benign	Uterine fibroids

IHC staining for cytokeratin, vimentin and factor VIII is graded from '+' to '+ + +'. [a]BSO: bilateral salpingo-oophrectomy

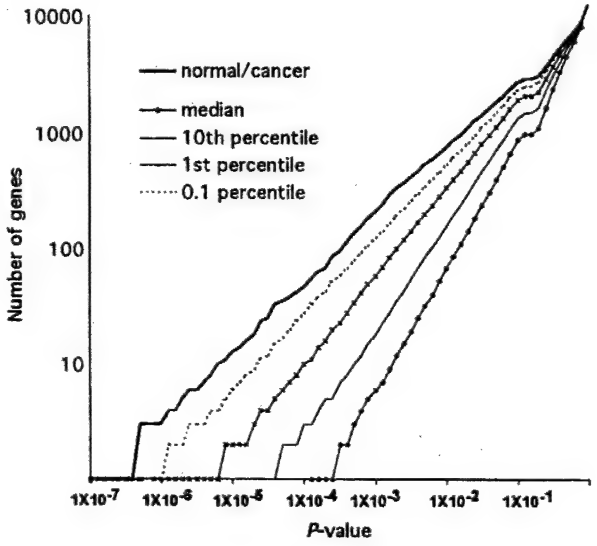

Figure 1 The gene expression differences between HOSE and CSOC samples are statistically significant. The number of genes with *P*-values less than various threshold levels (Materials and methods) were calculated for the normal/malignant classification and plotted. Random groupings were also generated and tested. The median and various confidence levels for these random groupings are also plotted. A confidence level of 1%, for example, indicates that < 1% of the random groupings had a higher number of genes that were differentially expressed with *P*-values below the indicated *P*-value threshold

Wnt5a frizzled 7) were among the genes over expressed in CSOC. Genes strongly correlated with the HOSE phenotype were equally diverse. *StAR*, *adipophilin*, and *fibulin2* encode proteins expressed in ovarian tissue. Other HOSE-specific genes reflect the epithelial nature of the HOSE (e.g., *PEM*, *plakophilin*, *merocin*, *Muc1*).

Hierarchical clustering of HOSE and CSOC gene expression

To visualize the gene expression distinction between HOSE and CSOC, we used hierarchical clustering (Figure 2). This analysis was carried out using ~1500 genes with significant variation across samples (see Materials and methods). Whereas the 'neighborhood analysis' sorts genes by their degree of correlation to the normal/malignant classification, the hierarchical clustering algorithm groups experimental samples according to the overall similarity in their gene expression pattern. The dendogram pictured in Figure 2b illustrates the main segregation of the gene expression patterns. The majority (26 out of 30) samples segregated correctly to normal and malignant clusters, according to their original tissue diagnosis. Three CSOC samples (C889, C858 and C918) clustered on a sub branch within the HOSE group, while one HOSE sample (H263) clustered with the CSOC samples. The only distinctive feature of H263 culture was that it was derived from an ovary with benign cysts and stromal hyperplasia (Table 2).

The main subgroups of genes driving the separation of HOSE and CSOC are shown in Figure 2c–f. For presentation purpose only a segment of each cluster is shown. As expected, some of the genes recognized here included the genes that were also selected based on the Student's *t*-test as being preferentially expressed in HOSE or CSOC. One group of genes separating out the HOSE cluster from the rest of samples is comprised of genes that are highly expressed in the normal cells (e.g. *gap junction protein*, *carbonic anhydrase IX* and *XII*, *stanniocalcin*, *fibulin 2*, *plakophilin*) (Figure 2c). Also included in this cluster are two potential tumor suppressor genes, *Mxi1* and *DOC1* (Lee and Ziff, 1999; Mok *et al*., 1994).

Within the CSOC division, there were additional subgroups. Statistically significant distinctions among different subgroups could not be established, but we note several 'molecular portraits'. For instance, a subgroup of seven samples (C843, C846, C839, C824, C823, C834 and C817) was characterized by intense expression of the genes encoding proteasome-related proteins, *nm23*, *placental protein 15*, and *karyopherin alpha 6* (Figure 2d). The second subgroup of four samples (C824, C823, C834 and C817) clustered together because of high expression levels of genes associated with cell proliferation (e.g. *CDC2*, *cyclinA2*, *cyclinB1*, *CDC28 protein kinase 2*, *CDC20*) (Figure 2e). This fraction of samples may represent an actively cycling group of tumor cells with more aggressive behavior. The third subgroup of five samples (C886, C844, C917, C866 and C798) clustered together mainly due to higher expression levels of genes encoding

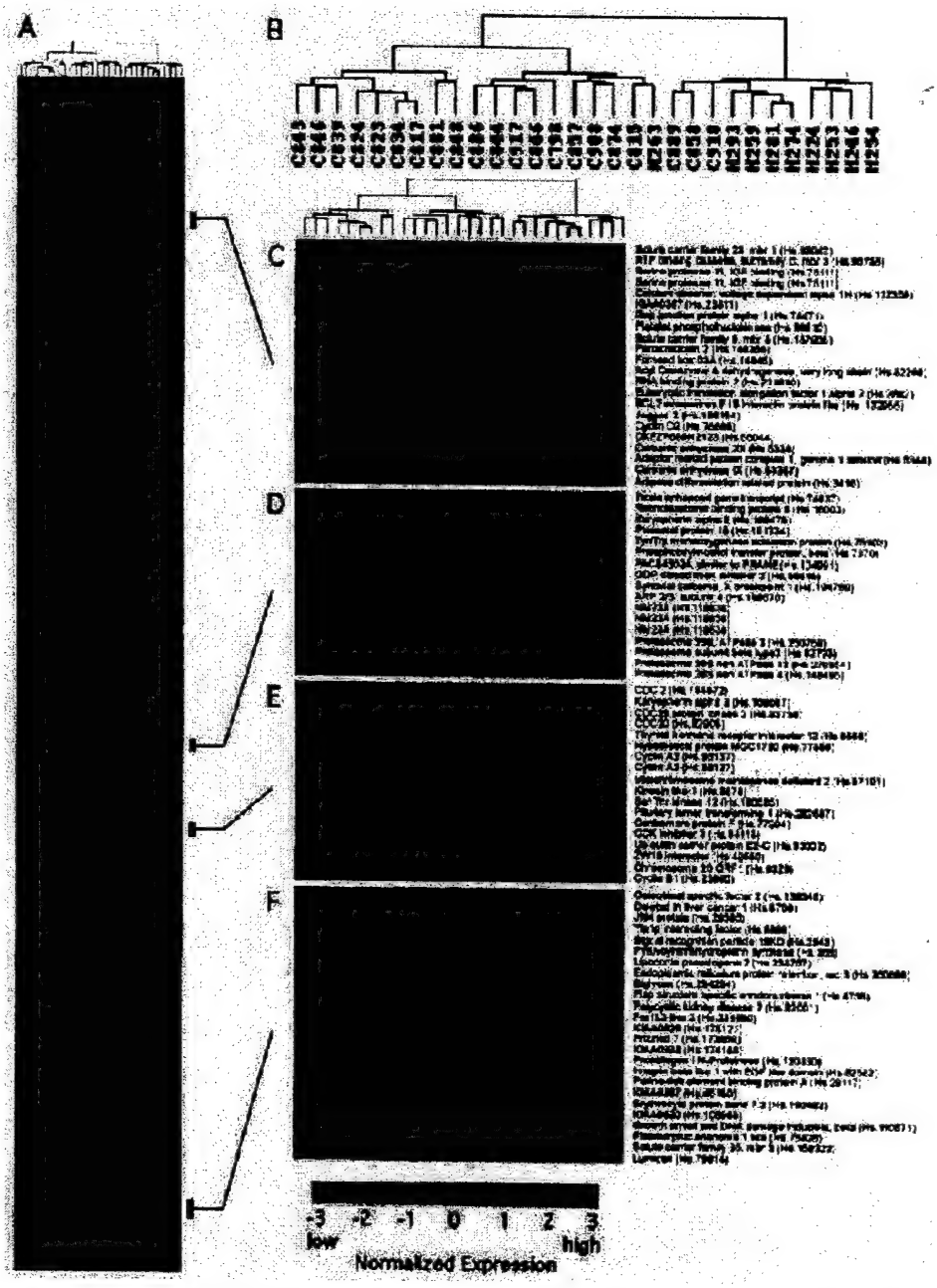

Figure 2 Hierarchical clustering of HOSE and CSOC samples. (**a**) Gene expression patterns in nine HOSE and 21 CSOC samples are shown. Columns represent individual samples and rows represent genes. Each cell corresponds to the level of expression of a particular gene in a given sample. All values have been normalized to a mean of 0 and a standard deviation of 1. A visual dual color code is utilized with red and green indicating relatively high and low expression levels, respectively. Cluster and Treeview programs were usd to generate these figures (Eisen *et al.*, 1998). The scale of color saturation, which reflects the gene expression levels, is shown below. (**b**) Dendogram illustrating the separation of samples based on their degree of similarity as measured by the Pearson correlation coefficient. (**c**) Group of genes with high level of expression in HOSE. (**d**–**f**) Groups of genes with relative high expression in CSOC. The groups are denoted as the 'proteolysis' group (**d**), 'proliferation' group (**e**), and 'ECM/cell adhesion group' (**g**), based on the predominance of particular type of genes in each group. Commonly used alias of the gene name is provided with the corresponding UniGene number (http://www.ncbi.nlm.nih.gov/UniGene/). The scale at the bottom shows the relationships between color saturation and the normalized gene expression levels

extracellular matrix proteins and cell adhesion receptors (e.g. *OSF2*, *biglycan*, *procollagen I N-proteinase*, *integrin β1 like protein*, *band 7.2 protein*, *lumican*) (Figure 2f).

Validation of cancer cell-specific gene expression

Four genes (*Wnt5a*, *OSF2*, *PAI2* and *TGM2*) were selected for RT–PCR analysis. RNA from three HOSE and seven CSOC samples used in the array

analysis were randomly chosen and used as templates. There was a rough correlation between the intensity of the bands and the gene expression levels from the oligonucleotide array studies when the RT–PCR products after a limited, and presumably non-saturating, number of amplification cycles were analysed by gel electrophoresis (Figure 3).

The expression of Wnt5a, OSF2, PDGF-α receptor (PDGFRα), and n-chimerin in ovarian tissue was also examined by RT–PCR. A qualitative difference in the levels of RT–PCR products in tumors compared to the normal ovaries was readily visible for each of four genes (Figure 4a). In the case of PDGFRα and OSF2, which were not detected in the normal ovaries, RT–PCR products were detected in 10/15 (for PDGFRα) and 13/15 (for OSF2) ovarian tumors. The different sizes RT–PCR products in OSF2 are due to alternative splicing at the 3′ end of the coding region (Horiuchi *et al.*, 1999). Similarly, higher levels of RT–PCR products were detected for Wnt5a and n-chimerin in eight out of 15 and nine out of 15 tumor samples, respectively. RT–PCR products were also demonstrated for TGM2 in tumor samples, but not in the normal ovaries (data not shown). RT–PCR for PAI2 gave similar levels of products in normal ovaries and tumors (data not shown).

For OSF2 and TGM2, we examined protein expression in ovarian tissues by immunoblot. Polyclonal rabbit anti-OSF2 antibodies detected a group of proteins migrating at ~90 kD six out of 10 tumors (Figure 4b). In three normal ovaries tested, OSF2

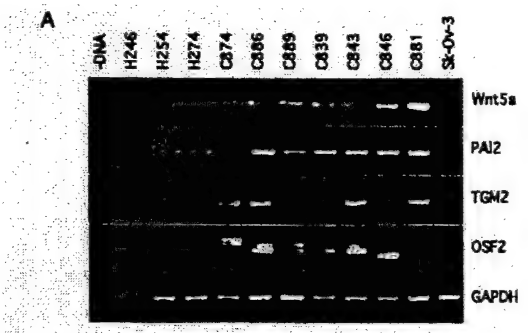

B

Gene	H246	H254	H274	C874	C886	C889	C839	C843	C846	C881
Wnt5a	1039	1909	103	1061	2136	1444	16117	28422	5052	20603
PAI2	77	5414	3670	77	108544	5847	6556	23078	27908	38547
TGM2	1858	-486	259	11868	27364	494	10144	89488	52446	34470
OSF2	470	1156	1466	16420	46724	2494	48591	41538	46088	34112

Figure 3 Validation of gene expression in cells. (a) Expression differences detected by microarrays were verified by RT–PCR for Wnt5a, PAI2, TGM2, and OSF2. GAPDH was used as a control to standardize RT–PCR. H246, H254 and H274 are HOSE (normal). C874, C886, C889, C839, C843, C846 and C881 are CSOC (cancer). Sk-Ov-3 is an ovarian carcinoma cell line. (b) Gene expression levels as determined by microarrays are shown

Table 3 Genes preferentially expressed in CSOC (cancer) cells than in HOSE (normal) cells (>2.5)

Probe set	*GeneBank accession*	*Gene description*	*Mean CSOC*	*Mean HOSE*	*CSOC/HOSE*	*P-value*
37185_at	Y00630	Arg-Serpin (plasminogen activator-inhibitor 2, PAI-2)	16672	1374	12.1	0.00683
38404_at	M55153	Transglutaminase (TGM2)	33268	2916	11.4	0.00005
32275_at	X04470	Antileukoprotease (ALP)	3473	334	10.4	0.03556
38087_s_at	W72186	zd69b10.s1 Homo sapiens cDNA	3003	300	10	0.02948
39069_at	AF053944	Aortic carboxypeptidase-like protein (ACLP)	5062	540	9.4	0.00007
41389_s_at	U46193	Renal cell carcinoma antigen RAGE-3	5501	707	7.8	0.00179
32666_at	U19495	Intercrine-alpha (hIRH)	2264	313	7.2	0.00053
37892_at	J04177	Alpha-1 type XI collagen (COL11A1)	6372	899	7.1	0.0424
36993_at	M33210	Colony stimulating factor 1 receptor (CSF-1R)	8094	1266	6.4	0.00134
1771_s_at	J03278	Platelet-derived growth factor (PDGF) receptor	8480	1494	5.7	0.00077
753_at	D86425	Osteonidogen	3839	703	5.5	0.00134
33878_at	W27472	31d4 Homo sapiens cDNA	1741	323	5.4	0.03259
1451_s_at	D13666	Osteoblast specific factor 2 (OSF-2os)	26710	5050	5.3	0.00002
33834_at	L36033	Pre-B cell stimulating factor homolog (SDF1b)	1551	300	5.2	0.00464
32242_at	AL038340	DKFZp566K192_s1 Homo sapiens cDNA	4970	968	5.1	0.01104
33862_at	AF017786	Phosphatidic acid phosphohydrolase homolog (Dri42)	3225	657	4.9	0.00601
36965_at	U13616	Ankyrin G (ANK-3)	1430	300	4.8	0.01987
34747_at	X83535	Membrane-type matrix metalloproteinase	2370	501	4.7	0.00784
34283_at	AL050125	DKFZp586F071	1457	315	4.6	0.00271
37484_at	X68742	Integrin, alpha subunit	2733	597	4.6	0.00396
1491_at	M31166	Tumor necrosis factor-inducible (TSG-14)	18067	4031	4.5	0.0064
35396_at	U54804	Has2	2741	644	4.3	0.00034
425_at	X67325	HSP27 Homo sapiens p27	8725	2055	4.2	0.00916
40126_at	Z97200	DNA sequence from PAC 79C4 on chromosome 1q24	1774	435	4.1	0.00602
1669_at	L20861	Proto-oncogene (Wnt-5a)	7247	1810	4	0.00213
40512_at	X51408	*n-chimerin*	1833	461	4	0.00441
35555_r_at	AF104902	ZIC2 protein (ZIC2)	2343	590	4	0.00005
39473_r_at	W29065	56g2 Homo sapiens cDNA	1909	491	3.9	0.01909
33222_at	AB017365	Fizzled-7	2156	571	3.8	0.0001
36025_at	AB002335	Human mRNA for KIAA0337 gene	1540	422	3.7	0.00017

GeneBank accession numbers and the corresponding description of the gene is provided for each U95Av2 Affymetrix probe sets. The fold difference between CSOC and HOSE samples, *P*-value for differential expression, mean hybridization signal intensity in CSOC and HOSE samples are included. The complete data set is available at http://www.cancer.mednet.ucla.edu/ovarian

Table 4 Genes preferentially expressed in HOSE (normal) cells than in CSOC (cancer) cells (> 2.5)

Probe set	*GeneBank accession*	*Gene description*	*Mean CSOC*	*Mean HOSE*	*HOSE/CSOC*	*P-value*
35174_i_at	X70940	Elongation factor 1 alpha-2	2557	18584	7.3	0.00427
38800_at	D45352	HUMHG17416 Homo sapiens cDNA	2183	13756	6.3	0.03607
35822_at	L15702	Complement factor B	647	3656	5.6	0.03023
34343_at	U17280	Steroidogenic acute regulatory protein (StAR)	1540	8341	5.4	0.01536
1616_at	D14838	FGF-9	543	2926	5.4	0.03282
40309_at	X66839	MaTu MN mRNA for p54/58N protein	1851	9803	5.3	0.00084
38469_at	M35252	CO-029	554	2927	5.3	0.00399
917_g_at	L18983	Tyrosine phosphatase (IA-2/PTP)	760	3952	5.2	0.00075
36324_at	X68487	A2b adenosine receptor	1116	5479	4.9	0.00372
40314_at	AJ002309	Synaptogyrin 3	330	1491	4.5	0.04952
32001_s_at	M80482	Subtilisin-like protein (PACE4)	847	3783	4.5	0.04526
39593_at	AI432401	tg73b09.x1 Homo sapiens cDNA	314	1396	4.4	0.00478
37657_at	Y16270	PALM gene, exon 1 and joined cds	1360	5737	4.2	0.00876
35081_at	D14838	FGF-9	410	1642	4	0.03383
39061_at	D28137	BST-2	5974	22523	3.8	< 0.00001
39215_at	AL021155	Brain Natriuretic Protein (BNP)	31480	114924	3.7	0.00003
35698_at	Y00318	Complement control protein factor I	1097	3976	3.6	0.00291
32963_s_at	W27549	32d11 Homo sapiens cDNA	336	1213	3.6	0.00503
40900_at	AI382123	te30a09.x1 Homo sapiens cDNA	1673	5903	3.5	0.00094
33442_at	AB002365	KIAA0367 gene, partial cds	1597	5553	3.5	0.0004
33767_at	X15306	NF-H gene, exon 1 and joined cds	1077	3734	3.5	0.02746
38167_at	AB020704	KIAA0897 protein, partial cds	388	1327	3.4	0.00515
1955_s_at	AF035528	Smad6 mRNA	533	1792	3.4	0.02164
34378_at	X97324	Adipophilin	12985	42865	3.3	0.00038
1346_at	S72043	Growth inhibitory factor (GIF)	5540	17752	3.2	0.01022
32783_at	X82494	Fibulin-2	7149	22596	3.2	0.01367
37248_at	U83411	Carboxypeptidase Z precursor	3178	10041	3.2	0.00797
38783_at	J05581	Polymorphic epithelial mucin (PEM)	530	1663	3.1	0.0433
40017_at	AL050214	DKFZp586H2123	1914	5813	3	0.00043
40642_at	AI312646	qp77f0.1x1 Homo sapiens cDNA	698	2115	3	0.00114

GeneBank accession numbers and the corresponding description of the gene is provided for each U95Av2 Affymetrix probe sets. The fold difference between CSOC and HOSE samples, *P*-value for differential expression, mean hybridization signal intensity in CSOC and HOSE samples are included

expression was negligible. TGM2 was expressed in eight out of 10 tumors, but not in the normal ovaries. In three tumors (T1354, T1357 and T1475), an additional anti-TGM2 immunoreactive band migrating at ~65 kD is seen. This faster migrating band may represent the previously reported TGM2 isoform (Fraij *et al*., 1992).

OSF2 immunohistochemistry (IHC)

The OSF2 expression in ovarian tissue was also examined by IHC (Table 5). In serous papillary carcinoma samples, eight out of 26 displayed intermediate to strong (2+ to 3+) OSF2 staining. In some tumors, the OSF2 staining was heterogeneous, with areas corresponding to invasive foci and regions with poor histological differentiation displaying a stronger staining. OSF2 staining was weak in 12 and absent in the remaining six tumor samples. In serous borderline tumors, only two of seven samples stained weakly (1+) for OSF2 in ~10% of cells. Eight of the nine normal ovaries displayed no OSF2 staining. One normal ovarian tissue showed weak staining (1+, in ~20% of cells) in an area corresponding to benign cystic proliferation. Representative photographs of OSF2 staining in ovarian tissue are shown in Figure 5.

Discussion

We utilized an ovarian cancer model that is based on *in vitro* expansion of normal and malignant ovarian epithelial cells (Karlan *et al*., 1995; Mok *et al*., 1994). In this model, all cultured cells are epithelial, based on positive staining for cytokeratin, and grossly uniform (Ismail *et al*., 2000; Karlan *et al*., 1995). Reliance on cultured cells introduces potential problems related to the secondary gene expression changes stemming from *in vitro* selection and variability in culture conditions. Some of the gene expression variation seen in different HOSE and CSOC samples and incorrect clustering of three CSOC and one HOSE samples may reflect this *in vitro* expansion bias (see Figure 2). However, these problems are offset by the fact that the use of expanded primary cultures is more likely to reveal gene expression changes that are cancer cell specific.

Two lines of evidence indicate that distinct cells are cultured from the EOC than the normal ovary. First, when the gene expression levels were sorted by degree of their correlation to class distinction (i.e., CSOC *vs* HOSE) by the 'neighborhood analysis' method, there was an unusually high density of genes that followed the idealized pattern of this class distinction, as compared to equivalent random patterns. Second, the hierarchical clustering algorithm uncovered a clear

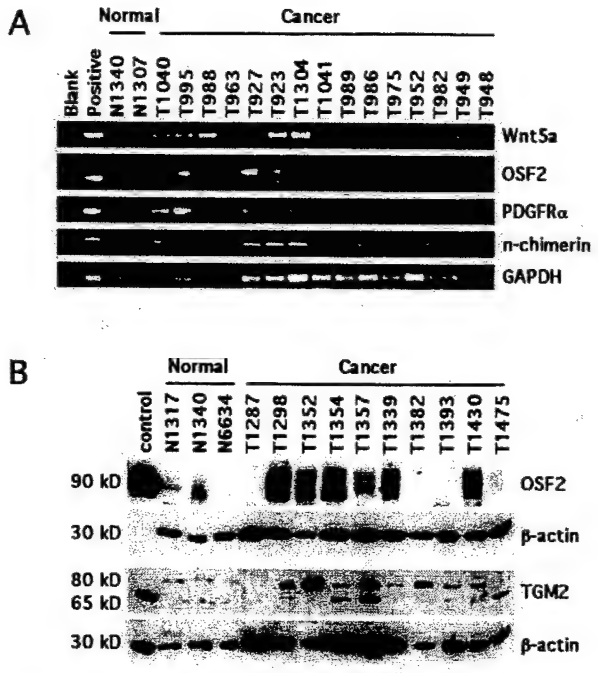

Figure 4 Validation of gene expression differences in tumor samples. (a) Expression of Wnt5a, OSF2, PDGFRα, and *n-chimerin* in ovarian tissues were examined by RT–PCR. GAPDH was used as a control to standardize RT–PCR. N1304 and N1370 are normal ovarian tissue. T948 to T1304 are serous papillary ovarian carcinomas. (b) Expressions of OSF2 and TGM2 in ovarian tissues were examined by immunoblotting. N1317, N1340, and N6634 are normal ovarian tissue. T1287 to T1475 are serous papillary ovarian carcinomas. Protein integrity in lysates was verified by immunoblotting for β-actin. Culture media from CSOC line C272 and the lysate of an ovarian xenograft were used as positive control for OSF2 and TGM2, respectively

Table 5 OSF2 immunohistochemistry

			Staining		
Tissue	*n*	*0*	*1+*	*2+*	*3+*
Normal ovaries	9	8	1[a]		
Borderline tumors	7	5	2[b]		
EOC	26	6	12	4	4

IHC staining was graded from 0 (no staining) to 3+ (strong staining). [a]Staining was in the area of benign cystic proliferation. [b]Staining was in ~20% of the cells in the tumor. EOC = epithelial ovarian carcinoma

separation between the normal cells from malignant cells. This separation represents the main division of our clustering tree, followed by smaller subdivisions distinguishing separate fractions within the CSOC sample group. These findings, together with the previous observation that CSOC cells, but not HOSE cells, contain chromosome abnormalities (Ismail *et al.*, 2000) support the use of cultured epithelial cells in gene expression studies.

The gene expression profiles of three CSOC (C889, C858, and C918) and one HOSE (H263) were sufficiently different, resulting in their clustering away from the main divisions of the dendogram (Figure 2). There were no consistent features of the three CSOC cultures, in the histology of the tumors which there were derived from, immunoreactivity to keratin, vimentin, or Factor VIII, or culture passage number, that would account for the differences in gene expression pattern. It is possible that a subtle, unrecognized, variation in the handling of the cultured cells might have skewed the gene expression. Another possibility is that the differences in their gene expression pattern reflect their distinct cellular characteristics. In this regard, it is interesting that H263 were cultured from an ovary with stromal hyperplasia and that the cultured cells had a much stronger immunoreactivity to cytokeratin than the other HOSE cultures (Table 2).

The list of differentially expressed genes includes genes that have previously been associated with the neoplastic process as well as those that have not been recognized as transformation related genes in ovarian or other human cancers. Among these, *OSF2* (also known as *periostin*), which encodes a secreted protein related to the axon guidance molecule fasciclin-1 of insect (Takeshita *et al.*, 1993), ranks high ($P = 0.00002$). The frequency of OSF2 positivity in CSOC cultures was ~70% by Northern blot analysis in our previous study (Ismail *et al.*, 2000), which correlates closely with the observed frequency of OSF2 staining in tumors (77%, 31% intermediate to strong and 46% weak staining). In tumors, anti-OSF2 antibodies stained intensely in the cytoplasm of the cancer cells (Figure 5), indicating that the cancer cells express OSF2. Two recent studies have reported that the serum OSF2 levels are elevated in lung cancer and thymoma patients (Sasaki *et al.*, 2001a,b), raising the possibility that the OSF2 expression status may provide a prognostic or predictive information for EOC.

Other genes of potential interest include *PDGFRα*, *Wnt5a TGM2*, and *n-chimerin*. Previous studies have shown PDGF and/or PDGFRα are over-expressed in EOC, suggesting a functional role of PDGF via autocrine growth stimulation (Henriksen *et al.*, 1993; Link *et al.*, 1996). The availability of tyrosine kinase inhibitors with specificity towards PDGF receptors affords an opportunity to test the role of PDGF axis in the pathogenesis of EOC. The *Wnt* genes encode a family of secreted growth factors critical for embryonic pattern formation and cell lineage differentiation (Cadigan and Nusse, 1997). While Wnt5a protein is not known to be transforming, it is implicated in the regulation of progenitor cell proliferation and up-regulated in breast cancer (Lejeune *et al.*, 1995; Yamaguchi *et al.*, 1999). TGM2 is a GTP-binding protein that participates in protein transamidation and has been suggested to play a role in Rho signaling and cell cycle and apoptosis (Antonyak *et al.*, 2001; Nanda *et al.*, 2001; Singh *et al.*, 2001). N-chimerin is a GTPase-activating protein for Rac1 and Cdc42Hs and may regulate cell motility by inducing the formation of lamellipodia (Kozma *et al.*, 1996).

Analysis of genes with stronger expression in HOSE offers insight into genes that may play a permissive role

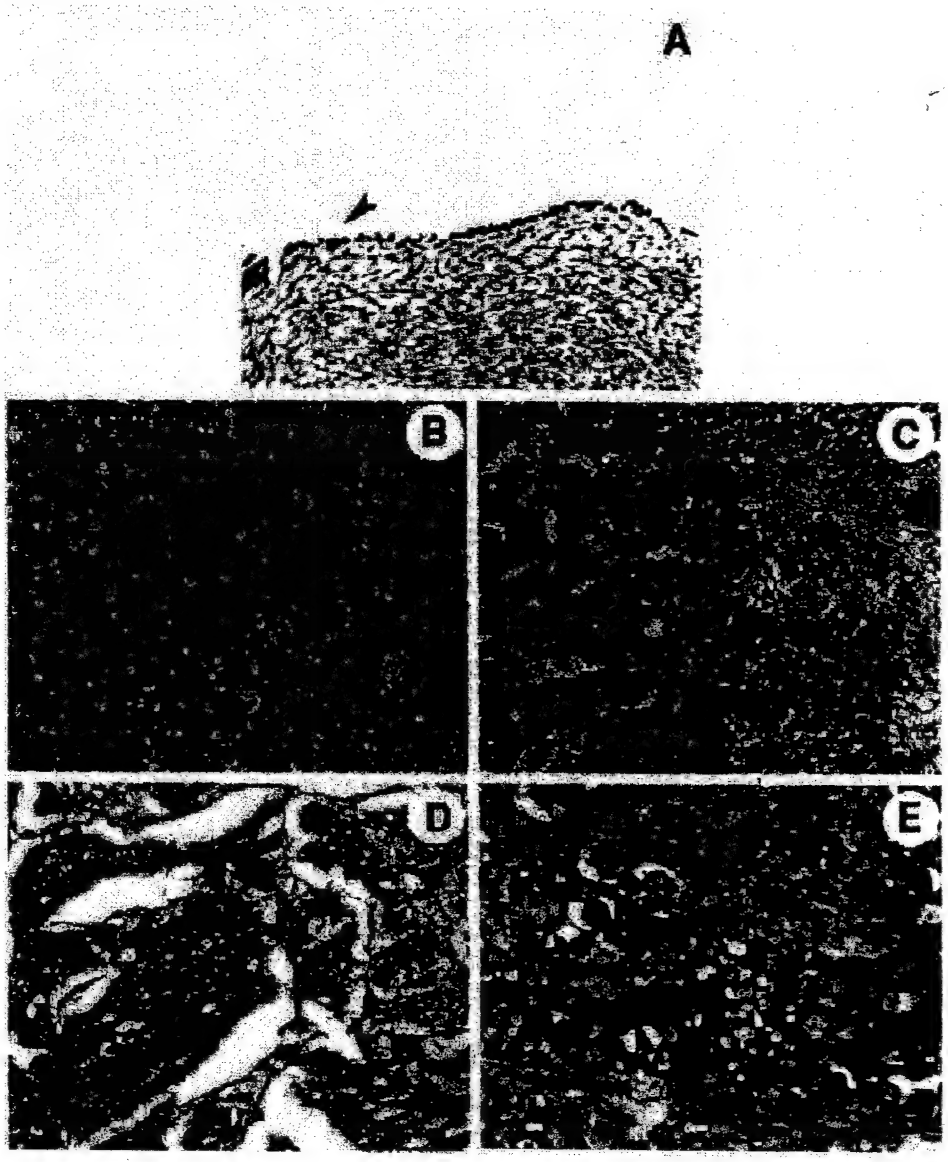

Figure 5 OSF2 expression in ovarian tissue. IHC staining for OSF2 in paraffin embedded tissue slides are shown. (a) Normal ovary. An arrowhead indicates the surface epithelial layer of the normal ovary. (b–d) EOC (serous papillary). Digitally enlarged photograph (d) illustrates intense cytoplasmic staining of OSF2 in carcinoma cells. The original images were digitally captured at 200× magnification

in the neoplastic process and/or govern differentiation. The only gene with tumor suppressor function revealed in our study is *Mxil* (Lee and Ziff, 1999). Other genes with strong signal in HOSE include *plakophilin*, *stanniocalcin*, *adipophilin*, *BST2*, *StAR*, *PACE4*, *prostacyclin synthetase* and *Muc1*. These genes are expressed in a tissue-restricted manner and may represent differentiation specific genes (Heid *et al.*, 1998; Ishikawa *et al.*, 1995; Mains *et al.*, 1997; Mertens *et al.*, 1996; Stasko and Wagner, 2001). The down-regulation of these genes may reflect cellular de-differentiation associated with neoplastic transformation.

We demonstrate that cultured epithelial cells provide a unique method for studying gene expression in a cell-autonomous manner. Genes that are differentially expressed in a cancer cell-specific manner may help us understand the pathogenesis of EOC and could be targeted for the development of diagnostic or therapeutic tools.

Materials and methods

Primary ovarian epithelial cell cultures

Primary cultures of ovarian surface epithelial cells were initiated by explanting ovarian surface scrapings or dissected ovarian surface fragments (Auersperg *et al.*, 1994; Ismail *et al.*, 2000; Karlan *et al.*, 1995). Their epithelial nature was verified by IHC using antibodies against cytokeratin

(AE1:AE3; Roche, Indianapolis, IN, USA), vimentin (Roche) and factor VIII (Calbiochem, San Diego, CA, USA). Both normal and malignant primary cells were grown in identical culture conditions and harvested at ~85% confluence.

Oligonucleotide arrays

Total RNA was extracted from each culture using RNA STAT-60 reagent (Tel-Test Inc, Friendswood, TX, USA) and purified using the RNeasy Mini Kit (Qiagen Inc, Valencia, CA, USA). Double-stranded cDNA was synthesized using the HPLC purified T7-(dT)24 primer (Genset Corp, La Jolla, CA, USA) and cDNA Superscript Choice System (Gibco BRL, Carlsbad, CA, USA). Biotinylated cRNA probe was obtained using the Bioarray High Yield RNA Transcript Labeling Kit (Enzo Biochem Inc, Farmingdale, NY, USA). Fifteen μg of labeled cRNA was incubated in 40 mM Tris-acetate, pH 8.1, 0.1 M potassium acetate, 30 mM magnesium acetate at 94°C for 35 min and hybridized to U95Av2 Genechips (Affymetrix, Santa Clara, CA, USA). The expression level for each probe set was calculated using the Affymetrix Microarray Suite (version 4.0.1) (Affymetrix). Briefly, the expression level was based on an average of differences between the perfect match-mismatch probe pairs for each gene. The values of the perfect match–mismatch pairs outside three standard deviations from the mean intensity (i.e. Affymetrix parameter STP set three) were discarded as outliers. The intensities across different chips were normalized to a target intensity of 2500 using global normalization scaling. All values below the intensity of the background (300) across experiments were set equal to the background.

Data analysis

All genes were ranked by their probability of being significantly differentially expressed between the two sample types as determined using the Student's *t*-test. The fold change in the mean of each gene between the normal and malignant samples was also calculated. The 'neighborhood analysis' (Golub *et al.*, 1999) was carried out using the same measure of differential expression as used in the Student's *t*-test,

$$t = \frac{|\mu_1 - \mu_2|}{\sqrt{\frac{\sigma_1^2}{n_1 - 1} + \frac{\sigma_2^2}{n_2 - 1}}}$$

where μ_i, σ_i and n_i are the mean, standard deviation and number of samples, respectively, of sample group i. *P*-values were then calculated based on the *t*-value (Press *et al.*, 1992). Random groupings (or permutations) of the samples were generated with one group containing the same number of samples as the original normal group, and the other containing the same number as the original malignant group. Random groupings were performed 10 000 times, and the mean and various significance levels for the number of genes with *P*-values greater than a threshold level were determined. The hierarchical clustering analysis (Eisen *et al.*, 1998) was carried out using ~1500 genes with significant variation across samples (as defined by a standard deviation (σ) greater than 1000 and a coefficient of variation (σ/μ) greater than 0.3) and an Affymetrix 'present' call in at least half of the experiments. We used the Pearson coefficient of correlation as a measure of linkage among genes and respectively, samples. No transformation of the data was performed prior to clustering.

RT–PCR

The Superscript II system was used for reverse transcription, starting with 5 μg of total RNA and oligo-dT primer in a 20 μl reaction volume. The RT product (0.5 μl) and primers (50 ng) were heated at 94°C for 90 s, followed by 27–30 rounds of amplification (30 s denaturing at 94°C, 30 s annealing at 60°C, 30 s extension at 72°C, followed by a final extension at 72°C for 10 min). The primer sequences are: Wnt5a (forward (F): GCAACAAGGTAATTGCGTGC-CATTCAG, reverse (R): CAGTGATACGCTGCAACA-CCTCTGTG), TGM2 (F: GCTGTGAGGAATGCTCT-GCAG, R: GCAACTAGTAGGTGCTTCACAATGGTG), PAI2 (F: GAACTCAGATCCATTCTGAGAAGC, R: GC-AATTCTGAGGCACACAGCTCATC), OSF2 (F: GTGGT-AGCACCTTCAAAGAAATC, R: CCTGAGAACGACC-TTCCCTTAATCG), PDGFRα: (F: CACTCTCTTCAGA-GGTCTGCGAG, R: CACTCTCTTCAGAGGTCTGCG-AG), *n-chimerin* (F: ATGAGATCTCCAGAACTAGACG, R: GCTAATCATGCAATAGCTTGAG), GAPDH (F: GA-TTCCACCCATGGCAAATTCC, R: CACGTTGGCAGT-GGGGAC), and β-actin (F: TGCGTGACATTAAGGA-GAAG, R: GCTCGTAGCTCTTCTCCA).

Immunoblotting

Frozen tissues were homogenized in a buffer containing 25 mM HEPES, pH 7.5, 150 mM sodium chloride, 12.5 mM EDTA, 1 mM DTT, 1% Triton X-100, 10% glycerol, and 1 mM each of aprotinin, leupeptin and phenylmethylsulfonyl fluoride. Twenty μg of protein in sample buffer were separated on a 7.5% SDS gel, transferred to a nitrocellulose membrane, and blotted with rabbit anti-OSF2 serum (1:3000), rabbit anti-TGM2 antibody (5 μg per ml; Neomarkers, Fremont, CA, USA), or anti-β actin antibody (1:10 000; Sigma, St Louis, MO, USA). A horseradish peroxidase-conjugated anti-rabbit antibody (1:10 000; Transduction Laboratories, Lexington, KY, USA) was used as the secondary and protein bands were visualized by chemiluminescence (Pierce, Rockford, IL, USA). Rabbit anti-OSF2 serum was generated using a bacterially produced 784 aa OSF2 derived from EST clone ID:1091416 (GenBank Accession AA599197) as the immunogen.

IHC

Paraffin-embedded ovarian tissue slides were processed for antigen retrieval by heating in 10 mM sodium citrate, pH 6.0 at 95°C for 25 min. The slides were blocked with 3% goat serum in 25 mM Tris, 150 mM sodium chloride, pH 7.5 for 30 min and then incubated with anti-OSF2 serum (1:1200) for 30 min. Subsequent substrate-chromogen development was carried out using a DAKO En Vision™+System, Peroxidase (DAB) kit (DAKO, Carpinteria, CA, USA), following the manufacturer's instructions. Staining was graded from 0 (no staining) to 3+ (strong staining) by a board certified pathologist (J Rao).

Acknowledgments
We thank C Denny, S Nelson and S Cole for helpful comments, and Z Chen (UCLA Microarray Core and Gene Expression Core) for assistance with the chip hybridization. This work was supported by grants from the United States Army Medical Research and Materiel Command (DAMD 17919503), NCI Training Grant (T32CA09297) (to D Matei), and an Alfred P Sloan Foundation/DOE postdoctoral fellowship (to TG Graeber).

References

Antonyak MA, Singh US, Lee DA, Boehm JE, Combs C, Zgola MM, Page RL and Cerione RA. (2001). *J. Biol. Chem.*, **276**, 33582–33587.

Auersperg N, Maines-Bandiera SL, Dyck HG and Kruk PA. (1994). *Lab. Invest.*, **71**, 510–518.

Bell DA and Scully RE. (1994). *Cancer*, **73**, 1859–1864.

Cadigan KM and Nusse R. (1997). *Genes Dev.*, **11**, 3286–3305.

Cheng JQ, Godwin AK, Bellacosa A, Taguchi T, Franke TF, Hamilton TC, Tsichlis PN and Testa JR. (1992). *Proc. Natl. Acad. Sci. USA*, **89**, 9267–9271.

Dubeau L. (1999). *Gynecol. Oncol.*, **72**, 437–442.

Eisen MB, Spellman PT, Brown PO and Botstein D. (1998). *Proc. Natl. Acad. Sci. USA*, **95**, 14863–14868.

Foster KA, Harrington P, Kerr J, Russell P, DiCioccio RA, Scott IV, Jacobs I, Chenevix-Trench G, Ponder BA and Gayther SA. (1996). *Cancer Res.*, **56**, 3622–3625.

Fraij BM, Birckbichler PJ, Patterson Jr MK, Lee KN and Gonzales RA. (1992). *J. Biol. Chem.*, **267**, 22616–22623.

Golub TR, Slonim DK, Tamayo P, Huard C, Gaasenbeek M, Mesirov JP, Coller H, Loh ML, Downing JR, Caligiuri MA, Bloomfield CD and Lander ES. (1999). *Science*, **286**, 531–537.

Greenlee RT, Murray T, Bolden S and Wingo PA. (2000). *CA Cancer J. Clin.*, **50**, 7–33.

Heid HW, Moll R, Schwetlick I, Rackwitz HR and Keenan TW. (1998). *Cell Tissue Res.*, **294**, 309–321.

Henriksen R, Funa K, Wilander E, Backstrom T, Ridderheim M and Oberg K. (1993). *Cancer Res.*, **53**, 4550–4554.

Horiuchi K, Amizuka N, Takeshita S, Takamatsu H, Katsuura M, Ozawa H, Toyama Y, Bonewald LF and Kudo A. (1999). *J. Bone Miner. Res.*, **14**, 1239–1249.

Hough CD, Sherman-Baust CA, Pizer ES, Montz FJ, Im DD, Rosenshein NB, Cho KR, Riggins GJ and Morin PJ. (2000). *Cancer Res.*, **60**, 6281–6287.

Ishikawa J, Kaisho T, Tomizawa H, Lee BO, Kobune Y, Inazawa J, Oritani K, Itoh M, Ochi T and Ishihara K *et al.* (1995). *Genomics*, **26**, 527–534.

Ismail RS, Baldwin RL, Fang J, Browning D, Karlan BY, Gasson JC and Chang DD. (2000). *Cancer Res.*, **60**, 6744–6749.

Jacobs I and Bast Jr RC. (1989). *Hum. Reprod.*, **4**, 1–12.

Karlan BY, Baldwin RL, Cirisano FD, Mamula PW, Jones J and Lagasse LD. (1995). *Gynecol Oncol.*, **59**, 67–74.

Kozma R, Ahmed S, Best A and Lim L. (1996). *Mol. Cell. Biol.*, **16**, 5069–5080.

Lee TC and Ziff EB. (1999). *J. Biol. Chem.*, **274**, 595–606.

Lejeune S, Huguet EL, Hamby A, Poulsom R and Harris AL. (1995). *Clin. Cancer Res.*, **1**, 215–222.

Link Jr CJ, Kohn E and Reed E. (1996). *Gynecol. Oncol.*, **60**, 347–354.

Mains RE, Berard CA, Denault JB, Zhou A, Johnson RC and Leduc R. (1997). *Biochem. J.*, **321**, 587–593.

Marks JR, Davidoff AM, Kerns BJ, Humphrey PA, Pence JC, Dodge RK, Clarke-Pearson DL, Iglehart JD, Bast Jr RC and Berchuck A. (1991). *Cancer Res.*, **51**, 2979–2984.

Mertens C, Kuhn C and Franke WW. (1996). *J. Cell Biol.*, **135**, 1009–1025.

Mok SC, Wong KK, Chan RK, Lau CC, Tsao SW, Knapp RC and Berkowitz RS. (1994). *Gynecol Oncol.*, **52**, 247–252.

Nanda N, Iismaa SE, Owens WA, Husain A, Mackay F and Graham RM. (2001). *J. Biol. Chem.*, **276**, 20673–20678.

Ono K, Tanaka T, Tsunoda T, Kitahara O, Kihara C, Okamoto A, Ochiai K, Takagi T and Nakamura Y. (2000). *Cancer Res.*, **60**, 5007–5011.

Petricoin EF, Ardekani AM, Hitt BA, Levine PJ, Fusaro VA, Steinberg SM, Mills GB, Simone C, Fishman DA, Kohn EC and Liotta LA. (2002). *Lancet*, **359**, 572–577.

Press WH, Teukolsky SA, Vettering WT and Flannery BP. (1992). *Numerical Recipes for C++*. 2nd edn. Cambridge UK: Cambridge University Press, pp 226–229.

Sasaki H, Auclair D, Fujai I, Kiriyama M, Yamakawa Y, Fuji Y and Chen LB. (2001a). *Cancer*, **92**, 843–848.

Sasaki H, Auclair D, Kaji M, Fukai I, Kiriyama M, Yamakawa Y, Fujii Y and Chen LB. (2001b). *Cancer Lett.*, **172**, 37–42.

Schummer M, Ng WV, Bumgarner RE, Nelson PS, Schummer B, Bednarski DW, Hassell L, Baldwin RL, Karlan BY and Hood L. (1999). *Gene*, **238**, 375–385.

Shayesteh L, Lu Y, Kuo WL, Baldocchi R, Godfrey T, Collins C, Pinkel D, Powell B, Mills GB and Gray JW. (1999). *Nat. Genet.*, **21**, 99–102.

Singh US, Kunar MT, Kao YL and Baker KM. (2001). *EMBO J.*, **20**, 2413–2423.

Slamon DJ, Godolphin W, Jones LA, Holt JA, Wong SG, Keith DE, Levin WJ, Stuart SG, Udove J and Ullrich A *et al.* (1989). *Science*, **244**, 707–712.

Stasko SE and Wagner GF. (2001). *Dev. Dyn.*, **220**, 49–59.

Takahashi H, Behbakht K, McGovern PE, Chiu HC, Couch FJ, Weber BL, Friedman LS, King MC, Furusato M and LiVolsi VA *et al.* (1995). *Cancer Res.*, **55**, 2998–3002.

Takeshita S, Kikuno R, Tezuka K and Amann E. (1993). *Biochem. J.*, **294**, 271–278.

Welsh JB, Zarrinkar PP, Sapinoso LM, Kern SG, Behling CA, Monk BJ, Lockhart DJ, Burger RA and Hampton GM. (2001). *Proc. Natl. Acad. Sci. USA*, **98**, 1176–1181.

Yamaguchi TP, Bradley A, McMahon AP and Jones S. (1999). *Development*, **126**, 1211–1223.

Young RC, Perez CA and Hoskins WJ. (2001). *Cancer: Principles and Practice of Oncology*. DeVita VT, Hellman S and Rosenberg SA (eds). Philadelphia: Lippincott Williams and Wilkins, pp. 1226–1263.

[CANCER RESEARCH 62, 5358–5364, September 15, 2002]

Periostin Secreted by Epithelial Ovarian Carcinoma Is a Ligand for $\alpha_V\beta_3$ and $\alpha_V\beta_5$ Integrins and Promotes Cell Motility[1]

Lindsay Gillan, Daniela Matei, David A. Fishman, C. S. Gerbin, Beth Y. Karlan, and David D. Chang[2]

Department of Medicine [L. G., D. M., C. S. G., D. D. C.], Department of Microbiology, Immunology and Molecular Genetics [D. D. C.], and Department of Obstetrics and Gynecology [B. Y. K.], David Geffen School of Medicine at UCLA, Los Angeles, California 90095, Division of Gynecologic Oncology, Cedars-Sinai Medical Center, Los Angeles, California 90048 [B. Y. K.], and Gynecologic Oncology, Northwestern University, Chicago, Illinois 60611 [D. A. F.]

ABSTRACT

Periostin (PN) is a secreted protein that shares a structural homology to the axon guidance protein fasciclin I in insects. Previously, we reported that PN expression is up-regulated in epithelial ovarian tumors. We further examined the role of PN in ovarian cancer. PN is expressed in several normal tissues but not in normal ovaries and has a tendency for higher expression in fetal tissues. Ovarian cancer cells secrete PN, which can accumulate in malignant ascites of ovarian cancer patients. Purified recombinant PN supports adhesion of ovarian epithelial cells that can be inhibited by monoclonal antibodies against $\alpha_V\beta_3$ or $\alpha_V\beta_5$ integrin, but not by anti-β_1 integrin antibody. Furthermore, $\alpha_V\beta_3$ integrin, but not β_1 integrins, colocalizes to the focal adhesion plaques formed on PN. Cells plated on PN form fewer stress fibers and are more motile compared with those plated on fibronectin. We propose PN functions as a ligand for $\alpha_V\beta_3$ and $\alpha_V\beta_5$ integrins to support adhesion and migration of ovarian epithelial cells.

INTRODUCTION

EOC[3] arises from the epithelial cells covering the surface of the ovaries (1, 2). EOC is a highly malignant disease, usually presenting with widespread i.p. metastasis (3). The i.p. dissemination is believed to be initiated by exfoliation of cancer cells, followed by their adhesion to the mesothelium that covers the peritoneal cavity. Although the precise mode of i.p. spread of EOC is not known, there are several unique features of ovarian epithelium that may facilitate this process. First, the ovarian epithelial cells can adopt a mesenchymal phenotype and lack the tight cell junctions (4), making them prone to exfoliation. Second, the ovarian epithelium is in direct contact with the peritoneal cavity. Once shed from the tumor, cancer cells are free to disseminate throughout the peritoneal cavity, carried by the flow of the peritoneal fluid.

The adhesion of ovarian epithelial cells to the ECM involves both integrin-dependent and independent mechanisms (5–8). Integrins are transmembrane heterodimeric receptors involved in both cell-cell and cell-ECM interactions (9). The functions of integrins are not limited to cell adhesion, but also involve activation of cytosolic signaling cascades to mediate cell proliferation, cell survival, and cell migration (10, 11). Integrin expression is frequently altered in cancer cells (12, 13), which together with the changes in the ECM composition alters the adhesion and motility of cancer calls. Malignant ovarian epithelial cells also secrete their own ECM proteins including fibulin-1, tenascin-c, and VN (7, 14, 15).

PN (formerly called osteoblast-specific factor-2) was originally identified as a 811-amino acid protein secreted by osteoblasts (16). It shares a structural homology to insect fasciclin I and can bind heparin (17) and support adhesion of osteoblasts (18), leading to a hypothesis that it functions to recruit and attach osteoblasts to the periosteum. Previously, we reported that PN mRNA expression is up-regulated in ovarian tumors (19). In addition, two recent reports showed that serum levels of PN are elevated in patients with thymoma (20) and non-small cell lung cancer (21).

We further characterized the expression and function of PN. PN transcripts were expressed in a number of normal organs, with a tendency for higher expression in fetal tissues. IHC analysis using polyclonal anti-PN antisera showed specific staining within the cancer cells in epithelial ovarian tumors. Purified recombinant PN promoted $\alpha_V\beta_3$- and $\alpha_V\beta_5$-dependent cell adhesion and spreading. Interestingly, ovarian epithelial cells spread on PN formed less stress fibers and were more motile, suggesting that PN secreted by the cancer cells may enhance their motility and invasiveness.

MATERIALS AND METHODS

PN cDNA. The full-length PN cDNA (periostin-bm) was derived from the expressed sequence tag clone ID:1091416 (GenBank accession no. AA599197). The coding sequence of this clone consists of 782 amino acids and differs from the published sequence (GenBank accession no. D13666) at the amino acid position 290 (Ile rather than Phe) and 421 (Asp rather than Val).

Anti-PN Antibodies. Rabbit anti-PN antibodies were generated using bacterially expressed NH_2-terminal hexa-histidine-tagged PN as the immunogen. The coding region of PN was cloned into the pQE60 (Qiagen Inc., Valencia, CA) vectors and transformed into bacterial cells (BL21). The bacteria were cultured in LB-amp at 37°C to an early exponential phase of growth ($OD_{600} \approx 0.5$) before the addition of 1 mM isopropyl-1-thio-β-D-galactopyranoside. After and additional 3 h, bacteria were harvested and PN-his proteins were purified under denaturing conditions using Ni-NTA beads (Qiagen Inc.).

Ovarian Epithelial Cells. HOSE and CSOC correspond to epithelial cells derived from the normal ovary and EOC. These primary cultures were prepared as described previously (19, 22) and maintained in MCDB 105:199 (1:1) medium supplemented with 10% FBS, penicillin (100 units/ml), and streptomycin (100 μg/ml). H281-hTERT was derived from HOSE cultures by transducing the catalytic subunit of hTERT (23). CSOC848-hTERT and CSOC272-hTERT/E7 were derived from CSOC culture by transducing hTERT alone or hTERT and the human papilloma virus E7 subunit. These cells have been passaged >70 times and are considered continuous cell lines. Sk-ov-3 human ovarian carcinoma cells were obtained from the American Type Culture Collection (Manassas, VA) and maintained in McCoy's 5A medium supplemented with 10% FBS.

Immunoblot Analysis of PN. When cell growth reached confluency, the culture media was replaced to complete medium without serum and incubated for an additional 4–5 days to obtain conditioned media. Ovarian ascites samples were from women with ovarian cancer (FIGO stage III or IV) undergoing debulking procedures. Nonovarian ascites were from patients undergoing therapeutic paracentesis for clinically indicated reasons. The conditioned media and ascitic fluids were centrifuged at 10,000 × *g* for 15 min and fractionated on a 6% SDS-polyacrylamide gel under reducing condition. The proteins were transferred to a nitrocellulose membrane and blotted with

Received 4/22/02; accepted 7/17/02.

The costs of publication of this article were defrayed in part by the payment of page charges. This article must therefore be hereby marked *advertisement* in accordance with 18 U.S.C. Section 1734 solely to indicate this fact.

[1] Supported by grants from the United States Army Medical Research and Materiel Command (DAMD17919503) and the National Cancer Institute (Training Grant T32CA09297; to D. M.).

[2] To whom requests for reprints should be addressed, at UCLA School of Medicine, Division of Heme-Onc, Factor 11-934, 10833 Le Conte Avenue, Los Angeles, CA 90095-1678. Phone: (310) 825-9759; Fax: (310) 825-6192; E-mail: ddchang@mednet.ucla.edu.

[3] The abbreviations used are: EOC, epithelial ovarian cancer; ECM, extracellular matrix; PN, periostin; FN, fibronectin; VN, vitronectin; IHC, immunuhistochemistry; HOSE, human ovarian surface epithelia; CSOC, Cedars Sinai ovarian carcinoma; hTERT, human telomerase; FBS, fetal bovine serum; mAb, monoclonal antibody.

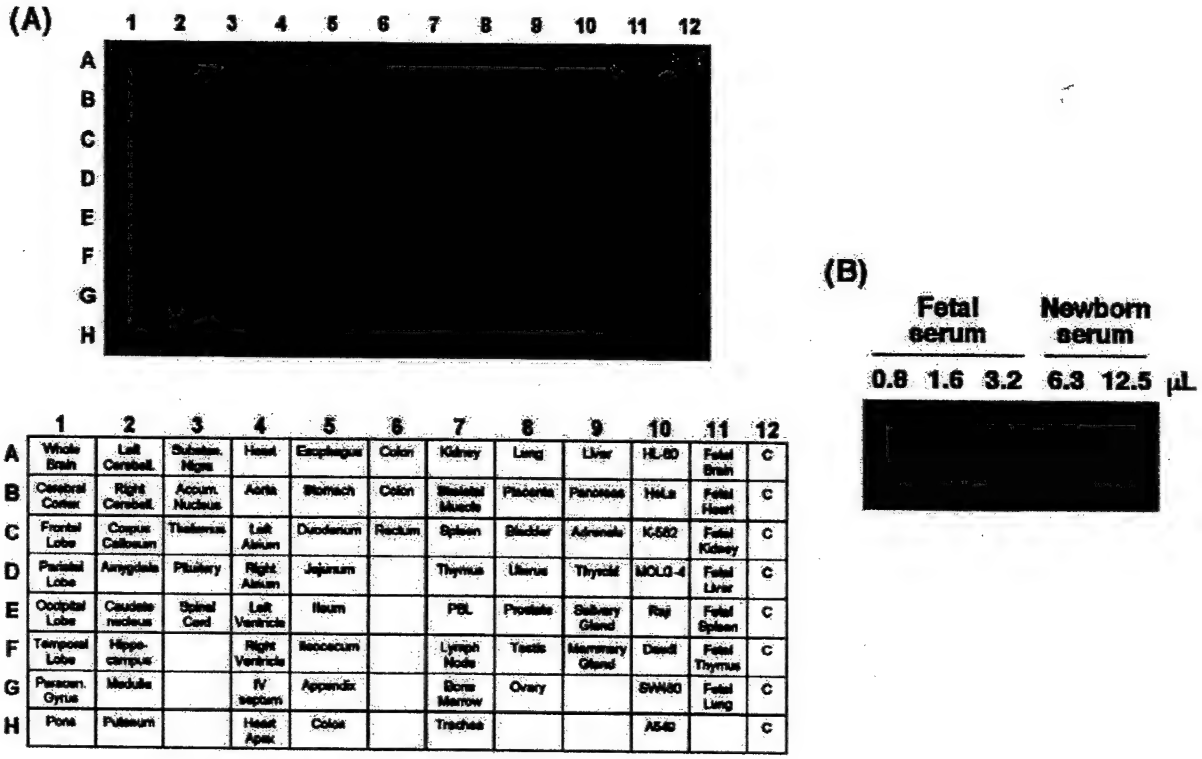

Fig. 1. Oncofetal pattern of PN expression. *A*, a multiple tissue expression array (BD Biosciences Clontech, Palo Alto, CA) that contains mRNA from 76 human tissues and cancer cell lines (*bottom*) arrayed on a nylon membrane was hybridized with ^{32}P-labeled PN cDNA probe (*top*) to determine the tissue distribution of periostin expression. *B*, indicated amounts of FBS (Gemini Bio-Products, Woodland Hills, CA) and newborn calf serum (Gemini Bio-Products) were immunoblotted with anti-PN antibodies.

anti-PN antibodies (1:5,000). After incubation with a horseradish peroxidase-conjugated antirabbit antibody (1:10,000; Transduction Laboratories, Lexington, KY), protein bands were visualized by chemiluminescence (Pierce Chemical Co., Rockford, IL).

IHC. Paraffin-embedded ovarian tissue slides were processed for antigen retrieval by heating in 10 mM sodium citrate (pH 6.0) at 95°C for 25 min. The slides were blocked with 3% goat serum in 25 mM Tris-HCl, 150 mM NaCl (pH 7.5) for 30 min and then incubated with anti-PN antibodies (1:1200) for 30 min. Subsequent substrate-chromogen development was carried out using a DAKO EnVision+ System, Peroxidase (DAB) kit (DAKO, Carpinteria, CA).

Preparation of Recombinant PN from Sf-9 Cells. A COOH-terminal hexa-histidine-tagged PN (PN-his) was expressed in the insect Sf-9 cells using the Bac-to-Bac Baculovirus Expression System (Invitrogen Corp., Carlsbad, CA). Briefly, a hexa-histidine tag was added to the COOH terminus of the PN cDNA using PCR, and the resulting fusion construct was cloned into the pFastBac1 plasmid. The isolated recombinant plasmid was transformed into *Escherichia coli* DH10BAC cells harboring a baculovirus shuttle vector, and white colonies representing the clones that have undergone transposition were isolated. High molecular weight DNA was prepared from the isolated clones and used to transfect Sf-9 cells. The recombinant baculovirus was prepared as conditioned culture media and used to infect 2×10^9 Sf-9 cells at a multiplicity of infection of 5. PN-his was purified from 1000 ml of conditioned medium obtained 72 h after the infection. Briefly, the conditioned medium was adjusted to pH 8 with 1 M Tris and loaded onto a 10-ml heparin-Sepharose column (Amersham Biosciences, Piscataway, NJ) equilibrated with wash buffer [0.1 M NaCl in 20 mM Tris-HCl (pH 8)]. The column was washed with 10× bed volumes of wash buffer, and the bound proteins were eluted with 1 M NaCl in 20 mM Tris-HCl (pH 8). PN-his protein in the pooled fractions was bound to Ni-NTA beads (Qiagen Inc.). After washing the Ni-NTA beads extensively in a buffer containing 20 mM Tris-HCl (pH 8), 500 mM KCl, 20 mM imidazole, and 10% (v/v) glycerol, PN-his protein was eluted in a buffer containing 20 mM Tris-HCl (pH 8), 100 mM KCl, 100 mM imidazole, and 10% (v/v) glycerol.

Solid Phase Binding Assay. Exponentially growing ovarian epithelial cells were harvested by treatment with 0.05% trypsin/0.02% EDTA and suspended in serum-free media supplemented with soybean trypsin inhibitor (0.5 mg/ml). Fifty thousand cells were added to the 96-well plates that have been coated with PN (0.5–10 μg/ml), FN (0.5–10 μg/ml; Roche Diagnostic Corp., Indianapolis, IN), or BSA (1% w/v). After a 1-h incubation at 37°C, the wells were washed three times with Tris-buffered saline, fixed with 3.7% (v/v) formaldehyde in Tris-buffered saline for 30 min, and stained with 1% (w/v) toluidine blue overnight. After washing with distilled water until no trace of free dye was visible, the cells were lysed in 2% (w/v) SDS for 10 min. The absorbance (600 nm) of toluidine blue was measured and converted into cell number, using a standard curve generated from cells bound to poly-L-lysine (1 mg/ml)-coated wells. To demonstrate the specificity of cell binding to PN, the coated wells were preincubated with anti-PN antibodies (1:25 and 1:100) for 30 min, before carrying out the adhesion assay. Inhibitory anti-integrin mAbs LM609 (anti-$\alpha_v\beta_3$; Chemicon Inc., Temecula, CA) and PIF6 (anti-$\alpha_v\beta_5$; Chemicon Inc.) were used at 10 μg/ml. The mAb P4C10 (anti-β_1; Invitrogen Corp.) was used at 1:100 dilution.

***In Situ* Immunofluorescence.** Cells in serum-free growth media [MCDB 105:M199 (1:1) supplemented with 1% BSA] were plated on FN-coated (10 μg/ml), PN-coated (10 μg/ml), or VN-coated (5 μg/ml; Promega Corp., Madison, WI) glass coverslips. After 5 h, cells were fixed with 3.7% formaldehyde in PBS for 10 min and permeabilized with 0.5% Triton X-100 for 5 min. Focal adhesions were visualized by staining paxillin with anti-paxillin antibody (BD Transduction Laboratories, San Diego, CA). Integrin staining was carried out the mAb TS2/16 (anti-β_1; American Type Culture Collection), LM609 (Chemicon Inc.), or PIF6 (Chemicon Inc.) for 1 h before fixation. Cy-3-conjugated goat antimouse IgG (Jackson ImmunoResearch Laboratories, West Grove, PA) was used as the secondary antibody. Actin filaments were stained with rhodamine-conjugated phalloidin (Molecular Probes Inc., Eugene, OR).

Time-Lapse Migration Microscopy. CSOC cells were plated on Delta-T glass dishes (0.5 mm; Bioptechs Inc., Butler, PA) that have been coated with PN or FN at 10 μg/ml or VN at 5 μg/ml. One and a half hours after plating the cells, the medium was refreshed and cell migration was monitored from images captured at 20-min interval from a Nikon Diaphot microscope equipped with

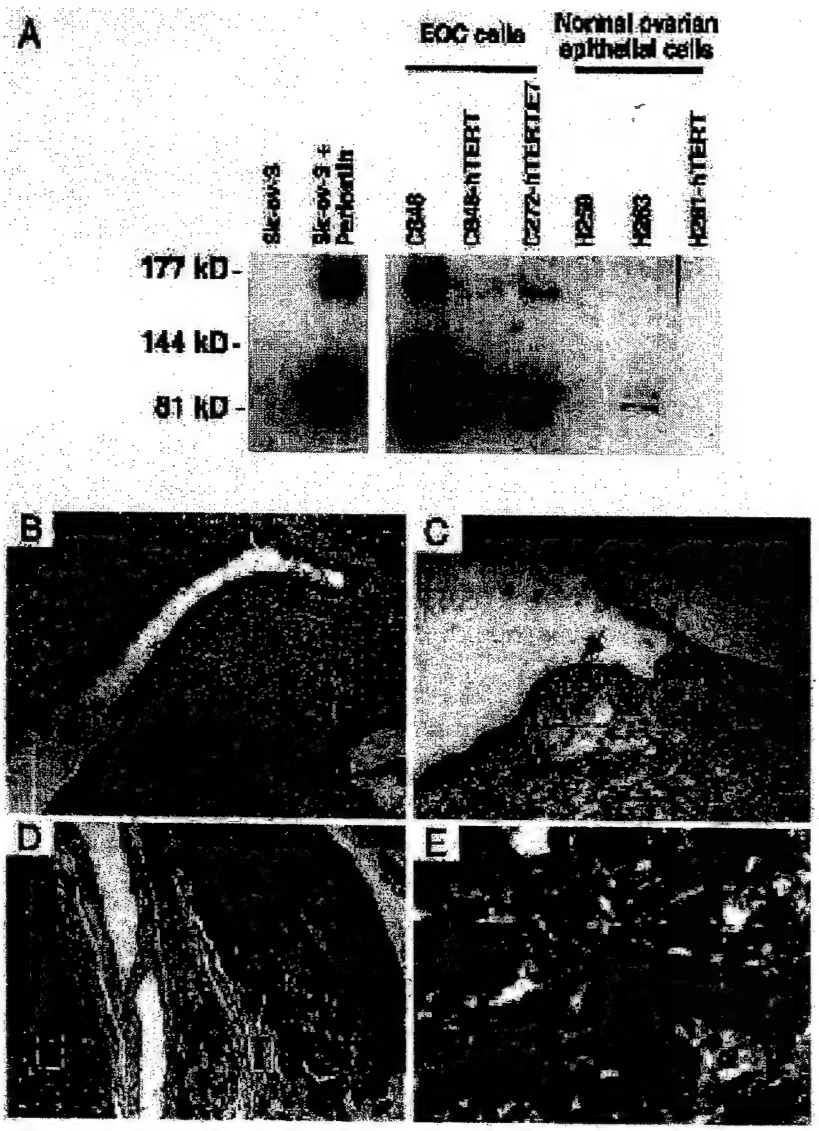

Fig. 2. PN is produced by EOC cells. *A*, cells were grown to confluency in complete growth media, rinsed to remove any traces of serum, and cultured for 96–120 h in growth media in the absence of serum. The conditioned media (10 μl) were immunoblotted with anti-PN antibodies. Sk-ov-3 cells transfected with the PN cDNA is shown for comparison. *C848*, EOC-derived primary epithelial culture; *C848-hTERT*, EOC-derived epithelial cell line expressing hTERT; *C272-hTERT/E7*, EOC-derived epithelial cell line expressing hTERT and the HPV16 E7 protein; *H259* and *H263*, primary epithelial cultures derived from normal ovaries; *H282-hTERT*, normal ovarian epithelial cell line expressing hTERT. *B–E*, IHC staining for PN in paraffin-embedded slides of normal ovaries (*B* and *C*) and EOC (*D* and *E*) are shown. The tissue shown in *D* contains both tumor (*T*) and adjacent normal ovarian tissue (*N*). The *arrows* in *B* and *C* indicate the surface epithelial cell layer.

a digital camera. The positions of the nuclei (n = 39 for FN; n = 31 for PN; n = 42 for VN) were tracked to measure cell movement. Cell velocity was calculated in micrometers per 8 h using the Image-Pro software (Media Cybernetics, Silver Springs, MD). Cell migration was carried out under serum-free conditions.

RESULTS

Tissue Distribution of PN Expression. PN was expressed in a wide range of normal adult tissues, notably in the aorta, stomach, lower gastrointestinal tract, placenta, uterus, and breast (Fig. 1*A*). Expression of PN in the normal ovaries was negligible. Interestingly, the expression of PN was high in the majority of fetal tissue. This fetal pattern of expression was also suggested when the circulating level of PN in bovine serum was estimated. In immunoblot analysis, a strong ~90 kDa band corresponding to PN can be readily detected from 0.8 μl of FCS (Fig. 1*B*). We were unable to detect a specific signal for PN in up to 12.5 μl of newborn calf (Fig. 1*B*).

Ovarian Cancer Cells Secrete PN. Anti-PN antisera detect a family of closely migrating proteins of ~90 kDa in the conditioned media of cultured epithelial cells derived from EOC (Fig. 2*A*). PN was either absent or low in the conditioned media of the normal ovarian epithelial cells. PN undergoes alternative splicing (18), which accounts for the appearance of multiple bands of ~90 kDa size. The immunoblot analysis also revealed an additional higher molecular weight band migrating ~170 kDa. This form is also seen in the conditioned media of Sk-ov-3 cells that have been transfected with the PN cDNA and is likely to represent a covalently linked multimer rather than an alternatively spliced isoform.

We next examined the expression of PN in ovarian tumor by IHC. In the normal ovary, PN expression was negligible in the stroma or the surface epithelia (Fig. 2, *B* and *C*). Anti-PN antisera (1:1200 dilution) stained tumor nodule, but not the adjacent normal ovarian tissue (Fig. 2*D*). In another EOC sample, intense staining could be seen in the carcinoma cells (Fig. 2*E*). Staining with preimmune sera in the same tumor samples was negligible, even at a 3-fold higher concentration (1:400 dilution; data not shown).

PN Accumulates in the Ovarian Ascites. EOC often disseminates into the peritoneal cavity as tumor implants and creates large volumes of ascites. Immunoblot analysis revealed the presence of PN in 20 of the 21 ascites from ovarian cancer patients (Fig. 3*A*). The concentra-

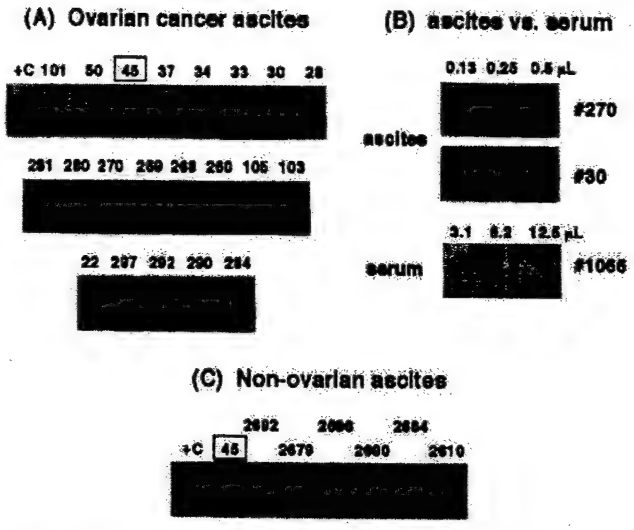

Fig. 3. PN accumulates in ascites of women with ovarian cancer. *A*, equal volumes of malignant ascites from patients with ovarian cancer were immunoblotted with anti-PN antibodies. The conditioned media of the C272-hTERT/E7 cell line was used as the positive control. *B*, indicated volumes of ascites (270 and 30) and serum from one patient (1066) were immunoblotted with anti-PN antisera. *C*, equal volumes of ascites from patients with pancreatic cancer (2692), leiomyoma (2679), uterine sarcoma (2686), multiple myeloma (2690), cirrhosis (2664), and breast cancer (2610) were immunoblotted with anti-PN antisera. The conditioned media of the C272-hTERT/E7 cell line was used as the positive control. For comparison, ascites from an ovarian cancer patient (45) is included.

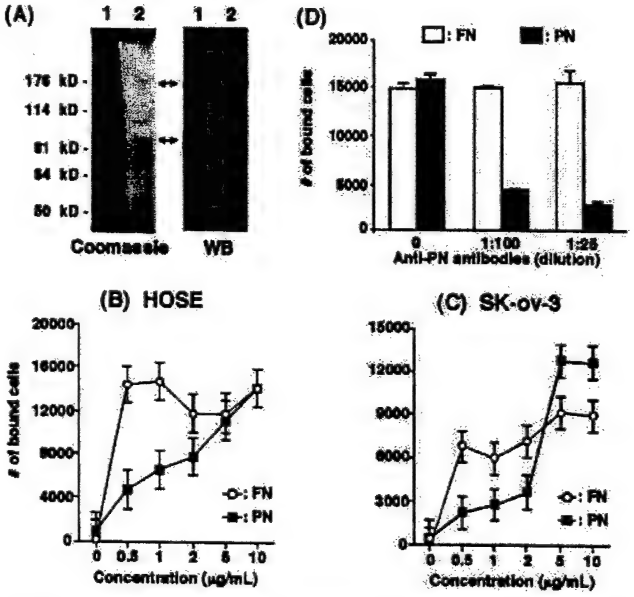

Fig. 4. Recombinant PN supports cell adhesion. *A*, Ni-NTA column-purified recombinant PN-his protein produced in insect cells (*Lane 1*) and bacterial cells (*Lane 2*) were fractionated by SDS-PAGE and stained with Coomassie (*left*) or immunoblotted with anti-PN antibodies (*right*). *B* and *C*, primary human ovarian epithelial cells (HOSE) and Sk-ov-3 were added to a 96-well plate (15,000/well) that had been coated with 0.5–10 µg/ml of PN (■) or FN (○) and incubated at 37°C for 1 h. *D*, Sk-ov-3 cells were adhered to a 96-well plate coated with 10 µg/ml of PN or FN in the presence of anti-PN antibodies. The dilutions of anti-PN antibodies are indicated. Cell adhesion was carried out under a serum-free condition in McCoy's 5A. Bound cells were enumerated from dye uptake (see "Materials and Methods").

tion of PN in ascites was variable but estimated at ~1 µg/ml (our unpublished results). In a semiquantitative immunoblot analysis, the concentrations of PN in the ascites of patients 270 and 30 were >100-fold higher than that in serum (Fig. 3*B*). PN was also in the ascites of a breast cancer patient (2610), but was absent or low in ascites from nonovarian cancer patients (Fig. 3*C*).

Recombinant PN Supports the Adhesion of Ovarian Epithelial Cells. Baculovirus-produced recombinant PN migrated as a ~90 kDa protein, similar to the endogenous protein (Fig. 4*A*). The Ni-NTA column purified PN fraction contained additional protein bands, but was free of FN or VN (our unpublished results). PN-coated surfaces supported the attachment of HOSE and Sk-ov-3 in a concentration-dependent manner (Fig. 4, *B* and *C*). At a coating concentration of 5 µg/ml, PN supported cell adhesion equivalent to FN. Anti-PN antibodies specifically inhibited the adhesion of Sk-ov-3 cells to PN, reducing cell adhesion by >82% at 1:25 dilution (Fig. 4*D*). Anti-PN antibodies did not affect cell adhesion to FN.

The adhesion of Sk-ov-3 cells to PN-coated surface required divalent cation (our unpublished results). The addition of manganese, which can increase the ligand-binding affinity of some integrins, including $\alpha_V\beta_3$ (24), further enhanced adhesion of Sk-ov-3 cells to PN nearly 2-fold (Fig. 5*A*). The effect on manganese on the adhesion of Sk-ov3 cells to FN was less dramatic. Sk-ov-3 cells express the β_1, $\alpha_V\beta_3$, and $\alpha_V\beta_5$ integrins (Fig. 5*B*). The attachment of Sk-ov-3 cells to a PN-coated plate was inhibited by anti-$\alpha_V\beta_3$ (LM 609; $P < 0.001$) or anti-$\alpha_V\beta_5$ mAb (PIF6; $P < 0.001$), and further inhibited by the addition of both antibodies (Fig. 5*C*). Conversely, while the function blocking mAb to β_1 integrins (P4C10) inhibited the attachment of Sk-ov-3 cells to FN ($P < 0.001$; Fig. 5*D*), it did not affect the attachment of Sk-ov-3 cells to PN. The adhesion of Sk-ov-3 cells to FN was partially inhibited by mAb PIF6 ($P = 0.253$).

Ovarian Epithelial Cells Display Motile Phenotype When Spread on PN. On FN, ovarian epithelial cells form well-defined focal adhesion plaques throughout the cell body (Fig. 6*A*). Dense stress fibers emanating from the focal adhesion plaques can be visu-

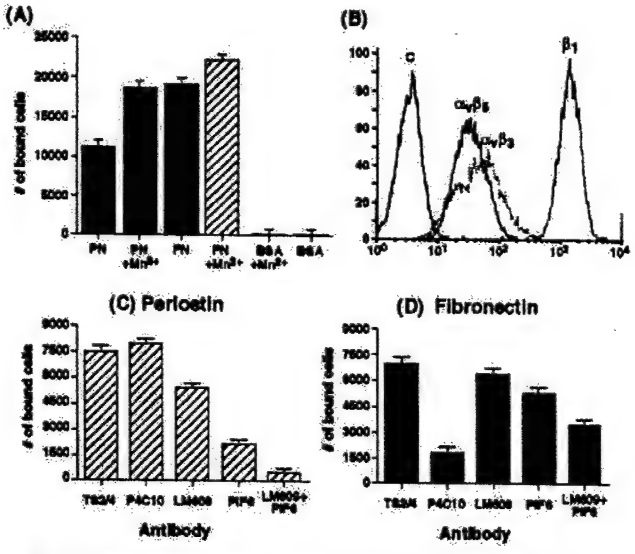

Fig. 5. PN adhesion is α_V integrin dependent. *A*, Sk-ov-3 cells (25,000) were added to a 96-well plate that had been coated with PN (10 µg/ml), FN (10 µg/ml), or BSA (1% v/v). Cell adhesion was carried out under a serum-free condition in McCoy's 5A (contains 0.8 mM Mg^{2+}). When indicated, $MnCl_2$ was added to 1 mM. After 1 h at 37°C, bound cells were enumerated from dye uptake. *B*, surface expression of β_1 and α_V integrins were analyzed by fluorescence-activated cell sorting. Sk-ov-3 cells were incubated with mAb against β_1-integrin (P4C10), $\alpha_V\beta_3$ (LM609), $\alpha_V\beta_5$ (PIF6), or $\alpha_L\beta_2$ (TS 2/4) for 30 min at 4°C, followed by FTIC-labeled goat antimouse IgG. Leukocyte integrin $\alpha_L\beta_2$ is not expressed in nonhematopoeitic cells, and the staining with TS2/4 mAb served as the control. *C* and *D*, Sk-ov-3 cells were incubated with P4C10, LM609, PIF6, or TS2/4 mAb before adding to a 96-well plate (10,000/well) that had been coated with PN or FN at 10 µg/ml. Cell adhesion was carried out in the absence of serum. After 1 h at 37°C, bound cells were enumerated from dye uptake.

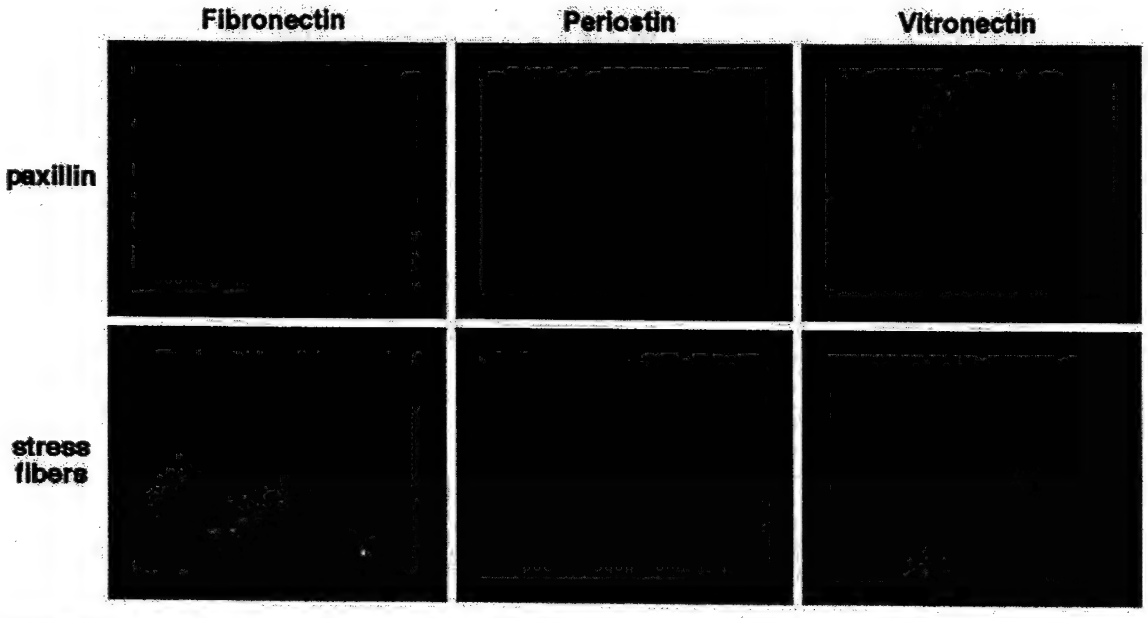

Fig. 6. Cells plated on PN have a motile phenotype. C848-hTERT cells were cultured without serum on glass coverslips that have been coated with FN (*A* and *D*), PN (*B* and *E*), or VN (*C* and *F*). After 5 h at 37°C, the cells were fixed and stained with anti-paxillin (*A–C*) or rhodamine-conjugated phalloidin (*D–F*).

alized in these cells with rhodamine-conjugated phalloidin (Fig. 6*D*). On PN, ovarian epithelial cells formed less stress fibers and focal adhesion plaques. In addition, the focal adhesion plaques were distributed mainly at the forward edge of the cell (Fig. 6*B*). This distribution of the focal adhesion plaques to the forward edge was unique to the cells spread on PN and was not seen in the cells spread on VN which, similar to PN, mediates $\alpha_V\beta_3$- or $\alpha_V\beta_5$-dependent cell spreading (Fig. 6*C*).

The type of integrins localizing to the focal adhesion plaques was also influenced by the composition of ECM. When cells were seeded onto substrates coated with FN in the absence of serum, β_1 integrins were localized to punctated regions throughout the cell body, similar to the localization of the focal adhesion protein paxillin (Fig. 7*A*). Under these conditions, $\alpha_V\beta_3$ integrins were distributed diffusely and could not be localized to the focal adhesion plaques (Fig. 7*D*). On a PN-coated surface, an entirely different pattern emerged, where $\alpha_V\beta_3$ integrins were found in a punctated pattern at the periphery of plasma membrane, similar to the distribution of focal adhesion protein paxillin, whereas the distribution of β_1 integrins were diffuse (Fig. 7, *B* and *E*). On VN, both β_1 and $\alpha_V\beta_3$ integrins localized to the focal adhesion plaques (Fig. 7, *C* and *F*).

PN Enhances Cell Motility. When ovarian epithelial cells were plated on a PN-coated surface, they frequently adopted a fan shape with a definable forward and trailing edge (see Figs. 6 and 7). This

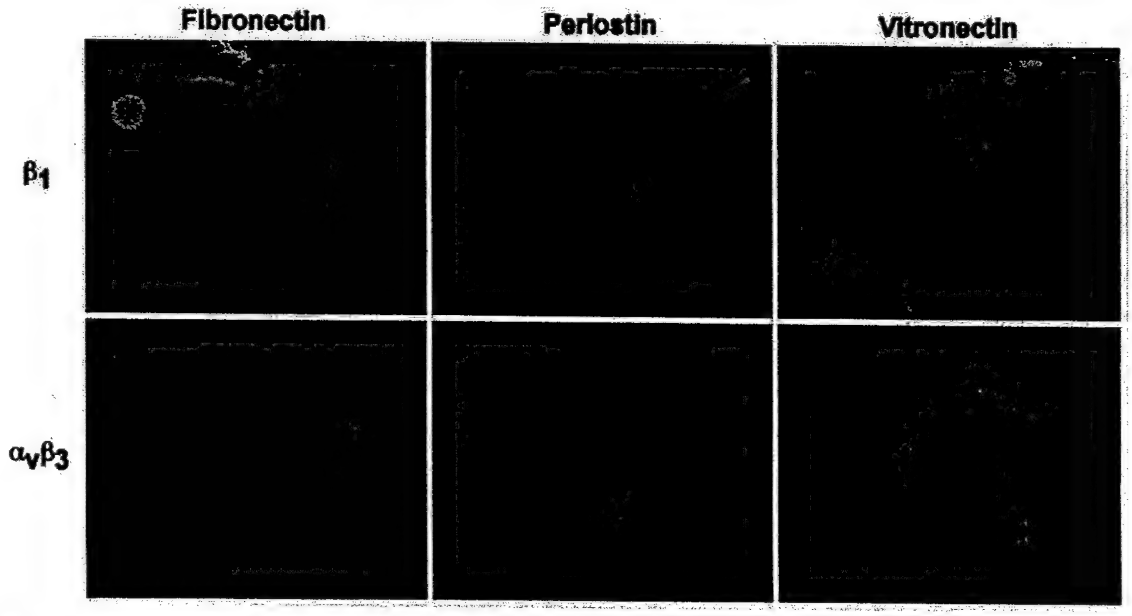

Fig. 7. PN directs $\alpha_V\beta_3$ integrins to focal adhesion plaques. C848-hTERT cells were cultured without serum on glass coverslips coated with FN (*A* and *D*), PN (*B* and *E*), or VN (*C* and *F*). After 4 h, cells were stained with anti-β_1-integrin (*A–C*) or $\alpha_V\beta_3$ integrin (*D–F*) antibodies for 1 h and then were fixed and incubated with goat Cy-3 conjugated antimouse IgG.

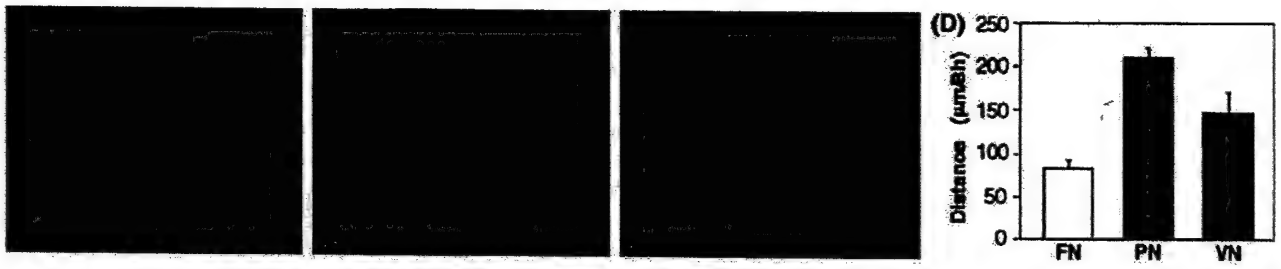

Fig. 8. PN enhances cell motility of ovarian epithelial cells. C848-hTERT cells were plated on (*A*) FN-coated (10 μg/ml), (*B*) PN-coated (10 μg/ml), or (*C*) VN-coated (5 μg/ml) Delta-T dishes, and cell migration was monitored with a time-lapse photography over an 8-h period. Cell movements were traced from digital images that have been captured at a 20-min interval (*A–C*) to obtain cell velocity (*D*; see "Materials and Methods").

finding and the reduced number of stress fibers in these cells suggested that cells might be more motile on PN. We monitored the movement of cells with time-lapse microscopy (Fig. 8). On a PN-coated surface, cell motility was significantly higher (210 ± 13 μm/8 h) compared with a FN-coated surface (80 ± 10 μm/8 h; $P < 0.001$). The motility of ovarian cells on a VN-coated surface was 148 ± 22 μm/8 h ($P < 0.05$), better than on FN, but not as efficient as on PN.

DISCUSSION

PN is structurally similar to fasciclin I, an insect neuronal adhesion protein (25, 26), and is composed of four internal repeat domains of about 120–160 amino acids. The only other fasciclin domain protein in mammals is βig-h3, which was identified as a transforming growth factor-β-induced gene in human adenocarcinoma cells (27). The fasciclin domain-containing proteins function as adhesion molecules. Fasciclin I can mediate homotypic cell adhesion (28), whereas purified recombinant βig-h3 supports $\alpha_1\beta_1$ integrin-dependent adhesion of chondrocytes and fibroblasts (29). βig-h3 contains an RGD motif near the COOH terminus, but this integrin recognition site can be deleted without affecting cell adhesion (29). PN does not contain an RGD motif.

The COOH-terminal region of PN, outside the four fasciclin domains, undergoes alternative splicing to generate multiple PN isoforms. The immunoblot also revealed a larger form of PN migrating at ~170 kDa that could not be accounted for by alternative splicing. ECM proteins, notably FN and VN, form disulfide-bound dimer or multimer (30, 31). The ~170-kDa form likely is a multimer (probably a dimer) of PN. This form is stable under reducing condition, indicating that it is not disulfide bound. The functions of different isoforms of PN need further investigation.

PN is overexpressed in a number of human tumors. To date, our group has examined PN expression in over 40 ovarian tissues and found that up to 30% of tumors are strongly positive for PN staining, with another 46% showing weak to moderate staining (our unpublished results). Besides EOC, PN expression is up-regulated in glioblastoma (32), non-small cell lung cancers (33), and melanoma (our unpublished results), and the serum levels of PN are elevated in patients with thymoma (21) and lung cancer (20). PN is expressed in most normal tissues, except in the brain, ovary, and hematopoeitic organs. The broad tissue distribution of PN expression suggests that it has a more generalized function that is not limited to bone formation. PN expression tends to be higher in fetal tissues, and the serum level of PN in fetal calf is significantly higher than that in newborn calf. This preferential expression in fetal tissue, together with its up-regulation in tumors, suggests PN has an "oncofetal" pattern of expression, similar to VN and the ED-B isoform of FN (34–36).

We have not been able to detect any significant change in the serum levels of PN in women with ovarian cancer compared with the normal controls (our unpublished results). However, the majority of ascites from ovarian cancer patients contains high levels of PN. We have shown that ovarian epithelial cancer cells secrete PN, which most likely accounts for the accumulation of PN in the ascites. Alternatively, carcinomatosis and the generalized inflammatory process associated with it may up-regulate PN expression from the mesothelial cells lining the peritoneal cavity. One contributing factor for the development of ascites is the increased permeability of vessels (37). A passive transfer of PN in circulation to the peritoneal cavity, however, is viewed unlikely because the level of PN in ascites can exceed 100 times that in serum or plasma.

Purified PN supports integrin-dependent adhesion and spreading of ovarian epithelial cells. First, the adhesion requires divalent cation and can be stimulated by Mn^{2+}, which increases the ligand-binding activity of several integrins (38). Second, the mAbs to $\alpha_v\beta_3$ or $\alpha_v\beta_5$ integrin suppressed the adhesion individually, and completely abolished the adhesion when combined. Third, when cells were allowed to spread on PN, $\alpha_v\beta_3$ integrin localized to the focal adhesion plaques, whereas the β_1 integrins were distributed diffusely throughout the cell. On FN, an opposite staining pattern emerged with the β_1 integrins localizing to the focal adhesion plaques and $\alpha_v\beta_3$ integrin being distributed diffusely. The dependence of cell surface distribution of integrins on ECM composition has been reported previously (39, 40). Altogether, these findings indicate that $\alpha_v\beta_3$ and $\alpha_v\beta_5$ integrins play a pivotal role in the PN-induced cell adhesion and spreading.

PN also confers more motile features to the adherent cells. Compared with cells spread on FN or VN, cells spread on PN display a recognizable front and trailing edge. In these cells the focal adhesion plaques are localized to the front of the cell, rather than being distributed throughout the ventral surface, as seen in cells spread on FN or VN. In addition, cells form fewer stress fibers on PN. The formation of focal adhesion plaques and organized actin stress fibers requires tension (41), which in part depends on the rigidity of the substrate (42). One possible explanation for our finding is that PN, compared with FN or VN, is a more pliable substrate. Alternatively, PN, through clustering α_v integrins, may trigger a different set of signals that favors motile features. The different morphological features of cells spread on FN *versus* PN correlate with cell motility. When cell motility was followed by time-lapse microscopy, cells were more motile on PN than FN.

Our finding that ovarian epithelial carcinoma cells secrete PN, which then accumulates in ascites, suggests that this oncofetal protein may play a role in the pathogenesis of EOC. PN, through promoting $\alpha_v\beta_3$ or $\alpha_v\beta_5$ integrin-dependent adhesion and migration of ovarian epithelial cells could promote i.p. dissemination. Another common feature of EOC is large volume ascites, stemming from neovascularization and vascular endothelial growth factor-induced increase in vascular permeability. One factor believed to be important in the

recruitment and proliferation of endothelial cells is the production of VN at the site of tumor. Like VN, PN could potentially stimulate neovascularization by serving as an "onco-matrix" protein to support $\alpha_V\beta_3$ or $\alpha_V\beta_3$ integrin dependent migration of endothelial cells.

ACKNOWLEDGMENTS

We thank J. Lao (University of California, Los Angeles, CA) for the gift of nonovarian ascites samples. We also thank D. Maron for the construction of the bacterial his-PN expression construct and H. Kim for preparing the bacterial his-PN recombinant protein.

REFERENCES

1. Auersperg, N., Edelson, M. I., Mok, S. C., Johnson, S. W., and Hamilton, T. C. The biology of ovarian cancer. Semin. Oncol., *25:* 281–304, 1998.
2. Young, R. C., Perez, C. A., and Hoskins, W. J. Cancer of the ovary. *In:* V. T. DeVita, S. Hellman, and S. A. Rosenberg (eds.), Cancer: Principles and Practice of Oncology, pp. 1226–1263. Philadelphia: Lippincott Williams & Wilkins, 2001.
3. Perez, R. P., Godwin, A. K., Hamilton, T. C., and Ozols, R. F. Ovarian cancer biology. Semin. Oncol., *18:* 186–204, 1991.
4. Auersperg, N., Pan, J., Grove, B. D., Peterson, T., Fisher, J., Maines-Bandiera, S., Somasiri, A., and Roskelley, C. D. E-cadherin induces mesenchymal-to-epithelial transition in human ovarian surface epithelium. Proc. Natl. Acad. Sci. USA, *96:* 6249–6254, 1999.
5. Cannistra, S. A., Kansas, G. S., Niloff, J., DeFranzo, B., Kim, Y., and Ottensmeier, C. Binding of ovarian cancer cells to peritoneal mesothelium in vitro is partly mediated by CD44H. Cancer Res., *53:* 3830–3838, 1993.
6. Strobel, T., and Cannistra, S. A. β1-Integrins partly mediate binding of ovarian cancer cells to peritoneal mesothelium in vitro. Gynecol. Oncol., *73:* 362–367, 1999.
7. Carreiras, F., Cruet, S., Staedel, C., Sichel, F., and Gauduchon, P. Human ovarian adenocarcinoma cells synthesize vitronectin and use it to organize their adhesion. Gynecol. Oncol., *72:* 312–322, 1999.
8. Cruet, S., Salamanca, C., Mitchell, G. W., and Auersperg, N. $\alpha v\beta 3$ and vitronectin expression by normal ovarian surface epithelial cells: role in cell adhesion and cell proliferation. Gynecol. Oncol., *75:* 254–260, 1999.
9. Hynes, R. O. Integrins: versatility, modulation, and signaling in cell adhesion. Cell, *69:* 11–25, 1992.
10. Schwartz, M. A., Schaller, M. D., and Ginsberg, M. H. Integrins: emerging paradigms of signal transduction. Annu. Rev. Cell Dev. Biol., *11:* 549–599, 1995.
11. Lafrenie, R. M., and Yamada, K. M. Integrin-dependent signal transduction. J. Cell. Biochem., *61:* 543–553, 1996.
12. Varner, J. A., and Cheresh, D. A. Integrins and cancer. Curr. Opin. Cell Biol., *8:* 724–730, 1996.
13. Mizejewski, G. J. Role of integrins in cancer: survey of expression patterns. Proc. Soc. Exp. Biol. Med., *222:* 124–138, 1999.
14. Clinton, G. M., Rougeot, C., Derancourt, J., Roger, P., Defrenne, A., Godyna, S., Argraves, W. S., and Rochefort, H. Estrogens increase the expression of fibulin-1, an extracellular matrix protein secreted by human ovarian cancer cells. Proc. Natl. Acad. Sci. USA, *93:* 316–320, 1996.
15. Wilson, K. E., Bartlett, J. M., Miller, E. P., Smyth, J. F., Mullen, P., Miller, W. R., and Langdon, S. P. Regulation and function of the extracellular matrix protein tenascin-C in ovarian cancer cell lines. Br. J. Cancer, *80:* 685–692, 1999.
16. Takeshita, S., Kikuno, R., Tezuka, K., and Amann, E. Osteoblast-specific factor 2: cloning of a putative bone adhesion protein with homology with the insect protein fasciclin I. Biochem. J., *294:* 271–278, 1993.
17. Sugiura, T., Takamatsu, H., Kudo, A., and Amann, E. Expression and characterization of murine osteoblast-specific factor 2 (OSF-2) in a baculovirus expression system. Protein Expr. Purif., *6:* 305–311, 1995.
18. Horiuchi, K., Amizuka, N., Takeshita, S., Takamatsu, H., Katsuura, M., Ozawa, H., Toyama, Y., Bonewald, L. F., and Kudo, A. Identification and characterization of a novel protein, periostin, with restricted expression to periosteum and periodontal ligament and increased expression by transforming growth factor β. J. Bone Miner. Res., *14:* 1239–1249, 1999.
19. Ismail, R. S., Baldwin, R. L., Fang, J., Browning, D., Karlan, B. Y., Gasson, J. C., and Chang, D. D. Differential gene expression between normal and tumor-derived ovarian epithelial cells. Cancer Res., *60:* 6744–6749, 2000.
20. Sasaki, H., Auclair, D., Kaji, M., Fukai, I., Kiriyama, M., Yamakawa, Y., Fujii, Y., and Chen, L. B. Serum level of the periostin, a homologue of an insect cell adhesion molecule, in thymoma patients. Cancer Lett., *172:* 37–42, 2001.
21. Sasaki, H., Auclair, D., Fukai, I., Kiriyama, M., Yamakawa, Y., Fujii, Y., and Chen, L. B. Serum level of the periostin, a homologue of an insect cell adhesion molecule, as a prognostic marker in non-small cell lung carcinomas. Cancer (Phila.), *92:* 843–848, 2001.
22. Karlan, B. Y., Baldwin, R. L., Cirisano, F. D., Mamula, P. W., Jones, J., and Lagasse, L. D. Secreted ovarian stromal substance inhibits ovarian epithelial cell proliferation. Gynecol. Oncol., *59:* 67–74, 1995.
23. Meyerson, M., Counter, C. M., Eaton, E. N., Ellisen, L. W., Steiner, P., Caddle, S. D., Ziaugra, L., Beijersbergen, R. L., Davidoff, M. J., Liu, Q., Bacchetti, S., Haber, D. A., and Weinberg, R. A. hEST2, the putative human telomerase catalytic subunit gene, is up-regulated in tumor cells and during immortalization. Cell, *90:* 785–795, 1997.
24. Felding-Habermann, B., O'Toole, T. E., Smith, J. W., Fransvea, E., Ruggeri, Z. M., Ginsberg, M. H., Hughes, P. E., Pampori, N., Shattil, S. J., Saven, A., and Mueller, B. M. Integrin activation controls metastasis in human breast cancer. Proc. Natl. Acad. Sci. USA, *98:* 1853–1858, 2001.
25. Zinn, K., McAllister, L., and Goodman, C. S. Sequence analysis and neuronal expression of fasciclin I in grasshopper and *Drosophila*. Cell, *53:* 577–587, 1988.
26. Wang, W. C., Zinn, K., and Bjorkman, P. J. Expression and structural studies of fasciclin I, an insect cell adhesion molecule. J. Biol. Chem., *268:* 1448–1455, 1993.
27. Skonier, J., Neubauer, M., Madisen, L., Bennett, K., Plowman, G. D., and Purchio, A. F. cDNA cloning and sequence analysis of β ig-h3, a novel gene induced in a human adenocarcinoma cell line after treatment with transforming growth factor-β. DNA Cell Biol., *11:* 511–522, 1992.
28. Elkins, T., Hortsch, M., Bieber, A. J., Snow, P. M., and Goodman, C. S. *Drosophila* fasciclin I is a novel homophilic adhesion molecule that along with fasciclin III can mediate cell sorting. J. Cell Biol., *110:* 1825–1832, 1990.
29. Ohno, S., Noshiro, M., Makihira, S., Kawamoto, T., Shen, M., Yan, W., Kawashima-Ohya, Y., Fujimoto, K., Tanne, K., and Kato, Y. RGD-CAP ((β)ig-h3) enhances the spreading of chondrocytes and fibroblasts via integrin $\alpha(1)\beta(1)$. Biochim. Biophys. Acta, *1451:* 196–205, 1999.
30. Mosher, D. F., and Johnson, R. B. In vitro formation of disulfide-bonded fibronectin multimers. J. Biol. Chem., *258:* 6595–6601, 1983.
31. Declerck, P. J., De Mol, M., Alessi, M. C., Baudner, S., Paques, E. P., Preissner, K. T., Muller-Berghaus, G., and Collen, D. Purification and characterization of a plasminogen activator inhibitor 1 binding protein from human plasma. Identification as a multimeric form of S protein (vitronectin). J. Biol. Chem., *263:* 15454–15461, 1988.
32. Lal, A., Lash, A. E., Altschul, S. F., Velculescu, V., Zhang, L., McLendon, R. E., Marra, M. A., Prange, C., Morin, P. J., Polyak, K., Papadopoulos, N., Vogelstein, B., Kinzler, K. W., Strausberg, R. L., and Riggins, G. J. A public database for gene expression in human cancers. Cancer Res., *59:* 5403–5407, 1999.
33. Sasaki, H., Lo, K. M., Chen, L. B., Auclair, D., Nakashima, Y., Moriyama, S., Fukai, I., Tam, C., Loda, M., and Fujii, Y. Expression of periostin, homologous with an insect cell adhesion molecule, as a prognostic marker in non-small cell lung cancers. Jpn. J. Cancer Res., *92:* 869–873, 2001.
34. Felding-Habermann, B., and Cheresh, D. A. Vitronectin and its receptors. Curr. Opin. Cell Biol., *5:* 864–868, 1993.
35. Castellani, P., Dorcaratto, A., Pau, A., Nicola, M., Siri, A., Gasparetto, B., Zardi, L., and Viale, G. The angiogenesis marker ED-B+ fibronectin isoform in intracranial meningiomas. Acta Neurochir., *142:* 277–282, 2000.
36. Midulla, M., Verma, R., Pignatelli, M., Ritter, M. A., Courtenay-Luck, N. S., and George, A. J. Source of oncofetal ED-B-containing fibronectin: implications of production by both tumor and endothelial cells. Cancer Res., *60:* 164–169, 2000.
37. Nagy, J. A., Masse, E. M., Herzberg, K. T., Meyers, M. S., Yeo, K. T., Yeo, T. K., Sioussat, T. M., and Dvorak, H. F. Pathogenesis of ascites tumor growth: vascular permeability factor, vascular hyperpermeability, and ascites fluid accumulation. Cancer Res., *55:* 360–368, 1995.
38. Plow, E. F., Haas, T. A., Zhang, L., Loftus, J., and Smith, J. W. Ligand binding to integrins. J. Biol. Chem., *275:* 21785–21788, 2000.
39. Singer, I. I., Scott, S., Kawka, D. W., Kazazis, D. M., Gailit, J., and Ruoslahti, E. Cell surface distribution of fibronectin and vitronectin receptors depends on substrate composition and extracellular matrix accumulation. J. Cell Biol., *106:* 2171–2182, 1988.
40. Dejana, E., Colella, S., Conforti, G., Abbadini, M., Gaboli, M., and Marchisio, P. C. Fibronectin and vitronectin regulate the organization of their respective Arg-Gly-Asp adhesion receptors in cultured human endothelial cells. J. Cell Biol., *107:* 1215–1223, 1988.
41. Burridge, K., and Chrzanowska-Wodnicka, M. Focal adhesions, contractility, and signaling. Annu. Rev. Cell Dev. Biol., *12:* 463–518, 1996.
42. Felsenfeld, D. P., Schwartzberg, P. L., Venegas, A., Tse, R., and Sheetz, M. P. Selective regulation of integrin–cytoskeleton interactions by the tyrosine kinase Src. Nat. Cell Biol., *1:* 200–206, 1999.

Association of Urokinase-Type Plasminogen Activator and Its Inhibitor with Disease Progression and Prognosis in Ovarian Cancer[1]

Gottfried Konecny,[2, 3] Michael Untch,[3] Astrid Pihan, Rainer Kimmig, Martina Gropp, Petra Stieber, Herrmann Hepp, Dennis Slamon, and Mark Pegram

Division of Hematology-Oncology, Department of Medicine, University of California at Los Angeles, School of Medicine, Los Angeles, California 90095-1678 [G. K., D. S., M. P.], and Departments of Obstetrics and Gynecology [M. U., A. P., R. K., M. G., H. H.] and Clinical Chemistry [P. S.], Klinikum Grosshadern, Ludwig Maximillians Universität München, 81377 München, Germany

ABSTRACT

Purpose: **Urokinase-type plasminogen activator (uPA) and its inhibitor, plasminogen activator inhibitor (PAI)-1, have been shown to be related to poor prognosis in a variety of malignant solid tumors. Studies on the prognostic relevance of uPA and PAI-1 in ovarian cancer, however, have been inconclusive. The current study tests the hypothesis that elevated expression of uPA and PAI-1 is associated with prognosis and disease progression.**

Experimental Design: **uPA and PAI-1 were prospectively measured by quantitative ELISA in tumor samples from 103 ovarian cancer patients (82 primary invasive epithelial carcinomas, 9 low malignant potential tumors, and 12 recurrent ovarian carcinomas).**

Results: **uPA but not PAI-1 levels were consistently associated with malignant progression, with levels increased from low malignant potential tumors to primary tumors (uPA, $P = 0.04$; PAI-1, $P = 0.019$), from early to advanced disease stages (uPA, $P = 0.014$; PAI-1, $P = 0.23$), and from primary to intra-abdominal metastatic tumors (uPA, $P = 0.001$; PAI-1, $P = 0.16$). High uPA and PAI-1 levels were associated with residual tumor volumes of >1 cm ($P = 0.001$ and $P = 0.016$, respectively). Among invasive International Federation of Gynecologists and Obstetrician stages I–IV tumors, elevated levels of uPA (>5.5 ng/mg) and PAI-I (>18.8 ng/ml) were associated with a shortened progression-free survival (uPA, $P = 0.003$; PAI-1, $P = 0.039$) and overall survival (uPA, $P = 0.0002$; PAI-1, $P = 0.007$). In multivariate analysis, uPA retained prognostic independence for progression-free survival ($P = 0.037$) and overall survival ($P = 0.006$).**

Conclusions: **These data suggest that the uPA/PAI-1 axis may play an important role in the intra-abdominal spread and reimplantation of ovarian cancer cells. The prognostic relevance of uPA and PAI-1 supports their possible role in the malignant progression of ovarian cancer.**

INTRODUCTION

Ovarian cancer is the leading cause of death from gynecological malignancies and the fourth leading cause of cancer deaths among American women. Little is known about the molecular biology underlying the metastatic process of intra-abdominal dissemination in ovarian cancer. Invasion and metastasis of solid tumors requires proteolytic enzymes that degrade the extracellular matrix and basement membranes (1). Among the proteases involved are the plasminogen activators, of which uPA[4] and/or its inhibitor, PAI-1, have been suggested to play a central role (2–4). Binding of uPA to the uPA receptor (CD87) activates the protease and catalyzes the conversion of plasminogen to plasmin, which subsequently activates type IV collagenase (3), or directly degrades extracellular matrix proteins such as fibrin, lamin, laminins, and proteoglycans (4). The enzymatic activity of uPA is regulated by the plasminogen activator inhibitors, PAI-1 and PAI-2 (5, 6). Both uPA and PAI-1 have been associated with disease outcome as statistically independent prognostic markers in breast (7–9), lung (10), colon (11), kidney (12), and gastrointestinal (13) cancers.

In ovarian cancer, significantly elevated uPA and PAI-1 levels have been described (14–16), however, studies analyzing the clinical impact of uPA and PAI-1 in ovarian cancer have reported inconclusive results, with studies either claiming prognostic importance of PAI-1 (17, 18) or uPA (19), or demonstrating no prognostic relevance for either uPA or PAI-1 (16). The studies with significant results were either performed with patient subsets of advanced disease stages only (17, 18), or without multivariate analysis (19). On the basis of these limitations, the current study was designed with the objective of analyzing the prognostic relevance of uPA and PAI-1 on PFS or OS in uni- and multivariate analyses among patients with all

Received 10/23/00; revised 1/16/01; accepted 3/13/01.

The costs of publication of this article were defrayed in part by the payment of page charges. This article must therefore be hereby marked *advertisement* in accordance with 18 U.S.C. Section 1734 solely to indicate this fact.

[1] Supported in part by Ernst and Berta Grimmke-Stiftung, Düsseldorf, Germany, and by Department of Defense Grant DAMD17-00-1-9503.

[2] To whom requests for reprints should be addressed, at Division of Hematology-Oncology, Department of Medicine, 12-145 Factor Building, University of California at Los Angeles, School of Medicine, Los Angeles, CA 90095-1678. Phone: (310) 206-4156; Fax: (310) 825-6192; E-mail: gkonecny@ucla.edu.

[3] G. K. and M. U. share first-authorship.

[4] The abbreviations used are: uPA, urokinase-type plasminogen activator; PAI, plasminogen activator inhibitor; FIGO, International Federation of Gynecology and Obstetrics; PFS, progression-free survival; OS, overall survival; LMP, low malignant potential.

Table 1 Patient and disease characteristics in invasive primary epithelial ovarian cancers (n = 82)

		N	Percentage
Age			
Median	56		
Range	34–82		
Stage			
FIGO I		12	14.6
FIGO II		6	7.3
FIGO III		50	61.0
FIGO IV		14	17.1
Histology			
Serous		53	64.6
Mucinous		10	12.2
Endometroid		15	18.3
Undifferentiated		3	3.7
Clear cell		1	1.2
Grading			
G1		8	9.8
G2		28	34.1
G3		42	51.2
G4		4	4.9
Hormone receptor status (n = 70)			
ER-negative		27	38.6
ER-positive		43	61.4
PR-negative		41	57.1
PR-positive		29	42.9
uPA			
≤5.5		64	78.0
>5.5		18	22.0
PAI-1			
≤18.8		41	50
>18.8		41	50

disease stages as a cohort representative of primary ovarian cancer in general.

PATIENTS AND METHODS

Patients. One hundred and three consecutive patients (1993–1997) who were treated for ovarian carcinoma at the Department of Obstetrics and Gynecology of the University of Munich, Klinikum Grosshadern, Munich, Germany were enrolled in this study. Complete surgical staging was followed by standard operative procedures, including a bilateral salpingo-oophorectomy, total abdominal hysterectomy, retroperitoneal pelvic and periaortic lymphadenectomy, and partial resection of the small or large intestine, diaphragmatic peritoneum, or upper abdominal surgery if indicated in advanced disease. Ovarian cancer disease was classified according to the FIGO staging system. Postoperative macroscopically visible tumor was the criterion for defining the presence or absence of residual tumor. The tumors studied included 82 primary invasive epithelial carcinomas, 9 LMP tumors, and 12 recurrent ovarian carcinomas. The patient and disease characteristics of the 82 primary invasive carcinomas are summarized in Table 1. Complete follow-up information was available for 80 of these patients.

Sixty-nine of 82 patients with primary ovarian cancer received platinum-based chemotherapy. Of the remaining 13 patients who received a single-drug therapy (n = 2) or no adjuvant treatment (n = 11), most had early stage grade 1 carcinomas (n = 8) or unfavorable health conditions (n = 5). During initiation of the study, standard chemotherapy for primary ovarian cancer was carboplatin/cyclophosphamide with subsequent paclitaxel-containing regimens. A maximum of six cycles of chemotherapy was administered. Computed tomography scans of the abdomen were performed when disease progression was suspected on the basis of gynecological examination, vaginal ultrasound, patient symptoms, or increases in serum tumor markers. Disease progression was defined as a radiologically (computed tomography scan or nuclear magnetic resonance) proven disease recurrence or progression. Second-look procedures were not performed in this cohort. CA 125 and CA 72-4 levels were measured every three months by enzyme immunoassay (Abbott Laboratories, Chicago, IL) and RIA (Centocore, New York, NY), respectively. Median follow-up was 17 months (range, 1–55 months) for all patients. This study was performed after approval by the local Human Investigations Committee of the University of Munich, Munich, Germany. Informed consent was obtained from each patient or patient guardian.

Methods. Biopsies were obtained during surgery, and tissue sections were analyzed by histological assessment in all cases. The remainder of each sample was stored at −198°C in liquid nitrogen until use. Subsequently, frozen specimens of 500 mg wet weight were pulverized with a microdismembrator (Braun-Melsungen, Melsungen, Germany), suspended in 2 ml of Tris-buffered saline containing 1% Triton X-100 detergent (Sigma Chemical Co., Munich, Germany), and incubated at 4°C for 12 h, with subsequent ultracentrifugation at 100,000 × g for 45 min. Quantitative levels of uPA and PAI-1 were prospectively measured in the supernants using ELISA kits, as described (Ref. 20; Imubind uPA and Imubind PAI-1; American Diagnostica, Greenwich, CT). Briefly, the uPA ELISA uses a murine monoclonal capture antibody directed to the uPA β-chain, thus detecting all forms of human uPA and uPA complexes with PAI-1. The detection system uses a biotinylated antibody of uPA α-chain specificity. The PAI-1 ELISA uses a murine monoclonal capture antibody directed to active and inactive PAI-1 and PAI-1 complexes. The detection system uses a biotinylated antibody directed to an epitope that is noncompetitive with the above capture/binding site. Antigen concentrations for uPA and PAI-1 were measured in terms of ng/mg protein. Protein concentrations were measured using the protein assay reagent method (Pierce, Rockford, IL). Assays for estrogen and progesterone receptor content were performed with enzyme immunoassays (ER-EIA and PR-EIA, Abbott Laboratories, Chicago, IL), as described (21).

Statistical Analysis. Statistical analysis was performed using the SPSS statistical software program. Univariate and multivariate analyses were performed by the log-rank test and Cox's regression analysis, respectively. Two group comparisons assuming equal variance were performed using Student's t test (two-tailed). Nonparametric methods were used (Mann-Whitney U test) for non-normally distributed data. Ps of <0.05 were considered to be significant. The cutoff values of uPA and PAI-1 were calculated by log-rank statistic. A cutoff value for uPA and PAI-1 was identified that provided the maximum separation of patients with distinct prognosis with regards to PFS and OS. Survival curves were analyzed by the Kaplan-Meier method (22).

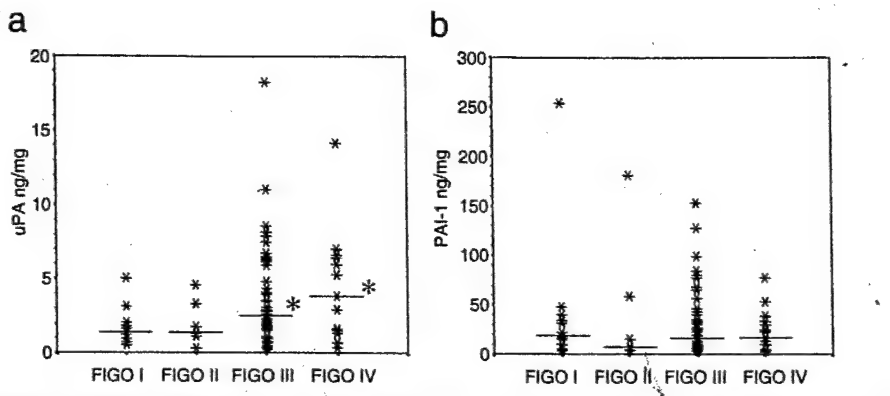

Fig. 1 Comparison of uPA (*A*) and PAI-1 (*B*) levels for all patients with primary ovarian cancer according to FIGO stage. Patients with advanced disease stages had significantly higher uPA but not PAI-1 concentrations compared with patients with early disease stages (uPA ng/mg protein, mean values ± SD; median): FIGO I, 1.7 ± 1.3 (1.5); FIGO II, 2.0 ± 1.6 (1.5); FIGO III, 3.7 ± 3.3 (2.5); FIGO IV, 4.2 ± 3.8 (3.4); $P = 0.014$; (PAI-1, ng/mg protein, mean values ± SD; median): FIGO I, 40.7 ± 68.7 (19.4); FIGO II, 44.7 ± 69.9 (10.7); FIGO III, 30.1 ± 33.3 (19.0); FIGO IV, 23.6 ± 21.5 (19.5); $P = 0.23$. *, $P = 0.014$ for FIGO stages III and IV compared with FIGO stages I and II. *Lines,* the median values.

RESULTS

uPA and PAI-1 concentrations were prospectively measured in tumor samples from 82 patients with primary ovarian cancer, 9 patients with LMP tumors, and 12 patients with recurrent ovarian carcinomas. Patient and disease characteristics of primary ovarian cancer patients are shown in Table 1. The expression of uPA in primary cancers was significantly associated with higher uPA concentrations among patients with higher FIGO stage disease [uPA ng/mg protein, mean values ± SD (median): FIGO I, 1.7 ± 1.3 (1.5); FIGO II, 2.0 ± 1.6 (1.5); FIGO III, 3.7 ± 3.3 (2.5); FIGO IV, 4.2 ± 3.8 (3.4); $P = 0.014$; Fig. 1*A*]. However, no significant association between PAI-1 concentrations and FIGO stage was found [PAI-1 ng/mg protein, mean values ± SD (median): FIGO I, 40.7 ± 68.7 (19.4); FIGO II, 44.7 ± 69.9 (10.7); FIGO III, 30.1 ± 33.3 (19.0); FIGO IV, 23.6 ± 21.5 (19.5); $P = 0.23$; Fig. 1*B*]. uPA and PAI-1 concentrations were significantly higher among primary ovarian cancers (FIGO I; $n = 12$) compared with LMP tumors [$n = 9$; uPA (mean ± SD)], 1.7 ± 1.2 *versus* 1.0 ± 1.2 ng/mg protein; $P = 0.04$; PAI-1 (mean ± SD), 40.7 ± 68.7 *versus* 9.0 ± 3.0 ng/mg protein; $P = 0.019$]. uPA concentrations among primary ovarian cancer patients (FIGO I-IV) were comparable with those measured in recurrent ovarian cancers [uPA (mean ± SD), 3.4 ± 3.1 *versus* 4.0 ± 2.9 ng/ml protein ($P = 0.5$)]; however, PAI-1 concentrations were significantly lower among recurrent ovarian cancers compared with primary ovarian cancers [PAI-1 (mean ± SD), 17.7 ± 15.2 *versus* 31.6 ± 41.5 ng/mg protein ($P = 0.035$)]. Among patients with advanced disease stages (FIGO III and IV), uPA and PAI-1 concentrations were compared between primary tumor sites ($n = 42$) and sites of metastases ($n = 21$). Intra-abdominal metastasis demonstrated significantly higher uPA but not PAI-1 concentrations [uPA (mean ± SD), 5.5 ± 3.8 *versus* 2.9 ± 2.8 ng/mg protein; $P = 0.001$; PAI-1 (mean ± SD), 33.8 ± 32.3 *versus* 24.8 ± 29.8 ng/mg protein; $P = 0.16$]. The relationship of uPA to PAI-1 among all ovarian cancer patients ($n = 103$) was analyzed and is shown in Table 2 and Fig. 2. The data demonstrate a significant positive association between uPA and PAI-1 as dichotomized variables or as continuous variables (χ^2 test, $P = 0.015$; Pearson correlation, $r = 0.22$; $P = 0.02$; Spearman's correlation, $r = 0.41$; $P < 0.001$). Ovarian cancer patients (FIGO I–IV) with elevated uPA levels (>5.5 ng/mg) also demonstrated significantly higher mean PAI-1 concentrations compared with those with lower uPA levels (PAI-1, 44 ± 32 *versus* 28 ± 43 ng/mg protein; $P = 0.003$).

Table 2 Significant association between uPA and PAI-1 for primary ovarian cancer patients ($n = 103$) using the defined cut-off value for uPA (5.5 ng/mg) and PAI-1 (18.8 ng/mg)[a]

	uPA-positive	uPA-negative	N
PAI-1-positive	15 (75%)	32 (39%)	47
PAI-1-negative	5 (25%)	51 (61%)	56
Total	20 (100%)	83 (100%)	100

[a] chi square; $P = 0.003$.

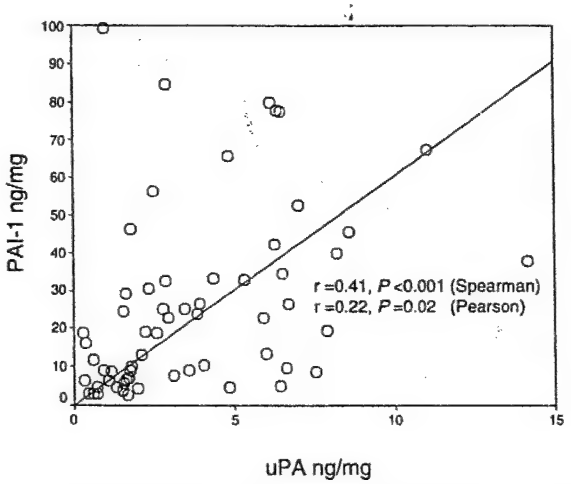

Fig. 2 Association between uPA and PAI-1 concentrations as continuous variables among 103 ovarian cancer patients [$r = 0.22$; $P = 0.02$ (Pearson); $r = 0.41$; $P < 0.001$ (Spearman)].

Table 3 Uni- and multivariate analyses of prognostic factors for PFS and OS in 80 patients with ovarian cancer, FIGO stages I–IV

The following parameters were included in the analyses: tumor stage (FIGO Stages I and II *versus* Stages III and IV), residual tumor (presence or absence), age (≤56 years *versus* >56 years), uPA (≤5.5 *versus* >5.5 ng/mg protein), PAI-1 (≤18.8 *versus* >18.8 ng/mg protein), and grading (G1, G2, G3, or G4).

	*P*s for PFS		*P*s for OS	
	Univariate	Multivariate	Univariate	Multivariate
FIGO stage	0.005	0.95	0.016	0.88
Residual tumor volume	<0.0001	0.0005	0.0003	0.025
uPA	0.003	0.037	0.0002	0.006
PAI-1	0.039	0.31	0.007	0.582
Age	0.059	0.0008	0.15	0.018
Grading	0.0002	0.962	0.004	0.882

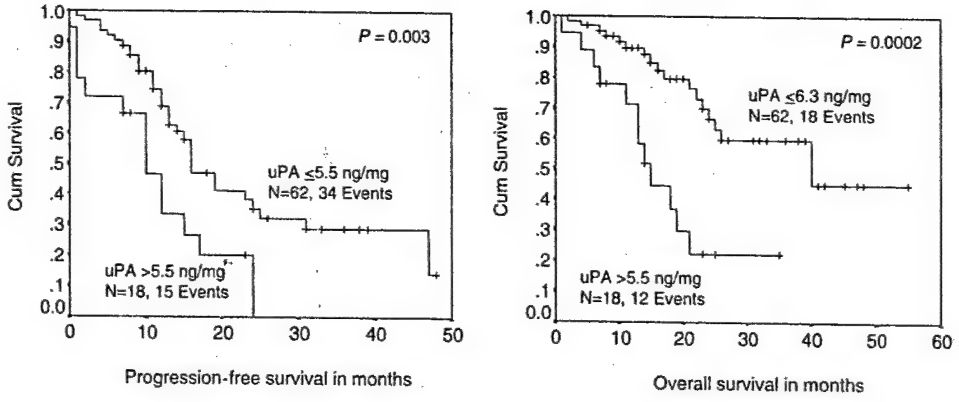

Fig. 3 Kaplan-Meier plots for PFS and OS of ovarian cancer patients, FIGO stages I–IV. Patients with uPA levels below the cutoff value (5.5 ng/mg protein) had improved median PFS and OS compared with patients with elevated levels (PFS, 16 *versus* 10 months; $P = 0.003$; OS, 40 *versus* 15 months; $P = 0.0002$).

Evaluation of uPA and PAI-1 on Prognosis (PFS and OS). Among invasive cancers of all stages, residual tumor volume, FIGO stage, and grading were significant prognostic factors for both PFS and OS in univariate analyses (Table 3). Patients with early disease stages (FIGO I and II; $n = 18$) had a significantly better prognosis than patients with advanced disease stages (FIGO III and IV; $n = 62$; median PFS, 47 *versus* 13 months; $P = 0.005$; median OS not reached for FIGO stages I and II patients *versus* 24 months for FIGO stages III and IV patients; $P = 0.016$). Likewise, patients with no residual tumor volume ($n = 28$) had a marked advantage in prognosis compared with patients with residual volume ($n = 52$; median PFS, 47 *versus* 12 months; $P < 0.0001$; median OS not reached for patients without residual disease *versus* 21 months for patients with residual disease; $P = 0.0003$). Age (≤56 or >56 years) demonstrated borderline significance for PFS ($P = 0.059$) and was not significant for OS ($P = 0.15$).

To evaluate the prognostic impact of uPA and PAI-1 levels on prognosis, we identified optimized cutoff values for separation of patients with distinct prognosis, using univariate analysis. A uPA value of 5.5 ng/mg provided the maximum separation of patients with regards to PFS and OS (log-rank test; $P = 0.003$ and 0.0002, respectively). A PAI-1 value of 18.8 ng/mg similarly provided the maximum separation of patients with regards to PFS and OS (log-rank test; $P = 0.039$ and $P = 0.007$, respectively). Among invasive cancers of all stages, patients with uPA concentrations below 5.5 ng/mg protein ($n = 62$) had an improved median PFS and OS compared with patients with elevated levels ($n = 18$; median PFS, 16 *versus* 10 months, $P = 0.003$; median OS, 40 *versus* 15 months, $P = 0.0002$; Fig. 3). Similarly, patients with PAI-1 levels below 18.8 ng/mg protein ($n = 40$) had an improved PFS and OS compared with patients with elevated levels ($n = 40$; median PFS, 19 *versus* 13 months, $P = 0.039$; median OS not reached for PAI-1-negative patients *versus* 21 months for PAI-1-positive patients, $P = 0.007$; Fig. 4). uPA concentration retained prognostic significance for OS in patients with residual tumor ($n = 54$; median OS, 24 *versus* 14 months; $P = 0.012$) and achieved borderline significance among patients with no residual tumor ($n = 28$; mean OS, 53 *versus* 20 months; $P = 0.06$). Neither estrogen and progesterone receptor status nor the volume of ascites (>500 *versus* ≤500 ml) or CA 125 values (>35 *versus* ≤35 units/ml) were significant prognostic factors in this cohort (data not shown). In multivariate analysis of patients with FIGO stages I–IV disease, which included the parameters of the FIGO stage, residual tumor volume, uPA, PAI-1, age and grading, the parameters of residual tumor volume, uPA, and age remained independent prognostic factors for PFS and OS (Table 3).

To compare this study with previous studies in which only patients with advanced disease stages were analyzed, the prognostic significance of uPA and PAI-1 in the subset of FIGO stages III and IV patients ($n = 62$) was analyzed. Among these invasive cancers, residual tumor volume ($P = 0.0007$), age ($P = 0.005$), and uPA ($P = 0.037$) were significant prognostic factors for PFS, whereas FIGO stage ($P = 0.10$) was only of borderline significance. FIGO stage ($P = 0.024$), residual tumor volume

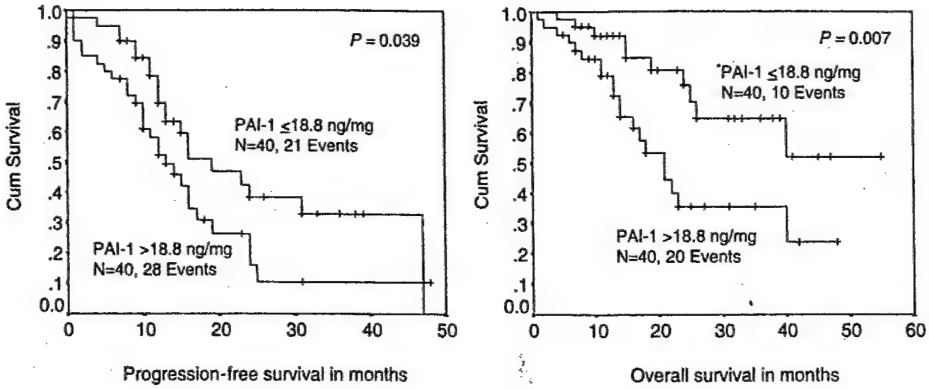

Fig. 4 Kaplan-Meier plots for PFS and OS of ovarian cancer patients, FIGO stages I–IV. Patients with PAI-1 levels below the cutoff value (18.8 ng/mg protein) had improved median PFS and OS compared with patients with elevated levels (PFS, 19 *versus* 13 months; $P = 0.039$; OS, median OS not reached for patients with PAI-1 levels ≤18.8 n/mg protein *versus* 21 months; $P = 0.007$).

($P = 0.012$), and uPA ($P = 0.003$) were significant prognostic factors for OS, whereas age ($P = 0.056$) and PAI-1 ($P = 0.066$) were of borderline significance. Interestingly, FIGO stage III or IV patients with optimal surgical cytoreduction ($n = 28$) had significantly lower uPA and PAI-1 concentrations than those with higher volumes (>1 cm; $n = 36$) [uPA (mean ± SD), 2.4 ± 2.4 *versus* 4.9 ± 3.7 ng/mg protein, $P = 0.001$; PAI-1 (mean ± SD), 22.9 ± 32.1 *versus* 33.1 ± 30.0 ng/mg protein, $P = 0.016$]. This suggests that the inability to optimally debulk patients could be related to the increased proteolytic activity in tumors observed in patients with higher residual volumes. In multivariate analysis of advanced ovarian cancer, including FIGO stage, residual tumor volume, age, and uPA, the parameters of residual tumor volume (PFS, $P = 0.0004$; OS, $P = 0.025$), uPA (PFS, $P = 0.07$; OS, $P = 0.007$) and age (PFS, $P = 0.0006$; OS, $P = 0.025$) retained independent prognostic importance.

DISCUSSION

In the present study, uPA concentrations were significantly higher in invasive tumors compared with LMP tumors, which have been recognized as a separate entity, as the clinical course of these tumors is far more favorable when compared with their invasive counterparts (23). Similarly, uPA levels were higher in metastatic lesions as compared with their respective primary tumors. Increasing levels of uPA were also significantly associated with advanced disease stages and with the amount (>1 cm) of residual tumor. Taken together, these findings demonstrate that uPA is associated with the malignant progression of epithelial ovarian cancer. The results are consistent with the hypothesis that elevated levels of uPA may contribute to invasiveness and metastasis of ovarian cancer. In contrast, PAI-1 content was not correlated with disease stage, which is in accordance with previous reports (16, 17), and no significant difference was found in PAI-1 content between primary and metastatic ovarian cancers as compared with uPA.

The present study is the first study to evaluate the prognostic significance of uPA and PAI-1 in uni- and multivariate analyses in a representative cohort of primary ovarian cancers of all stages. The level of uPA was an independent prognostic marker for both PFS and OS in multivariate analysis, using the cutoff values established for this cohort. Consistent with previous reports, we also confirmed the independent prognostic relevance of residual tumor volume and age in ovarian cancer (24–28). This is the first study to demonstrate the independent prognostic relevance of uPA in a nonselected group of ovarian cancer patients. In a recent report on 77 patients with primary ovarian cancer (FIGO stages I–III), Hoffmann *et al.* (19) were also able to demonstrate prognostic relevance of uPA for OS; however, they only performed univariate analysis. In contrast, van der Burg *et al.*, (16) who assessed uPA and PAI-1 among 90 patients ranging from stage I to stage IV disease, reported no correlation of uPA and PAI-1 with PFS or OS. The negative findings of that study possibly are attributable to the different laboratory assays, extraction procedures, and cutoff values used, as van der Burg *et al.* based median values as cutoff values for uPA and PAI-1 and measured uPA and PAI-1 concentrations in cytosols routinely prepared for ER and PR determinations.

Two previous studies support a poor prognosis associated with high PAI-1 content (17, 18). Chambers *et al.* (17) determined PAI-1 levels by immunohistochemistry in samples from 119 patients with FIGO stages I–IV disease, and PAI-1 was an independent prognostic factor among the 99 patients with FIGO stages III or IV disease; however uPA was not included in this analysis. Kuhn *et al.* (18) recently demonstrated the importance of PAI-1 as an independent prognostic marker for survival by assessing PAI-1 by ELISA among 84 ovarian cancer patients with FIGO stage IIIc disease. In the present study, the prognostic relevance of high PAI-1 levels for PFS and OS was confirmed in univariate analysis only when all disease stages were included in the analysis; however, this was not the case among the subset of patients with advanced disease for PFS, and for OS the effect was of borderline significance ($P = 0.066$), possibly because of the small sample size ($n = 64$) in subset analysis.

Not only did the previously mentioned studies use different extraction procedures or assay methods and different antibodies, but, also, different cutoff values were applied to separate patients into low- *versus* high-risk groups. Hoffmann *et al.* (19), who analyzed a comparable cohort (FIGO stages I–III) of primary ovarian cancer patients, detected uPA and PAI-1 levels in tissue pellets and selected a slightly lower

optimized cutoff value of 4.8 ng/ml for uPA. However, they did indicate that the uPA concentrations were ~30% lower if detection was performed in tissue pellets, as done in their study, compared with tissue homogenates, which were used in the present study.

The optimal cutoff value for uPA in this study was 5.5 ng/mg protein, meaning that 18 of 82 patients (22%) whose tumors revealed elevated uPA concentrations had a significantly shorter OS compared with those with lower uPA levels. To further establish the prognostic impact of uPA in ovarian cancer, the previously described cutoff value of 4.8 ng/ml protein for uPA was analyzed (data not shown). This cutoff value also provided clinically significant results in this study population, in which 22 of 82 patients (27%) had a significantly shorter survival compared with those with lower uPA concentrations ($P = 0.006$). uPA also retained independent prognostic significance with the selected cutoff value of 4.8 ng/mg protein in multivariate analysis, including FIGO stage, residual tumor volume, levels of PAI-1, age, and histological grade ($P = 0.0088$). These data, however, also demonstrate that suitable cutoff values for both uPA and PAI-1 must be further defined and validated in a prospective setting.

This study presents evidence that elevated levels of the uPA protease and, to a lesser extent, its inhibitor, PAI-1, are associated with the capacity of ovarian cancer cells to invade then metastasize in the peritoneum. Additional research, however, is necessary to understand the role of PAI-1 in this process. It has been suggested that PAI-1 can promote internalization of receptor-bound uPA, which allows recycling of the uPA receptor to the cell surface (29). In this way, the proteolytically active areas of the cell surface can be modified by PAI-1, thus regulating directed proteolytic activity of tumor cells (4). It recently has been described that competitive displacement of uPA from the cellular binding sites results in decreased proteolysis *in vitro*. Metastatic capacity was similarly inhibited when animals were given intermittent i.p. injections of uPA/IgG fusion protein capable of displacing uPA activity from the tumor cell surface (30). Assessment of uPA and PAI-1 levels may therefore allow identification of ovarian cancer patients at high risk and provide a rationale for a biologically directed therapy.

ACKNOWLEDGMENTS

We thank Sandra Lude and Margret Felber for their expertise, Wendy Aft for her kind support in preparing the manuscript, and Dr. Beth Karlan (Department of Obstetrics and Gynecology, Jonsson Comprehensive Cancer Center, University of California at Los Angeles, Los Angeles, CA) for critically reviewing the manuscript.

REFERENCES

1. Kohn, E. C., and Liotta, L. A. Molecular insights into cancer invasion: strategies for prevention and intervention. Cancer Res., *55:* 1856–1862, 1995.

2. Astedt, B., and Holmberg, L. Immunological identity of urokinase and ovarian carcinoma plasminogen activator released in tissue culture. Nature (Lond.), *261:* 595–597, 1976.

3. Dano, K., Andreasen, P. A., Grondahl-Hansen, J., Kristensen, P. Nielsen, L. S., and Skriver, L. Plasminogen activators, tissue degradation, and cancer. Adv. Cancer Res., *44:* 139–266, 1985.

4. Schmitt, M., Harbeck, N., Thomssen, C., Wilhelm, O., Magdolen, V., Reuning, U., Ulm, K., Hofler, H., Jänicke, F., and Graeff, H. Clinical impact of the plasminogen activation system in tumor invasion and metastasis: prognostic relevance and target for therapy. Thromb. Haemost., *78:* 285–296, 1997.

5. Conese, M., and Blasi, F. Urokinase/urokinase receptor system: internalization/degradation of urokinase-serpin complexes: mechanism and regulation. Biol. Chem. Hoppe Seyler, *376:* 143–155, 1995.

6. Cajot, J. F., Bamat, J., Bergonzelli, G. E., Kruithof, E. K., Medcalf, R. L., Testuz, J., and Sordat, B. Plasminogen-activator inhibitor type 1 is a potent natural inhibitor of extracellular matrix degradation by fibrosarcoma and colon carcinoma cells. Proc. Natl. Acad. Sci. USA, *87:* 6939–6943, 1990.

7. Duffy, M. J., O'Grady, P., Devaney, D., O'Siorain, L., Fennelly, J. J., and Lijnen, H. J. Urokinase-plasminogen activator, a marker for aggressive breast carcinomas. Preliminary report. Cancer (Phila.), *62:* 531–533, 1988.

8. Foekens, J. A., Schmitt, M., van Putten, W. L., Peters, H. A., Bontenbal, M., Jänicke, F., and Klijn, J. G. Prognostic value of urokinase-type plasminogen activator in 671 primary breast cancer patients. Cancer Res., *52:* 6101–6105, 1992.

9. Jänicke, F., Schmitt, M., Ulm, K., Gossner, W., and Graeff, H. Urokinase-type plasminogen activator antigen and early relapse in breast cancer. Lancet, *2:* 1049, 1989.

10. Pedersen, H., Brunner, N., Francis, D., Osterlind, K., Ronne, E., Hansen, H. H., Dano, K., and Grondahl-Hansen, J. Prognostic impact of urokinase, urokinase receptor, and type 1 plasminogen activator inhibitor in squamous and large cell lung cancer tissue. Cancer Res., *54:* 4671–4675, 1994.

11. Ganesh, S., Sier, C. F., Griffioen, G., Vloedgraven, H. J., de Boer, A., Welvaart, K., van de Velde, C. J., van Krieken, J. H., Verheijen, J. H., Lamers, C. B., *et al.* Prognostic relevance of plasminogen activators and their inhibitors in colorectal cancer. Cancer Res., *54:* 4065–4071, 1994.

12. Hofmann, R., Lehmer, A., Buresch, M., Hartung, R., and Ulm, K. Clinical relevance of urokinase plasminogen activator, its receptor, and its inhibitor in patients with renal cell carcinoma. Cancer (Phila.), *78:* 487–492, 1996.

13. Nekarda, H., Siewert, J. R., Schmitt, M., and Ulm, K. Tumour-associated proteolytic factors uPA and PAI-1 and survival in totally resected gastric cancer. Lancet, *343:* 117, 1994.

14. Kuhn, W., Pache, L., Schmalfeldt, B., Dettmar, P., Schmitt, M., Jänicke, F., and Graeff, H. Urokinase (uPA) and PAI-1 predict survival in advanced ovarian cancer patients (FIGO III) after radical surgery and platinum-based chemotherapy. Gynecol. Oncol., *55:* 401–409, 1994.

15. Casslén, B., Bossmar, T., Lelander, I., and Astedtm, B. Plasminogen activators and plasminogen activator inhibitors in blood and tumor fluids of patients with ovarian cancer. Eur. J. Cancer, *30A:* 1302–1311, 1994.

16. van der Burg, M. E., Henzen-Logmans, S. C., Berns, E. M., van Putten, W. L., Klijn, J. G., and Foekens, J. A. Expression of urokinase-type plasminogen activator (uPA) and its inhibitor PAI-1 in benign, borderline, malignant primary, and metastatic ovarian tumors. Int. J. Cancer, *69:* 475–479, 1996.

17. Chambers, S. K., Ivins, C. M., and Carcangiu, M. L. Plasminogen activator inhibitor-1 is an independent poor prognostic factor for survival in advanced stage epithelial ovarian cancer patients. Int. J. Cancer, *79:* 449–454, 1998.

18. Kuhn, W., Schmalfeldt, B., Reuning, U., Pache, L., Berger, U., Ulm, K., Harbeck, N., Spathe, K., Dettmar, P., Hofler, H., Jänicke, F., Schmitt, M., and Graeff, H. Prognostic significance of urokinase (uPA) and its inhibitor PAI-1 for survival in advanced ovarian carcinoma stage FIGO IIIc. Br. J. Cancer, *79:* 1746–1751, 1999.

19. Hoffmann, G., Pollow, K., Weikel, W., Strittmatter, H. J., Bach, J., Schaffrath, M., Knapstein, P., Melchert, F., and Pollow, B. Urokinase and plasminogen activator-inhibitor (PAI-1) status in primary ovarian carcinomas and ovarian metastases compared to benign ovarian tumors

as a function of histopathological parameters. Clin. Chem. Lab. Med., *37:* 47–54, 1999.

20. Jänicke, F., Pache, L., Schmitt, M., Ulm, K., Thomssen, C., Prechtl, A., and Graeff, H. Both the cytosols and detergent extracts of breast cancer tissues are suited to evaluate the prognostic impact of the urokinase-type plasminogen activator and its inhibitor, plasminogen activator inhibitor type 1. Cancer Res., *54:* 2527–2530, 1994.

21. Duffy, M. J., O'Siorain, L., Waldron, B., and Smith, C. Estradiol receptors in human breast carcinomas assayed by use of monoclonal antibodies. Clin. Chem., *32:* 1972–1974, 1986.

22. Kaplan, E. L., and Meier, P. Nonparametric estimation from incomplete observations. J. Am. Stat. Assoc., *53:* 457–481, 1958.

23. Trimble, C. L., and Trimble, E. L. Management of epithelial ovarian tumors of low malignant potential. Gynecol. Oncol., *55:* 52–61, 1994.

24. Hoskins, W. J., Bundy, B. N., Thigpen, J. T., and Omura, G. A. The influence of cytoreductive surgery on recurrence-free interval and survival in small-volume stage III epithelial ovarian cancer: a Gynecologic Oncology Group study. Gynecol. Oncol., *47:* 159–166, 1992.

25. Markman, M., Lewis, J. L., Jr., Saigo, P., Hakes, T., Rubin, S., Jones, W., Reichman, B., Curtin, J., Barakat, R., Almadrones, L., Morrissey, T., and Hoskins, W. Impact of age on survival of patients with ovarian cancer. Gynecol. Oncol., *49:* 236–239, 1993.

26. Omura, G. A., Brady, M. F., Homesley, H. D., Yordan, E., Major, F. J., Buchsbaum, H. J., and Park, R. C. Long-term follow-up and prognostic factor analysis in advanced ovarian carcinoma: the Gynecologic Oncology Group experience. J. Clin. Oncol., *9:* 1138–1150, 1991.

27. Ozols, R. F., Garvin, A. J., Costa, J., Simon, R. M., and Young, R. C. Advanced ovarian cancer: correlation of histologic grade with response to therapy and survival. Cancer (Phila.), *45:* 572–581, 1980.

28. Jänicke, F., Holscher, M., Kuhn, W., von Hugo, R., Pache, L., Siewert, J. R., and Graeff, H. Radical surgical procedure improves survival time in patients with recurrent ovarian cancer. Cancer (Phila.), *70:* 2129–2136, 1992.

29. Blasi, F. Urokinase and urokinase receptor: a paracrine/autocrine system regulating cell migration and invasiveness. Bioessays, *15:* 105–111, 1993.

30. Crowley, C. W., Cohen, R. L., Lucas, B. K., Liu, G., Shuman, M. A., and Levinson, A. D. Prevention of metastasis by inhibition of the urokinase receptor. Proc. Natl. Acad. Sci. USA, *90:* 5021–5025, 1993.

Cancer Gene Therapy (2002) 9, 567–572

www.nature.com/cgt

Long term follow-up of patients with recurrent ovarian cancer after Ad *p53* gene replacement with SCH 58500

Richard E Buller,[1] Mark S Shahin,[1] Jo Ann Horowitz,[2] Ingo B Runnebaum,[3,4] Vikas Mahavni,[1] Stan Petrauskas,[2] Rolf Kreienberg,[3,4] Beth Karlan,[5] Dennis Slamon,[5] and Mark Pegram[5]

[1]Department of Obstetrics and Gynecology, Division of Gynecologic Oncology, The University of Iowa Hospitals and Clinics, Iowa City, Iowa 52242-1009, USA; [2]Schering-Plough Research Institute, Kenilworth, New Jersey, USA; [3]University of Freiburg, Freiburg, Germany; [4]University of Ulm, Ulm, Germany; and [5]University of California, Los Angeles, California, USA.

Objective: We have previously reported the safety, efficient gene transfer, and favorable CA125 responses of individuals with recurrent ovarian cancer treated by *p53* gene replacement with the adenoviral vector SCH 58500. The purpose of the present investigation was to evaluate the long-term follow-up of these heavily pretreated patients subsequent to SCH 58500 dosing. **Methods:** Patients ($n=36$) were treated with either single-dose SCH 58500 in the phase I study or with multiple doses (MD) of SCH 58500 over multiple cycles in combination of platinum-based chemotherapy in the phase I/II portion of the study. Five patients were initially treated in the single-dose group and re-enrolled in the MD group. The MD group was evaluated both without the re-enrolled patients as MD1 ($n=19$), and as MD2 ($n=24$), which included them. Patients who were only treated on the single-dose arm were designated as SD ($n=12$). Most patients received additional chemotherapy at the discretion of their physicians on completion of the trial. The current analysis is a retrospective sequential cohort survival analysis. **Results:** The first patient was treated in March 1997 and the last patient completed SCH 58500 in September 1998. There was no difference in age at diagnosis, Karnofsky performance status, interval between diagnosis to SCH 58500, prior cycles or regimen of chemotherapy, platinum-free interval, percent platinum refractory patients, pretreatment CA125, or largest tumor volume between groups. Both MD groups had a slightly longer chemotherapy-free interval before SCH 58500 than the SD group. Median survival of individuals who received MD SCH 58500 with chemotherapy was 12–13.0 months, compared to only 5 months for those treated with SD SCH 58500. There are 10 long-term survivors more than 20 months after MD treatment for recurrent disease compared to only 2 long-term survivors after SD SCH 58500. **Conclusion:** The 12- to 13.0-month median survival in a heavily pretreated population with recurrent ovarian cancer compares favorably to the 16-month median survival for individuals treated with paclitaxel at the time of initial recurrence of this disease and is more than double the 5-month survival seen with palliative radiotherapy or paclitaxel failure. These data suggest that further study of SCH58500 is clearly indicated.

Cancer Gene Therapy (2002) **9,** 567–572 doi:10.1038/sj.cgt.7700473

Keywords:* p53*; gene therapy; ovarian cancer survival; adenovirus

Despite the addition of several new cytotoxic agents to our therapeutic armamentarium, the overall survival of individuals diagnosed with advanced-stage ovarian cancer remains disappointing.[1–4] In general, cytotoxic agents rely on a beneficial therapeutic index to effect greater damage to metastatic ovarian cancer than to normal host cells. The growing knowledge base of specific gene defects associated with ovarian cancer,[5,6] coupled with the observation that this disease responds to surgical cytoreduction[7–10] and tends to remain confined to the abdominal cavity throughout its course,[11,12] make it an attractive model for molecularly targeted therapeutics. We have recently demonstrated that mutation of the *p53* tumor suppressor gene leads to compromised ovarian cancer survival.[13] The results of a phase I/II trial of intraperitoneal adenoviral-mediated p53 gene replacement in recurrent ovarian cancer demonstrated safety, tolerability of doses limited only by infusion volume, and the manufacturing process.[14] Most importantly, repetitive gene transfer was the norm following multiple courses of

Received April 4, 2002.

Address correspondence and reprint requests to: Dr Richard E Buller, Department of Obstetrics and Gynecology, Division of Gynecologic Oncology, 200 Hawkins Drive — #4630 JCP, Iowa City, IA 52242-1009, USA. E-mail: richard-buller@uiowa.edu

Presented in part at the 9th International Conference on Gene Therapy of Cancer, San Diego, CA December 7–9, 2000.

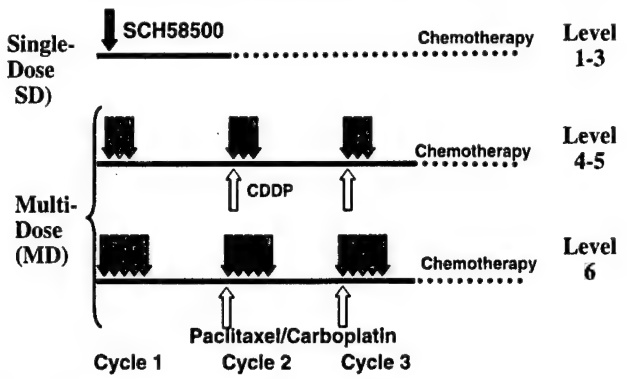

Figure 1 Schedule of therapy.

SCH 58500 despite the rapid development of an elevated antiadenoviral antibody titer. Favorable CA125 responses in the phase II portion of the study have encouraged us to evaluate the long-term follow-up of these patients. This analysis was not planned as part of the original trial and should be considered a nonrandomized sequential cohort retrospective analysis.

Methods

SCH 58500 is a replication-defective, recombinant, human adenoviral vector containing the cloned wild-type human *p53* gene.[15] Between 3/12/97 and 6/24/98, 36 patients with recurrent ovarian, peritoneal, or fallopian tube cancer enrolled in either a phase I escalating single-dose study of SCH 58500 at 7.5×10^{10} to 7.5×10^{12} particles, or a multiple-dose (MD) group of patients receiving sequential SCH 58500 (two to five doses per cycle) at 7.5×10^{12} to 7.5×10^{13} particles per dose, given either with intraperitoneal cisplatin (100 mg/m^2) or intravenous carboplatin/paclitaxel. The last dose of SCH 58500 was given in September 1998. Five patients elected to go onto the MD portion of the study from 1 to 8 months after completion of the phase I portion. The treatment schema is outlined in Figure 1. Dose levels 1–6 correspond to 7.5×10^{10}, 7.5×10^{11}, 2.5×10^{12}, 7.5×10^{12}, 2.5×10^{13}, 7.5×10^{13} particles/dose, respectively. Intraperitoneal delivery of SCH 58500 for 2–5 days per cycle at dose levels 4–6, and routine follow-up have been described.[14]

Follow-up information was collected from the time of study entry until patient death or through 05/21/01. A standard definition of platinum resistance was used: progression of disease while receiving carboplatin or cisplatin, or recurrence of disease within 6 months of completion of therapy.[4,16] The resistance is considered primary if it occurs during or following the initial treatment. The resistance is said to be secondary if it occurs during or following platinum retreatment of recurrent disease.

Statistical analysis of the association between clinical and treatment parameters between groups was evaluated using the chi-square test or Fisher exact test where appropriate. Student *t* test was used for comparison of the means. Survival curves were constructed using the Kaplan-Meier method and differences between curves were tested using the log rank test. All *P* values were two sided, and only those

Table 1 Comparison of SD and MD cohorts

	SD	MD1*	*P1*†	MD2‡	*P2*§
Sample size	12	19		24	
Age at diagnosis	62 [3]¶	59 [3]	NS	59 [2]	NS
Prior:					
Regimens of chemotherapy	3 [0.6]	2.2 [0.4]	NS	2.7 [0.4]	NS
Prior cycles of chemotherapy	14.8 [2.9]	9.7 [1.3]	NS	12.4 [1.8]	NS
Karnofsky performance status	85.0 [3.6]	91.7 [3.1]	NS	90.9 [3.4]	NS
Interval (months):					
Diagnosis to SCH 58500	22.0 [3.0]	18.4 [2.5]	NS	23.9 [3.4]	NS
Chemotherapy free	3.3 [0.7]	6.4 [1.0]	.02	5.7 [0.9]	.05
Platinum free	8.1 [1.6]	9.6 [1.2]	NS	10.0 [1.1]	NS
Pre SCH 58500:					
CA125 [U/dl]	1959 [939]	2012 [1404]	NS	1673 [1114]	NS
Tumor area (cm^2)‖	44 [11]	22 [14]	NS	21 [11]	NS
Platinum resistant (%)	7 (58%)#	11 (58%)**	NS	14 (58%)††	NS

*Includes only multiple-dose (MD) individuals who did not enter the single-dose (SD) regimen previously.

†*P1*=significance level of comparison of means between SD cohort and MD1 cohort. *P1*≤.05 is considered significant.

‡Includes *all* multiple-dose patients even if they had previously received a single dose of SCH 58500 in the dose escalation phase I trial.

§*P2*=same as for *P1*, but the comparison is between SD and MD2 cohorts.

¶[Standard error of means].

‖Largest CT measurable lesion width×length.

#Includes four patients with primary platinum resistance and three patients with initial complete response to primary/secondary treatment with platinum but failure to respond to secondary or tertiary treatment.

**Includes six patients with primary platinum resistance and five patients with initial complete response to primary/secondary treatment with platinum but failure to respond to secondary or tertiary treatment.

††Includes six patients with primary platinum resistance and eight patients with initial complete response to primary/secondary treatment with platinum but failure to respond to secondary or tertiary treatment.

Table 2 Long-term survivors following SCH 58500

Subject	Previous chemotherapy regimens	Interval from last platinum (mo)	SCH 58500 dose (*PN*)	Doses	Chemotherapy (route)	Survival* (mo)
207†	1. Carboplatin, cyclophosphamide 2. Cisplatin, etoposide 3. Paclitaxel, platinum 4. Carboplatin 5. SCH 58500	5.5	7.5×10^{12}	2	Cisplatin (i.p.)	35.8
212	1. Carboplatin, adriamycin, cyclophosphamide 2. Paclitaxel, carboplatin 3. Paclitaxel, cyclophosphamide, PBSC mobilization 4. Ifosfamide, carboplatin, etoposide, paclitaxel 5. Melphalan 6. Topotecan 7. SCH 58500	16.9	7.5×10^{12}	2	Cisplatin (i.p.)	35.3*
17	1. Paclitaxel, cisplatin	10.9	7.5×10^{12}	2	Cisplatin (i.p.)	35.8*
20†	1. Paclitaxel, carboplatin 2. Etoposide, ifosfamide 3. Carboplatin	3.9	2.5×10^{13}	3	Carboplatin/paclitaxel (i.v.)	34.3*
21	1. Paclitaxel, carboplatin	10.7	2.5×10^{13}	3	Carboplatin/paclitaxel (i.v.)	32.6*
22†	1. Paclitaxel, carboplatin	4.4	2.5×10^{13}	3	Carboplatin/paclitaxel (i.v.)	32.6
34†	1. Paclitaxel, carboplatin 2. Paclitaxel, cisplatin	3.8	7.5×10^{13}	5	Carboplatin/paclitaxel (i.v.)	27.8
11†	1. Paclitaxel, cisplatin 2. Carboplatin	3.8	2.5×10^{10}	1	None	24*
14†	1. Paclitaxel, cisplatin 2. Paclitaxel, cisplatin	8.2	7.5×10^{12}	1	None	24*
24	1. Carboplatin, cyclophosphamide	13.1	7.5×10^{13}	5	Carboplatin/paclitaxel (i.v.)	23.3‡
35	1. Paclitaxel, carboplatin 2. Topotecan	21.5	7.5×10^{13}	5	Carboplatin/paclitaxel (i.v.)	22.8*
28	1. Paclitaxel, carboplatin	12.3	7.5×10^{13}	5	Carboplatin/paclitaxel (i.v.)	20.0*

PN, particle number.
*Dead of disease.
†Considered platinum refractory.
‡Lost to follow up.

less than .05 were considered statistically significant. Statistical analyses were implemented using the SPSS 10.0 package (SPSS, Chicago, IL).

Results

Patients were grouped on the basis of entry into the single-dose arm (SD; $n=12$) and compared to a cohort who received only multidose (MD) SCH 58500 with chemotherapy (MD1; $n=19$), or MD, that included the five patients re-enrolled on MD following participation in the SD portion of the trial (MD2; $n=24$). The three groups were heavily pretreated with chemotherapy based on the number of prior chemotherapy cycles and regimens. Aside from a longer chemotherapy-free interval for the MD groups, Table 1 shows that there was no difference in the age at diagnosis of the original ovarian cancer, baseline Karnofsky performance status (KPS), number of prior regimens or cycles of chemotherapy, the interval from diagnosis to study entry, the platinum-free interval, mean CA125 or largest CT measurable lesions before dosing with SCH 58500. Platinum-resistant tumor made up 58% of each group. The SD group contained three (25%) patients who had received a

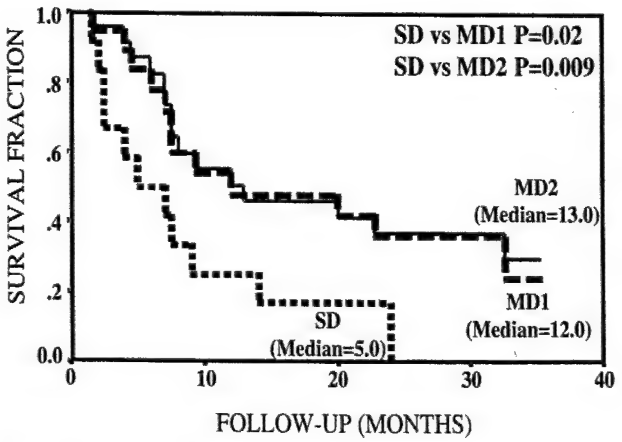

Figure 2 Survival following SCH 58500.

prior single, platinum-continuing regimen with documented complete response to treatment. Similarly the MD1 and MD2 groups each contained six patients (32% and 25%, respectively) who had received a prior single, platinum-containing regimen with documented complete response. Overall, complete responses to one or more platinum regimens were documented for 42%, 42%, and 42% of the SD, MD1, MD2 groups with a mean platinum-free interval of 11.6 [range: 6.7–23.1 months], 12.5 [range: 6.2–21.5 months], 13.3 [range: 6.2–21.5 months]. Platinum resistance could be subdivided into primary/secondary as follows: 25%/25%; 32%/26%; 25%/33% for the SD, MD1, MD2 groups, respectively.

The MD2 group contained 10 (42%) long-term survivors ≥20 months after study entry, as opposed to only 2 (17%) in the SD group. Potentially important parameters that characterize these long-term survivors are summarized in Table 2. Six subjects had received more than two prior platinum-containing regimens. Six of the 12 (50%) could be considered to have platinum-sensitive disease. The platinum-free interval from last treatment with any platinum drug to first dose of SCH 58500 averaged 10.3 months [range: 10.9–21.5 months]. In contrast, the other six patients were considered to have platinum-resistant disease, based on persistent disease after a primary treatment regimen or recurrence less than 6 months after completion of primary or secondary platinum-based therapy (average 4.4 months; range: 3.8–5.5 months). The mean pre-SCH 58500 CA125 was 362 U/dl [range: 53–1298]. Six patients did not have measurable disease on computed tomography (CT) so that the average, largest, CT-measurable lesion was 8.5 cm^2 [range: 0–56 cm^2]. The SD group had only one patient without CT-measurable disease. Three of six patients treated with intraperitoneal cisplatin at 100 mg/m^2 are the three longest survivors at nearly 3 years. None of the three had CT-measurable disease. One of these was considered to have a platinum-resistant cancer. None had a pathologic complete response to this treatment regimen.

Table 3 Treatment of recurrent ovarian cancer

Author	Prior regimens	Agent	Sample size	Median survival [range, mo]
Gershenson*[17]	1	Cisplatin	19	19.3 [5–39]
van der Burg†[19]	>1	Cyclophosphamide/carboplatin	30	12.0 [2–35+]
Vergot‡[20]	not stated	Hexamethylmelamine	61	9+(Responders) 5 (Nonresponders)
Rosen§[21]	1+	Hexamethylmelamine	20	9.3 [3–30+]
Markman¶[1]	1.8	Ifosfamide	57	9 [1–28+]
Eisenhauer‖[23]	1	Paclitaxel: 135 or 175 mg/m^2 over 24 or 3 hours	407	11.4 [1.5–27.4]
Einzig#[24]	1	Paclitaxel	34	27 (Responders) 6 (Nonresponders)
Thigpen**[4]	1	Paclitaxel	49	16.3 [3–27]
Tenbokkel††[2]	1	Topotecan	112	14.2 [0–14.5+]
	1	Paclitaxel	114	10.0 [0.17–6+]
Israel‡‡[3]	1.7	Liposomal doxorubicin	63	10 [0.25–33]
Corn§§[25]	>1	Palliative radiotherapy	33	4.5
Jänicke[10]	1	Secondary cytoreduction	30	2–8–29¶¶
Present study	2.4	SCH 58500‖‖×1	12	5.0 [1.5–24]
	3.0	SCH 58500##+cisplatin±paclitaxel	24	13.0 [1.6–35.3+]

*Progression-free interval from primary treatment 36 months. Seventy-four percent had a surgically documented complete primary response.

†Progression-free interval from previous treatment 12 months. Median prior therapy duration — 12 months, nine cycles. Actual number of regimens not reported: 28/30>4 cm^2 disease.

‡Only patients with progression, or stable disease, or relapse within 6 months after platinum therapy are included. A platinum-resistant population. Median number of platinum-containing courses=6.

§Mean of eight prior courses of cisplatin. Median survival: responders=15.1 months, nonresponders=5.8 months.

¶Platinum resistant population: 44% primary failure, 37% secondary platinum failure after a primary minimal partial response.

‖Measurable disease required for entry. Treatment interval > 6 months, 100% KPS, longer interval from first diagnosis correlate with better survival.

#Measurable disease required.

**Includes both platinum-sensitive (37%) and platinum-resistant (63%) patients. Measurable disease required.

††Includes approximately 53% platinum resistance rate in each arm. Measurable disease required.

‡‡Only 48/63 are epithelial ovarian cancers: 44/48 are platinum resistant; 21/48 have measurable disease.

§§Fifty-seven percent had >1 prior platinum regimens. All with measurable disease. 2/33 develop bowel obstruction.

¶¶Median survival is 29 months for no residual disease or recurrent >12 months after primary treatment. This drops to 8–9 months for <2 cm residual disease or a recurrence <12 months after primary treatment. With >2 cm residual disease, all are dead <8 months, median survival only 2 months.

‖‖Single-dose SCH 58500 escalated from 7.5×10^{10} to 7.5×10^{12} particles/dose.

##Multiple-dose SCH 58500 (2–5 doses/cycle) 7.5×10^{12} to 7.5×10^{13} particles/dose (cycle 1) with cisplatin alone or carboplatin+paclitaxel added in cycles 2 and 3.

Figure 2 shows survival curves for these three treatment groups. The median survival for the SD group was only 5 months [range: 1.5–24 months]. The last two patients died 24 months after dosing. In contrast, there are 10 individuals who lived more than 20 months following the phase II portion of this study. As of 05/21/01, there are still four long-term survivors at 23.3–35.8 months following study entry. Two of the longest survivors were treated on both arms of the study. One individual was lost to follow up at 23.3 months. Median survival for the MD1 group was 12 months [range: 1.6–35.3 months] and 13 months [range: 1.6–35.3 months] for the MD2 group. In both groups, survival was longer than for SD group patients (P=.02; MD1 vs SD, log rank test; P=.009; MD2 vs SD, log rank test).

Discussion

It can be said that there are no cures for recurrent ovarian cancer. Nonetheless, isolated indolent cases of what might be considered "chronic" ovarian cancer are well known to all who treat this disease. In general, unless there has been a prolonged treatment-free interval of two or more years without exposure to platinum-containing chemotherapy regimens, the interim prognosis for recurrent disease is rather dismal.[1–4,10,17–25] None of the patients in the present study had a platinum-free interval of more than 23 months. Only three patients were chemotherapy-free for greater than 12 months before study entry. Two of these were among the 12 long-term survivors. Table 3 presents median survival data for treatment of recurrent ovarian cancer under a variety of conditions. Survival varies from approximately four and a half months for those treated with palliative radiotherapy to as long as 19 months following retreatment with platinum. Several studies[17,18,22] indicate that the longest survival will be associated with the longer platinum-free intervals. This may be secondary to the development of a new cancer due to a field effect, rather than a "late recurrence" of the original disease.[26] Failure to respond to secondary paclitaxel treatment[24] is associated with only a 5-month median survival. This interval, as for those treated with palliative radiotherapy[25] or for hexamethylmelamine nonresponders,[20,21] matches the median survival for our SD SCH 58500 group. In contrast, median survival for individuals treated with multiple doses of SCH 58500 plus platinum-based chemotherapy was 12–13 months. Three individuals treated with intraperitoneal cisplatin and SCH 58500 lived nearly 3 years after dosing and one is still alive at 35.8 months. The heavily pretreated nature of all three groups suggests that the normal advantage to retreatment with the platinum drug plus multidose SCH 58500 may not be fortuitous. Furthermore, most of the patients had rather bulky disease. Jänicke et al[10] have shown that chemotherapy following secondary cytoreduction produces a median survival of only 2 months when residual disease is >4 cm^2. All of those patients expired within 8 months. Fully 23/36 [64%] of the patients in the current study exceeded this tumor volume.

This was not a randomized trial and potential differences between prior and subsequent chemotherapy following completion of SCH 58500 dosing (both SD and MD) may have influenced outcome. Patients in all groups went on to receive a variety of chemotherapy regimens at the discretion of the physicians following SCH 58500. It should be noted that at least 5 of the 12 SD patients were treated on a platinum regimen after dosing with SCH 58500. Furthermore, the survival differences hold true even if the single-dose patients who subsequently were treated with multiple doses of SCH 58500 and chemotherapy are excluded from analysis (SD vs MD1).

None of the patients treated with SCH 58500 could be considered to have had a clinical complete response. Thus, prolonged survival relative to historical controls suggests that either the combination of chemotherapy plus SCH 58500 may be synergistic or that multiple doses of SCH 58500 may affect a change in the nature of the cancer contributing to a chronicity of disease that favorably impacts survival. Because a single dose of SCH 58500 is enough to create a prolonged elevation of antiadenoviral antibody titters,[14] we cannot rule out a potential therapeutic effect of multidosing with SCH 58500 secondary to a peritoneal immune response. The effects of the different chemotherapy regimens (intraperitoneal cisplatin or intravenous carboplatin+paclitaxel) independent of SCH 58500 cannot be evaluated in this already complicated trial. Additional studies suggest that the potential therapeutic benefit for MD patients is independent of platinum retreatment.[27] Further study of this gene-specific agent delivered by a replication-deficient adenoviral vector would appear to be clearly indicated.

References

1. Markman M, Hakes T, Reichman B, et al. Ifosfamide and mesna in previously treated advanced epithelial ovarian cancer: activity in platinum-resistant disease. *J Clin Oncol.* 1992;10: 243–248.
2. Tenbokkel Huinink W, Gore M, Carmichael J, et al. Topotecan versus paclitaxel for the treatment of recurrent epithelial ovarian cancer. *J Clin Oncol.* 1997;15:2183–2193.
3. Israel VP, Garcia AA, Roman L, et al. Phase II study of liposomal doxorubicin in advanced gynecologic cancers. *Gynecol Oncol.* 2000;78:143–147.
4. Thigpen JT, Blessing JA, Ball H, et al. Phase II trial of paclitaxel in patients with progressive ovarian carcinoma after platinum-based chemotherapy: a gynecologic oncology group study. *J Clin Oncol.* 1994;12:1748–1753.
5. Aunoble B, Sanches R, Didier E, et al. Major oncogenes and tumor suppressor genes involved in epithelial ovarian cancer. *Int J Oncol.* 2000;16:567–576.
6. Lynch HT, Casey MJ, Lynch J, et al. Genetics and ovarian carcinoma. *Semin Oncol.* 1998;25:265–280.
7. Griffiths CT. Surgical resection of tumor bulk in the primary treatment of ovarian carcinoma. *Natl Cancer Inst Monogr.* 1975;42:101–104.
8. Hoskins WJ, Rubin SC, Dulaney E, et al. Influence of secondary cytoreduction at the time of second-look laparotomy on the survival of patients with epithelial ovarian carcinoma. *Gynecol Oncol.* 1989;34:365–372.
9. Hoskins WJ, McGuire WP, Brady MF, et al. The effect of diameter of largest residual disease on survival after primary cytoreductive surgery in patients with suboptimal residual epithelial ovarian carcinoma. *Am J Obstet Gynecol.* 1994;170: 974–979.

10. Jänicke F, Hölscher M, Juhn W, et al. Radical surgical procedure improves survival time in patients with recurrent ovarian cancer. *Cancer.* 1992;70:2129–2136.
11. Sood AK, Sorosky J, Dolan M, et al. Distant metastases in ovarian cancer: why do they occur? *Clin Cancer Res.* 1999;5: 2485–2490.
12. Geisler J, Geisler H. Brain metastases in epithelial ovarian carcinoma. *Gynecol Oncol.* 1995;57:246–249.
13. Shahin MS, Hughes JH, Sood AK, et al. The prognostic significance of p53 tumor suppressor gene alterations in ovarian carcinoma. *Cancer.* 2000;89:2006–2017.
14. Buller RE, Runnebaum IB, Karlan B, et al. A phase I/II trial of rAd/p53 (SCH 58500) gene replacement in recurrent ovarian cancer. *Cancer Gene Ther.* 2002;9:553–566.
15. Wills KN, Maneval DC, Menzel P, et al. Development and characterization of recombinant adenoviruses encoding human p53 for gene therapy of cancer. *Hum Gene Ther.* 1994;5:1079–1088.
16. Markman M, Iseminger KA, Hatch KD, et al. Tamoxifen in platinum-refractory ovarian cancer: a gynecologic oncology group ancillary report. *Gynecol Oncol.* 1996;62:4–6.
17. Gershenson DM, Kavanagh JJ, Copeland LJ, et al. Re-treatment of patients with recurrent epithelial ovarian cancer with cisplatin-based chemotherapy. *Obstet Gynecol.* 1989;73: 798–802.
18. Gore ME, Fryatt I, Wiltshaw E, et al. Treatment of relapsed carcinoma of the ovary with cisplatin or carboplatin following initial treatment with these compounds. *Gynecol Oncol.* 1990;36:207–211.
19. van der Burg MEL, Hoff AM, van Lent M, et al. Carboplatin and cyclophosphamide salvage therapy for ovarian cancer patients relapsing after cisplatin combination chemotherapy. *Eur J Cancer.* 1991;27:250–253.
20. Vergote,I, Himmelman A, Frankendal B, et al. Hexamethylmelamine as second-line therapy in platin-resistant ovarian cancer. *Gynecol Oncol.* 1992;47:282–286.
21. Rosen GF, Lurain JR, Newton M. Hexamethylmelamine in ovarian cancer after failure of cisplatin-based multiple-agent chemotherapy. *Gynecol Oncol.* 1987;27:173–179.
22. Markman M, Rothman R, Hakes T, et al. Second-line platinum therapy in patients with ovarian cancer previously treated with cisplatin. *J Clin Oncol.* 1991;9:389–393.
23. Eisenhauer EA, Huinink WW ten Bokkel, Swenerton KD, et al. European-Canadian randomized trial of paclitaxel in relapsed ovarian cancer: High-dose versus low-dose and long versus short infusion. *J Clin Oncol.* 1994;12:2654–2666.
24. Einzig AI, Wiernik PH, Sasloff J, et al. Phase II study and long-term follow-up of patients treated with taxol for advanced ovarian adenocarcinoma. *J Clin Oncol.* 1992;10:1748–1753.
25. Corn BW, Lanciano RM, Boente M, et al. Effective radiotherapeutic palliation after chemotherapy failure. *Cancer.* 1994;74:2979–2983.
26. Buller RE, Skilling JS, Sood AK, et al. Field cancerization: why late "recurrent" ovarian cancer is not recurrent. *Am J Obstet Gynecol.* 1998;178:641–649.
27. Buller RE, Shahin M, Karlan B, et al. Multidose intraperitoneal (IP) rad/p53 (SCH 58500) gene replacement combined with chemotherapy in heavily pretreated recurrent ovarian cancer is associated with prolonged survival. *Proc Am Soc Clin Oncol.* 2001;20:262a.

Cancer Gene Therapy (2002) 9, 553–566

www.nature.com/cgt

A phase I/II trial of rAd/*p53* (SCH 58500) gene replacement in recurrent ovarian cancer

Richard E Buller,[1] Ingo B Runnebaum,[2] Beth Y Karlan,[3] Jo Ann Horowitz,[4] Mark Shahin,[1] Thomas Buekers,[1] Stan Petrauskas,[4] Rolf Kreienberg,[5] Dennis Slamon,[3] and Mark Pegram[3]

[1]Department of Obstetrics and Gynecology, Division of Gynecologic Oncology, The University of Iowa Hospitals and Clinics, Iowa City, Iowa, USA; [2]Department of Obstetrics and Gynecology, University of Freiburg, Freiburg, Germany; [3]University of California, Los Angeles, California, USA; [4]Schering-Plough Research Institute, Kenilworth, New Jersey, USA; and [5]University of Ulm, Ulm, Germany.

Purpose: To determine the safety, gene transfer, host immune response, and pharmacokinetics of a replication-deficient adenovirus encoding human, recombinant, wild-type *p53* (SCH 58500) delivered into the peritoneal cavity (i.p.) alone and sequentially in combination with platinum-based chemotherapy, of patients with recurrent ovarian, primary peritoneal, or fallopian tube cancer containing aberrant or mutant p53. **Methods:** SCH 58500 was administered i.p. to three groups of patients with heavily pretreated recurrent disease. Group 1 ($n=17$) received a single dose of SCH 58500 escalated from 7.5×10^{10} to 7.5×10^{12} particles. Group 2 ($n=9$) received two or three doses of SCH 58500 given alone for one cycle, and then with chemotherapy for two cycles. The SCH 58500 dose was further escalated to 2.5×10^{13} particles/dose in group 2. A third group ($n=15$) received a 5-day regimen of SCH 58500 given at 7.5×10^{13} particles/dose per day i.p. alone for cycle 1 and then with intravenous carboplatin/paclitaxel chemotherapy for cycles 2 and 3. **Results:** No dose-limiting toxicity resulted from the delivery of 236/287 (82.2%) planned doses of SCH 58500. Fever, hypotension abdominal complaints, nausea, and vomiting were the most common adverse events. Vector-specific transgene expression in tumor was documented by RT-PCR in cells from both ascitic fluid and tissue biopsies. Despite marked increases in serum adenoviral antibody titers, transgene expression was measurable in 17 of 20 samples obtained after two or three cycles of SCH 58500. Vector was detectable in peritoneal fluid by 24 hours and persisted for as long as 7 days whereas none was detected in urine or stool. There was poor correlation between CT scans and CA125 responses. CA125 responses, defined as a greater than 50% decrement in serum CA125 from baseline, were documented in 8 of 16 women who completed three cycles of the multidose regimen. **Conclusion:** CT scans are not a valid measure of response to i.p. SCH 58500 due to extensive adenoviral-induced inflammatory changes. Intraperitoneal SCH 58500 is safe, well tolerated, and combined with platinum-based chemotherapy can be associated with a significant reduction of serum CA125 in heavily pretreated patients with recurrent ovarian, primary peritoneal, or fallopian tube cancer.

Cancer Gene Therapy (2002) **9,** 553–566 doi:10.1038/sj.cgt.7700472

Keywords:* p53*; gene therapy; ovarian cancer; CA125

It is projected that 23,400 women will be diagnosed with ovarian cancer and 13,900 will die from this disease during the year 2001.[1] These statistics make ovarian cancer the fifth leading cause of death among women in the United States. Ovarian cancer offers several unique opportunities for novel therapeutic intervention. First, despite the tendency to present at advanced International Federation of Gynecology and Obstetrics (FIGO) stage reflected by the observation that nearly 73% of ovarian cancers are no longer confined to the ovary at diagnosis,[2] this cancer often remains confined within the abdominal cavity throughout its course.[3,4] Second, initial, complete clinical responses are the expected norm following surgical cytoreduction and adjuvant systemic chemotherapy. Unfortunately, recurrence, progression, and death from disease is the eventual outcome for more than 75% of women diagnosed with epithelial ovarian cancer. Finally, because both primary[5,6] and secondary[7,8] surgical cytoreduction are cornerstones of the therapeutic approach to this cancer, tissue samples are often available for molecular genetic studies. Such studies have resulted in a better understanding of some of the molecular changes associated with ovarian cancer and how they may influence prognosis or response to treatment.

Received April 4, 2002.

Address correspondence and reprint requests to: Dr Richard E Buller, Department of Obstetrics and Gynecology, Division of Gynecologic Oncology, 200 Hawkins Drive — #4630 JCP, Iowa City, IA 52242-1009, USA. E-mail: richard-buller@uiowa.edu

Presented in part at the 7th International Conference on Gene Therapy of Cancer, San Diego, CA, November 19–21, 1998 and the 30th Annual Meeting of the Society of Gynecologic Oncologists, San Francisco, CA March 20–24, 1999.

Mutation of the *p53* tumor suppressor gene is one of the most frequent molecular genetic changes in cancer.[9,10] Wild-type p53 functions include roles in DNA repair following G1 cell cycle arrest, and directing irreparably damaged cells toward apoptotic pathways, thus maintaining the integrity of the genome.[11] Both *in vitro* and *in vivo* evidence suggests that cells with altered p53 function may be less responsive to certain chemotherapeutics than those that are able to express wild-type p53.[12,13] p53 dysfunction frequently results from mutations that can generate both missense and nonsense inactivating mutations. Rare gain of function mutations has also been described.[14] Nearly 70% of advanced stage ovarian cancers contain *p53* mutations and many of these mutations render the cancers p53 null.[15-17] Overall, *p53* null mutations can be associated with extremely poor prognosis reflected, at least in part, by early and distant metastasis.[4] These observations suggest that *p53* mutation is of fundamental importance in the progression of ovarian cancer.

Despite the association of distant metastasis with *p53* null mutation, most ovarian cancers usually remain confined to the abdominal cavity throughout their course and provide a unique opportunity for regional delivery of therapeutic agents. Intraperitoneal delivery of chemotherapy can provide a pharmacokinetic advantage over intravenous dosing by maximizing delivery of drug directly to tumor and minimizing systemic side effects.[18] A seminal study by the Gynecologic Oncology Group has demonstrated both response and survival advantage to women with minimal residual disease treated with intraperitoneal (i.p.) cisplatin after primary cytoreductive surgery for ovarian cancer.[19] Thus, ovarian cancer is a unique model for gene replacement strategies.[20,21]

Preclinical studies in several *in vivo* models have shown that delivery of wild-type *p53* to tumor cells can be achieved.[22-31] Extension of these studies, particularly in lung cancer, to phase I clinical trials has produced encouraging results.[32-36] To date, gene transfer in these systems has been accomplished with cationic lipids and a variety of viral vectors including the retroviruses and adenoviruses.[37] The use of an adenoviral vector, which has been rendered replication deficient, offers several advantages for therapeutic gene replacement strategies in cancer.[37] First, in contrast to retroviruses, adenoviral vectors efficiently transduce both dividing and quiescent cells. Second, they can be produced in high titers with particle numbers approaching the number of target cancer cells. Third, a bystander effect has been observed to occur following dosing with adenoviral vectors. Fourth, adenoviral vectors do not integrate into the host genome minimizing concerns regarding insertional mutagenesis. Taken together, these observations encouraged us to undertake a phase I/II trial of human recombinant adenoviral *p53* gene therapy with rAd/*p53* (SCH 58500) in recurrent ovarian cancer. Preliminary results have been presented in part.[38] The objectives of the study were: (a) to determine safety and tolerability to SCH 58500 alone and in combination with chemotherapy, (b) to determine the ability to transfer wild-type *p53* sequences into ovarian cancer cells *in vivo*, (c) to measure serum and ascites antibody responses to this form of therapy along with their influence on gene transfer, (d) to determine the pharmacokinetics of SCH 58500 in ascites and serum, and (e) to evaluate tumor response when multiple doses are delivered to patients over a 3-month period. Our findings indicate that gene transfer of SCH 58500 can be accomplished with minimal toxicity and that reduction in a surrogate marker, CA125, suggests the potential for clinical activity.

Methods

SCH 58500

SCH 58500 is a novel antineoplastic agent consisting of a recombinant adenoviral vector containing the cloned, human, wild-type *p53* tumor suppressor gene cDNA, which is under the control of the human cytomegalovirus immediate early promoter/enhancer element. SCH 58500 is derived from a type 5 adenovirus, a common serotype belonging to subgroup C, which has been rendered replication-defective through deletion of the viral genes E1a, E1b, and protein IX.[39] Vector is produced using GMP standards and has been tested for the presence of viral, bacterial, and other contaminants.

Tumor p53 *mutation status*

For screening, a representative primary or recurrent tumor sample from each patient who had signed informed consent was analyzed for *p53* mutation by immunohistochemistry utilizing both Pab 1801 (diluted 1:40) and Pab 240 (diluted 1:20) antibodies (Pharmingen, San Diego, CA). A positive stain with either antibody was considered to reflect aberrant tumor p53 protein and confirmed eligibility. Although this finding does not always reflect a p53 mutation, most authors consider immunopositive tumor to contain dysfunctional p53.[16] Sections with <10% of cells showing nuclear staining were considered negative. Such individuals were excluded from study entry unless a *p53* DNA sequence abnormality could be documented.[16]

Antiadenovirus antibody assay

An ELISA was used to measure antiadenovirus antibodies specific for adenoviral coat proteins (antihexon antibodies) in serum and ascites. Samples were assayed in parallel with normal human serum and a ratio of sample titer versus normal human serum titer was calculated. If this ratio was less than 0.28 the sample was considered negative.

Patient eligibility and exclusion criteria

Only female patients at least 18 years of age previously treated with surgery and chemotherapy for ovarian, fallopian tube, or primary peritoneal carcinoma now presenting with pathologically confirmed recurrence of disease were eligible. An elevated CA125 was not required for entry. For those individuals without malignant ascites at recurrence, we required surgically documented i.p. disease accessible to laparoscopic or percutaneous biopsy. A tumor *p53* mutation was required as described above. All treated individuals functioned with a Karnofsky performance status of at least 60% and a minimum life expectancy of 3 months. Standardized clinical laboratory tests were within normal limits.

Previous whole abdominal radiotherapy was not allowed. Before the first treatment cycle a contrast study of the abdomen demonstrated free flow of instilled agent. Either a spiral CT with i.p. contrast, or i.p. Hypaque (Nycomed, Princeton, NJ) in 500 mL of normal saline followed in 30 minutes with a conventional flat plate x-ray was used to determine adequate peritoneal distribution of the infuseate. Three eligible, consented patients did not receive treatment with SCH 58500 based on poor distribution of contrast. Initially, only patients serologically positive for antiadenovirus type 5 antibody at screening were treated.

Patients not eligible for the study included those pregnant or nursing, and those with presence of serious bacterial, viral, fungal, or parasitic infection. Patients with evidence of adenoviral infection, as determined by ELISA, at screening were excluded and the chronic use of immunosuppressant therapy or use of another investigational drug within 3 months of proposed treatment with SCH 58500 also resulted in exclusion. Known human immunodeficiency virus (HIV)-positive individuals were also excluded. Short-term bolus use of dexamethasone as an antiemetic, or as premedication for paclitaxel, was allowed.

Registration

An institutional human subjects review board approved informed consent was obtained before the performance of any test or evaluation not considered standard of care for patients with peritoneal carcinomatosis. The same consent detailed the treatment with SCH 58500 and alternatives. No patient received SCH 58500 without signing an informed consent.

SCH 58500 delivery

SCH 58500 was infused over 20 minutes into the peritoneal cavity *via* a Hickman (Bard Systems, Salt Lake City, UT), Tenckhoff (CR Bard, Murray Hill, NJ), or Porta Cath (SIMS Deltec, St. Paul, MN) catheter. In preliminary studies, all catheters were shown to be compatible with SCH 58500. The goals of the infusions were to use a constant volume for each dose, with the volume large enough to generate adequate i.p. distribution, while at the same time providing a tolerable total volume. To achieve these goals, some variability of infusion volumes was required. Patients with clinically significant, preexisting ascites underwent drainage of the ascites before dosing with SCH 58500. Patients in group 1 then received SCH 58500 in 1000 mL of 0.9% NaCl. Group 2 and 3 patients received SCH 58500 in 250 mL, for 2 (Level 4), 3 (Level 5), and 5 (Level 6) days. By the end of five daily administrations (i.e., level 6), a total infusion volume of 1250 mL had been reached. Any additional ascites that accumulated during the course of administration of multiple doses was not removed except in one patient who had a large volume of ascites with her recurrent disease. Following this patient's first dose in cycle 1, the day 2 dose was delayed 24 hours to allow for ascites drainage. In the absence of ascites, each dose of SCH 58500 was infused in 500 mL of 0.9% NaCl so that by the end of five daily administrations (i.e., level 6), a total infusion volume of 2500 mL had been reached. Patients were then rotated every 15 minutes for 2 hours into Trendelenberg, right lateral, left lateral, and sitting positions.

Treatments

This sequential cohort, nonrandomized study, was conducted in three groups of patients. Table 1 outlines the treatment schema for i.p. SCH 58500. For group 1 patients, a single treatment dose of SCH 58500 was escalated from 7.5×10^{10} particles to 7.5×10^{12} particles per dose in four steps. Three patients were to be treated with SCH 58500 at each dose level in this group. The decision to escalate or expand a dose level was based on review of safety data for the patients within the single-dose level cohort under study or after day 7 of the first cycle when multiple cycles were given. A single, potential dose-limiting toxicity (DLT; see Results) prompted us to expand level 2 from three to six patients. After initial safety data were obtained, two additional antiadenoviral antibody negative individuals were allowed to enter at level 1. Therefore, a total of 17 patients were treated in group 1. Patients treated in this group were allowed to enter the multiple-dose group (see below) if they continued to meet all eligibility criteria.

For group 2 patients ($n=9$), cytotoxic chemotherapy was added in cycles 2 and 3 to allow differentiation between SCH 58500 side effects when it was given alone in cycle 1 and those related to its combination with chemotherapy. The dose of SCH 58500 was further escalated to 2.5×10^{13} particles although single-day dosing was increased first to 2 and then to 3 days per treatment cycle. Six group 2 patients received single-agent i.p. cisplatin at 100 mg/m^2 on day 1 of cycles 2 and 3 for dose levels 4 and 5 only. A 30-minute infusion of cisplatin was delivered in 1 liter of 0.9% NaCl 1 hour following the SCH 58500 infusion. The rest of the multiple-cycle patients were treated with intravenous chemotherapy. Paclitaxel at 175 mg/m^2 was infused over 3 hours immediately before SCH 58500 on day 1 whereas carboplatin was infused over 30 minutes immediately after SCH 58500 on day 3 of cycles 2 and 3 at dose levels 5 and 6. The carboplatin dose was based on an area under the curve

Table 1 SCH 58500 treatment regimens

Dose level	Particles delivered	Treatment days	Chemotherapy	Cycles*
Group 1 — single-dose SCH 58500				
1	7.5×10^{10}	1	None	1
2	7.5×10^{11}	1	None	1
3	2.5×10^{12}	1	None	1
4	7.5×10^{12}	1	None	1
Group 2 — escalating-dose SCH 58500 plus chemotherapy				
4	7.5×10^{12}	2	Cisplatin (i.p.)	3
5	2.5×10^{13}	3	Cisplatin (i.p.)	3
5	2.5×10^{13}	3	Carboplatin/Taxol (i.v.)	3
Group 3 — multiple-dose SCH 58500 plus conventional chemotherapy				
6	7.5×10^{13}	5	Carboplatin/Taxol (i.v.)	3

*Treatments were repeated at 28-day intervals.

(AUC) of 6 mg/mL min with the GFR based on the Cockroff-Gault formula for creatinine clearance.[40] With multiple-dose, multiple-cycle regimens, paclitaxel was before the vector because of *in vitro* evidence that this agent enhances transfection efficiency of SCH 58500.[23]

Once safety was confirmed by interpatient escalation, group 3 patients (n=15) were treated with intravenous carboplatin and paclitaxel in combination with SCH 58500 at 7.5×10^{13} particles, dose level 6. The number of doses of SCH 58500 was escalated from 3 to 5 per cycle. For patients in this group, either measurable or evaluable disease was required. Measurable disease was defined as a bidirectionally measurable lesion with clearly defined margins on physical exam or x-ray, computed tomography (CT), or magnetic resonance image analysis. Evaluable disease was defined as an elevated CA125 tumor antigen level greater than two times the institutional norm.

Tumor sampling. Twenty-four to 72 hours following single-dose SCH 58500, or 24 hours after the last dose of SCH 58500 in each multiple dose of the study agent, the peritoneal cavity was drained to obtain tumor cells. Patients who did not have ascites with recurrence of their cancer, or who had inadequate ascites following SCH 58500 dosing, were separately consented to laparoscopy for cycles 1 and 3 to obtain tumor and normal tissue samples for the various PCR studies. Pathologic, or cytologic, examination confirmed the presence of malignant cells in the samples of all patients.

Toxicity. The study design with escalating doses of SCH 58500 was aimed to determine dose-limiting toxicities utilizing standard WHO criteria. Any grade 4 (G1; WHO) toxicity, or a grade 3 (G3) toxicity lasting greater than 1 week, was to be considered dose limiting (DLT), unless the event was obviously related to another procedure (e.g., anemia due to chronic test phlebotomy).

Nausea, vomiting, and anorexia were excluded as dose-limiting toxicities in patients receiving chemotherapy.

Patient monitoring. All single-dose patients were treated as inpatients. A qualitative ELISA kit (Cambridge Biotech, Worcester, MA) was used to confirm the absence of viral shedding in urine and stool samples before dosing, during treatment, and before hospital discharge. Vital signs were obtained before and periodically following the administration of SCH 58500. Physical exams, performance status, weight, and adverse event assessments were performed daily whereas the patients were hospitalized and at prescribed intervals following discharge: Day 7, 14, 21, and 2 months after dosing, then every 3 months until death. Laboratory data included serum and ascites sampling for pharmacokinetic studies, complete blood counts (CBC), fibrinogen, fibrin split products, PT, PTT, serum C_3, C_4, CH_{50}, electrolytes including magnesium, blood glucose, and CA125. Laboratory tests were performed at each visit, except CA125, which was monthly. Baseline abdominal and pelvic computed tomograms were obtained along with a chest x-ray before dosing. Follow-up scans were obtained at 28 days and as clinically indicated for patients who received multiple cycles of SCH 58500. Lesions were measured in two perpendicular directions. Standard response definitions were used, i.e., complete response (CR) required the disappearance of all gross evidence of disease for at least 4 weeks; partial response (PR) required a reduction in lesion size in excess of 50% lasting at least 4 weeks; progressive disease was said to have occurred on the basis of a 25% increase in lesion size; all other measurable disease cases were considered to define stable disease (SD). As an additional measure of response, changes in serum CA125 were evaluated. The 50% and 75% CA125 responses as defined by Rustin et al[41,42] have been shown to correlate well with conventional CT response measures.

Documentation of gene transfer and viral persistence. Total RNA was extracted and cDNA prepared from ascites or tissue biopsies. The QIAamp 96 Spin Blood Kit (Qiagen, Valencia, CA) was used to extract viral DNA from serum. Polymerase chain reactions were carried out utilizing primers specific for both the adenovirus and the *p53* gene as well as β-actin or glyceraldehyde 3-phosphate dehydrogenase (G3PD) collectively referred to as housekeeping genes or HKG. The MIMIC® (Clontech, Palo Alto, CA) reverse transcriptase technique allowed for semiquantitative comparisons of mRNA levels. Tripartite leader sequence-specific primers permitted the resolution of SCH 58500 sequence from host p53 sequence (See Results).

In situ *PCR.* Five-micrometer sections of formalin-fixed, paraffin-embedded tissue were placed on 1.2-mm silane-coated Perkin-Elmer (Foster City, CA) *in situ* PCR glass slides. Slides were baked 2–3 hours at 60°C to reduce RNA content. Slides were then treated sequentially with 0.02 N HCl, Proteinase K, and acetic acid. Thirty-five PCR cycles were carried out using dinitrophenyl-labeled primers (DNP) specific for SCH 58500. Following incubation with anti-DNP antibody conjugated to alkaline phosphatase, visualization was achieved by adding nitro-blue tetrazolium-5-bromo-4-chloro-3-indolyl phosphate as substrate and counterstaining with Nuclear Fast Red. Negative staining was pink, whereas positive staining was blue and nuclear.

Statistics. Differences in toxicities between SCH 58500 and SCH 58500 plus chemotherapy cycles were evaluated with Fisher's Exact test, 2-tailed. Mean CA125 changes were analyzed by ANOVA, or t tests as appropriate. A P value of $<.05$ was required for significance.

Results

Patient selection and characteristics

One hundred and fifty-five patients signed informed consent and entered into screening at three sites. Overexpression of p53 protein by immunohistochemistry was demonstrated for 79 of the 155 (51%) cancers tested. The Iowa site carried out p53 gene sequencing on 25 of 28 p53 immunonegative cancers screened at that institution. An additional 8 patients (7 with *p53* null mutations) met the p53 eligibility criteria in this fashion. So that 57% (88/155) of patients screened were eligible for entry. Overall, 36 patients were dosed with SCH 58500. Five patients were treated on both the single-dose arm of the study and the later multiple-dose program. Therefore, 41% (36/88) of the eligible patients representing

23% (36/155) of the patients screened were actually treated with SCH 58500. The mean age of the individuals dosed was 60 years (range: 39–76). Demographic and disease-related parameters for this cohort of heavily pretreated individuals with recurrent peritoneal carcinomatosis are summarized in Table 2. Most individuals had recurrent ovarian cancer. The mean interval from primary diagnosis to dosing with SCH 58500 was 778 days (range: 115–2360 days). The mean platinum-free interval to dosing with SCH 58500 was 263 days (range: 37–711 days). Nine of 36 patients had a platinum-free interval of more than one year. The mean number of prior chemotherapy regimens was 2.8 with 22% of individuals receiving four or more prior regimens and 33% receiving just one prior regimen. All individuals had previously received platinum-based chemotherapy, and all but two had prior treatment with a taxane. Three patients had recurrent disease evaluable only on the basis of laparoscopic biopsy. Fourteen patients could be considered to have small-volume disease, arbitrarily defined as less than or equal to 2 cm.

Toxicity

Two hundred and thirty-six different signs or symptoms were recorded as adverse events. These varied from single patient WHO grade 1 (G1) events such as increased earwax and nonspecific breast complaints to a G4 transient ischemic attack. Because adenoviral particles delivered in this study are more than a log higher than in any previously reported gene therapy trial, great attention was paid to complete reporting of all potential adverse events. From a practical standpoint, we have chosen to present all serious G3 or G4 events, but only the G1 and grade 2 (G2) events that occurred in three or more treated individuals. This of course underreports the total number of minor adverse events. Each treatment-related adverse event is recorded as the highest-grade toxicity experienced out of all treatment cycles received by that patient as explained in the legend to Table 3. The events are listed in this table on the basis of occurrence in either the single-dose or multiple-dose groups. To show that there was no cumulative toxicity, we have listed the five patients who were treated with multiple-dose SCH 58500 after completion of the single-dose portion of the study separately. The most common adverse events in the single-dose group included fever (47%), nausea (41%), edema (41%), abdominal complaints (41%), and anemia (29%). Seven patients experienced ≥5 different adverse events whereas only 1 patient had no adverse events at all. Eight G3 or G4 adverse events were reported in four patients. These included anemia (2:G3; 1:G4), abdominal complaints (1:G3), dehydration (1:G3), pain (1:G3), tachycardia (1:G3), and vomiting (1:G3). There was no unusual toxicity in the two serum antiadenoviral antibody negative patients dosed at level 1.

Fever was also the most common adverse event experienced by 100% of the multiple-dose patients. This sign developed within 2 to 4 hours of dosing. The highest reported temperature was 40.5°C. Four cycles were accompanied by G3 febrile responses (>40°C) among two different patients. After fever was noted in the initial dosing cohorts, patients were generally given prophylactic acetaminophen. The subsequent febrile responses were attenuated, but this may also have been due to the steroid premedication given before chemotherapy for cycles 2 and 3. Figure 1 demonstrates this observation graphically for a patient treated at dose level 5. In the multidose cohort, the next most frequent signs and symptoms related to SCH 58500 included hypotension (89%), a variety of abdominal complaints (79%), hypertension (68%), nausea (63%), tachycardia (58%), vomiting (58%), and fatigue (53%) — often in the same patient and cycle as the hypertension was noted. The blood pressure changes prevalent in this group were not seen at all in the single-dose group, but they were generally considered mild because only one G3 toxicity occurred. All of these most common adverse events, except hypertension, also occurred in 100% of the single-dose patients who reenrolled in the multiple-dose regimen. However, there was no progression of toxicity grade in those re-treated relative to those initially treated at the same dose of SCH 58500.

Forty-seven G3 or G4 toxicities were reported in 13 patients who received multiple-dose SCH 58500. Many of the new WHO G3 toxicities were probably related to chemotherapy because they usually appeared in cycles 2 and 3. The patient with congestive heart failure also developed a G4 neutropenia with concomitant thrombocytopenia in cycle 3. A few new low-grade adverse events were reported when chemotherapy was combined with SCH

Table 2 Study cohort demographics

Primary diagnosis	
Ovarian cancer	30
Peritoneal cancer	5
Fallopian tube cancer	1
Prior chemotherapy	
Mean number of regimens	2.8 range [1–8]
Mean treatment cycle	13 range [5–31]
Mean drugs × cycles	24.4 range [8–78]
SCH 58500 treatment	
Single dose	17
Multiple dose	24
Both	5
Interval: (days)	
Diagnosis to SCH 58500	777.7 range [115–2360] median=630
Platinum-free to SCH 58500 first dose*	263 range [37–711] median=261
Disease status	
Elevated CA125	33
CT measurable lesions†	
>2 cm	22
≤2 cm	5
Normal CA125 and CT scan	3

*The platinum-free interval for nine patients was ≥365 days.
†All CT-measurable disease was accompanied by an elevated CA125.

Table 3 Treatment-related adverse events*

Adverse event	Single-dose SCH 58500 (*N=17*)				Multiple-dose SCH 58500 (*N=19*)				Single- and multiple-dose SCH 58500 (*N=5*)			
	G1	G2	G3	G4	G1	G2	G3	G4	G1	G2	G3	G4
Abdominal complaints†	4	2	1	0	4	4	7	0	2	1	2	0
Anxiety	0	0	0	0	2	0	0	0	2	0	0	0
Anemia	1	1	2	1	0	3	1	0	0	0	1	1
Anorexia	1	0	0	0	5	0	1	0	2	0	0	0
Asthenia	0	0	0	0	2	4	2	0	2	0	0	0
Bradycardia	0	0	0	0	0	0	1	0	0	0	0	0
Chills	1	0	0	0	7	3	0	0	0	0	0	0
Cellulitis (Port)	1	0	0	0	3	1	0	0	0	1	0	0
CHF	0	0	0	0	0	0	1	0	0	0	0	0
Dehydration	0	0	1	0	2	0	0	0	0	0	1	0
Diaphoresis	2	0	0	0	2	0	0	0	0	0	0	0
Diarrhea	0	1	0	0	7	0	1	0	1	0	1	0
Dizziness	1	0	0	0	3	2	0	0	2	0	0	0
Dyspnea	1	0	0	0	3	1	0	0	0	0	0	0
Edema	6	1	0	0	0	1	1	0	1	0	0	0
Fatigue	2	2	0	0	3	3	4	0	2	3	0	0
Fever	3	5	0	0	1	16	2	0	2	3	0	0
Gastritis	0	0	0	0	0	0	1	0	0	0	0	0
Headache	0	0	0	0	8	1	0	0	1	0	0	0
Hypertension‡	0	0	0	0	10	3	0	0	1	1	0	0
Hypotension§	0	0	0	0	11	3	2	0	4	1	0	0
Lethargy	0	0	0	0	0	1	1	0	0	0	0	0
Loss of Consciousness	0	0	0	0	0	0	1	0	0	0	0	0
Malaise	1	0	0	0	3	4	2	0	2	0	0	0
Nausea	7	0	0	0	2	3	7	0	1	1	3	0
Neutropenia	0	0	0	0	0	0	0	1	0	0	0	0
Pain¶	1	2	1	0	4	2	1	0	0	2	0	0
Peritonitis	0	0	0	0	0	0	2	0	0	0	0	0
Tachycardia	1	0	1	0	11	0	0	0	5	0	0	0
Thrombocytopenia	0	0	0	0	0	0	0	1	0	0	0	0
TIA	0	0	0	0	0	0	0	1	0	0	0	0
Vomiting	4	1	1	0	2	3	6	0	2	2	1	0

*All WHO G3 or G4 toxicities and any toxicity, including G1 and G2 reported by three or more patients. Values are number of patients with a given event in each group. Only the worst toxicity level is reported for each patient, i.e., a G2 fever in cycle 1, G1 in cycle 2, and G3 in cycle 3 appears as a single entry, G3.

†Includes abdominal enlargement, bloating, contractions, cramping discomfort, distention, fullness, pain, pressure, or tenderness.

‡Hypertension: G1=asymptomatic transient increase by greater than 20 mmHg or to >150/100 if previously within normal limits; no treatment required. G2=recurrent or persistent increase by greater than 20 mmHg or to >150/100 if previously within normal limits; no treatment required. G3=requires therapy. G4=hypertensive crisis.

§Hypotension: G1=≥20 mmHg decrease in SBP or DBP requiring no therapy (including transient orthostatic hypotension). G2=≥20 mmHg decrease in SBP or DBP requiring fluid replacement or other therapy but not hospitalization. G3=requires therapy and hospitalization. G4=life-threatening.

¶Includes pain, back pain, breast pain, chest pain, substernal chest pain, or flank pain.

58500. These included lower extremity myalgias, myoclonus, ileus, gastritis with hematemesis, hyperactive bowel sounds, pulmonary hypertension, peripheral neuropathy, oliguria, mucositis, port site cellulitis, agitation, generalized weakness, and cachexia. Only three multiple-dose patients had ≤3 adverse events whereas 11 reported ≥10 adverse events. Overall, G3 toxicities accompanied approximately one-third of the treatment cycles. Antiemetics generally alleviated the gastrointestinal symptoms and were used prophylactically at the investigator's discretion. As the total amount of SCH 58500 delivered was increased, there was a trend toward more G3 adverse events: the number of adverse events went from 0.5 to 1.6 to 2.9 per patient as the treatment was advanced from single dose to level 4/5 and then to level 6. The addition of chemotherapy produced additional nausea and vomiting (P=.03, Fisher's exact test, 2-tailed). There was no trend for adverse events to worsen in a given individual as the number of doses delivered was increased. Likewise, there was no evidence of cumulative toxicity as patients progressed from the single-dose arm to treatment with multiple doses and multiple cycles.

One G4 toxicity occurred in a patient who became anemic in cycle 2. This complication along with the other G3 toxicities due to anemia occurred in individuals who were anemic at the start of the study and has been attributed to the volume of blood drawn for the multiple laboratory studies,

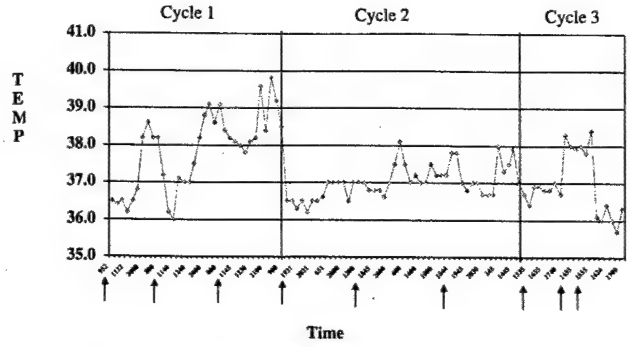

Figure 1 Typical febrile response to SCH 58500 over time with multiple doses and cycles. † indicates dose of i.p. SCH 58500 delivered. SCH 58500 toxicity by treatment cycle.

anemia of chronic disease, and anemia secondary to chemotherapy treatments. There was no evidence of hemolysis in any patients. One individual with liver metastasis and progressive disease following single-dose SCH 58500 at level 2 developed a potential DLT reflected by an increase in alkaline phosphatase from 57 U/L at baseline to 742 U/L 28 days following dosing. This was accompanied by an increase in AST to 106 U/L and ALT to 111 U/L. She refused a follow-up CT scan and died 51 days after dosing. The family declined a request for an autopsy. Because of this adverse event, three additional patients were treated at this dose level before moving on to level 3. Therefore, although one cannot rule out SCH 58500 as a cause of this potential DLT, the investigator felt that the clinical course of this patient was quite consistent with progression of disease as the proximal cause of these events. Supporting this conclusion was the additional observation that no other patient, at any dose, developed evidence of G3 or G4 hepatic toxicity. Five individuals (14%) developed potentially worrisome small bowel obstructions between 2 and 8 months after initial dosing. These events occurred both on the single-dose (n=2) and multiple-dose (n=3) arms. Only one episode was attributed to SCH 58500, rather than to disease progression and/or underlying adhesions. All five resolved with conservative nonsurgical management. Two i.p. catheter-related infections also complicated treatment and led to patient removal before completion of the anticipated number of cycles. Both were associated with abdominal Hickman (Bard Systems, Salt Lake City, UT) catheters. One of these individuals developed vancomycin-resistant enterococcal peritonitis. She was found to be a nasal carrier of this organism. Another individual developed a sterile pelvic abscess. Both patients received only five doses of SCH 58500 alone before withdrawal from the multiple-dose arm. Overall, 82.2% of the planned doses of SCH 58500 were delivered. In addition to the catheter problems outlined above, failure to complete the planned number of cycles of chemotherapy plus SCH 58500 resulted from disease progression (two patients), side effects (one patient), and a withdrawn consent (two patients).

Pharmacokinetics. SCH 58500–specific PCR was carried out on serum samples of all patients during cycle 1. Samples were obtained pretreatment at 15, 30 minutes, 1, 2, 4, 6, 12, 24, 36, 48, and 72 hours; and days 7, 14, 21, and 28 following administration of SCH 58500. Detectable serum levels of SCH 58500 were found in seven patients. In four of these, the levels were detectable but not quantifiable. Only one patient had a quantifiable level after 24 hours. There was no vector shedding in either urine or stool of any patient as determined by ELISA assay. One patient underwent a therapeutic thoracentesis 72 hours after dosing with SCH 58500 on the single-dose arm. The pleural fluid was positive for vector by ELISA. Patient peritoneal fluid analysis consistently demonstrated the presence of viral DNA for 24 hours. For a subset of three patients, viral DNA was detected on day 6 for one patient and day 7 for two. ELISA positive peritoneal fluid was noted for periods in excess of 1 year following the last dose of SCH 58500. However, we were unable to culture live virus or demonstrate infectivity by the FACS assay[43] from the prolonged ELISA positive fluid.

Tumor sampling

Following cycle 1, 22 patients had ascites sampled, 5 had a laparoscopic biopsy, and 11 had both. Only ascitic fluid was sampled after cycle 2. Following cycle 3, 8 patients had ascitic fluid sampled, 5 underwent laparoscopic biopsy, and 1 had both procedures.

Determination of gene transfer

The unique tripartite leader sequence incorporated into the recombinant *p53* gene sequence allowed us to differentiate

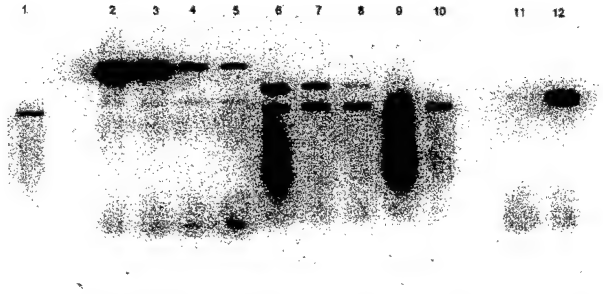

Figure 2 MIMIC® PCR assessment of gene transfer. The numbers correspond to lane numbers in a 3% agarose gel. Total RNA was extracted from a tumor biopsy obtained laparoscopically from a patient 72 hours after administration of a single dose of 2.5×10^{12} particles of SCH 58500. For this sample, the effect of serial dilution of β-actin message template cDNA prepared from tissue RNA and added to a MIMIC® PCR reaction is reflected by the decreasing intensity of the upper band in lanes 2–5 of the agarose gel. A precisely calculated amount (500 molecules) of β-actin MIMIC® has been spiked into the PCR reaction and results in the generation of the lower band in the same lanes. Lanes 11 (500 molecules of β-actin MIMIC®) and 12 (100,000 molecules of β-actin MIMIC®) have been used for quantitative calculations. Similarly 500 molecules of the p53 MIMIC® have been spiked into the PCR reactions run in lanes 6–8 from serial dilutions of the template cDNA. In these lanes the MIMIC® product is the lower band and corresponds to the single band in lane 1 (500 molecules of p53 MIMIC® without template cDNA). The upper band in lanes 6–8 represents p53 product containing the tripartite leader. In the absence of transfection, as in lanes 9 and 10, no upper band is seen because the wild-type p53 sequence does not contain sequence that will bind the leader sequence specific primers.

mRNA expression due to transduced *p53* gene from any host wild-type p53 mRNA co-isolated from contaminating normal cells. Figure 2 shows a gel containing both sample and MIMIC® PCR reaction that demonstrates this principle. The equivalence of band intensities in lane 7 at a 1:4 dilution of template cDNA allows for the calculation of the number of molecules of p53 mRNA isolated from the sample normalized for the sample β-actin message content. In this case 1.6 molecules of p53 transgene mRNA per 1000 molecules of β-actin message were detected. Similar studies were carried out using mRNA isolated from cells separated from ascites or from biopsies obtained at the indicated times and cycles for all patients treated. Figure 3 summarizes these results. Transgene expression was seen at doses as low as 7.5×10^{10} particles and consistently at or above 7.5×10^{11} particles per dose. Three samples were negative for β-actin and were excluded from this analysis. In two cases samples thawed during shipment. In another patient, a tumor biopsy obtained at day 3 was negative; however, her ascites was positive at day 7. Overall, transgene expression at the RNA level occurred in 3 of 5, 4 of 4, 3 of 3, 8 of 11, 9 of 11, and 25 of 28 samples analyzed for SCH 58500 doses of 7.5×10^{10}, 7.5×10^{11}, 2.5×10^{12}, 7.5×10^{12}, 2.5×10^{13}, and 7.5×10^{13} particles per dose, respectively. The most significant observation from this analysis is that transgene expression was detectable in 17 of 20 (85%) samples following multiple dosing with SCH 58500.

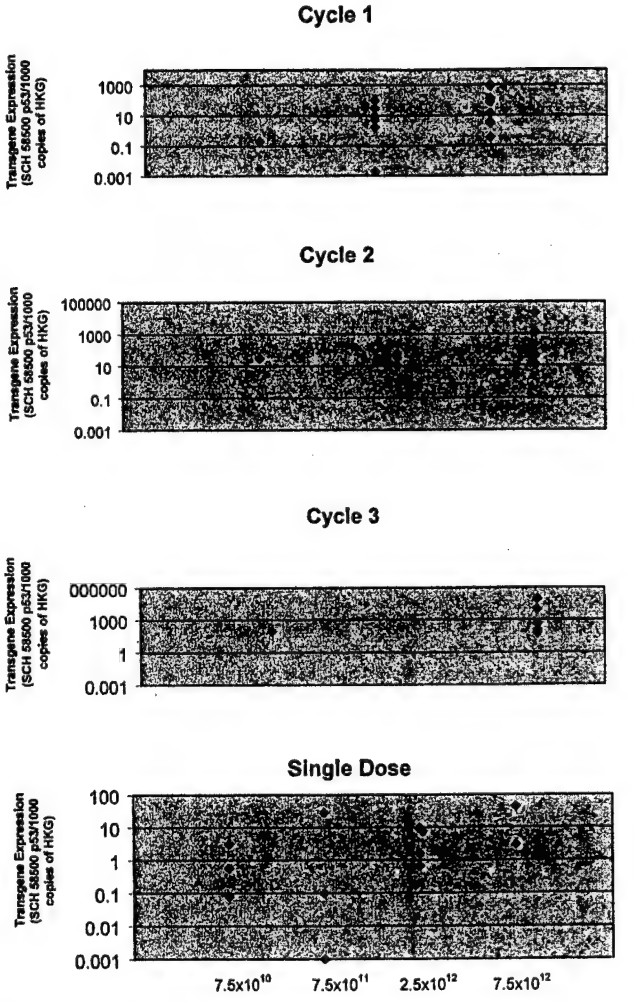

Figure 3 *p53* gene transfer following multidose i.p. delivery of SCH 58500. MIMIC® PCR reactions were carried out as described in the legend to Figure 1. Measurable levels of mRNA are plotted in the graphs according to cycle and dose of SCH 58500. Seven additional samples were RT-PCR positive, but at expression below levels that could be quantitated. Only 9 of 62 samples expressing β-actin were negative for p53 transgene expression.

Demonstration of vector-encoded DNA in tumor target cells

The RT-PCR transgene expression data presented above were generated from ascitic fluid cell pellets or tissue biopsies. Such samples may contain normal cells as well as tumor cells. Thus, whereas we have clearly demonstrated transgene expression in our biopsy and ascitic fluid samples, we have not demonstrated the presence of either agent or transgene product from within tumor cells. To achieve this goal, *in situ* PCR was carried out on sequential tissue samples from a single patient. The primers used were specific for SCH 58500. Figure 4A shows a sample obtained before dosing with SCH 58500. The pink stain indicates the absence of viral DNA. This contrasts with the blue nuclear stain of the sample shown in Figure 4B obtained after three cycles of SCH 58500. A negative control is shown in Figure 4C wherein *Taq* polymerase was omitted from the reaction. These results clearly demonstrate the presence of viral DNA within tumor cells. Finally, Figure 4D shows a hematoxylin and eosin stained section corresponding to the tissue sample in panels B and C. In this figure, apoptotic bodies and dying tumor cells are readily differentiated from healthy tumor cells deeper within the biopsy.

Antiadenoviral antibody response

Baseline serum antiadenoviral antibody titers ranged from 1:160 to 1:16,000 before the first dose of SCH 58500. A 2-fold rise in titer could be seen by day 3 following i.p. SCH 58500. Increases in titer on day 28 ranged from 2- to 1600-fold over screening values. For patients enrolled in the multiple-dose regimens, or those re-treated with SCH 58500, a transient decrease in antibody titer on the order of 2- to 4-fold was sometimes seen. Twelve- to fifty-fold increases over the baseline titer were observed for up to 11 months following a single dose of SCH 58500. With multiple dosing, continued increases in titer were measured to as high as 1:2,560,000. An immune response was documented in one of the two individuals treated at level 1 who entered with negative titers. There was no apparent correlation between change in antibody titer and alterations in CA125 levels (see below). Likewise, there was no correlation between the dose of SCH 58500 and the mean change in antibody titer or the mean change in antibody titer with transgene expression (data not shown).

Measures of response

Table 4 compares conventional CT response determinations to the change in CA125 measured from study entry to study

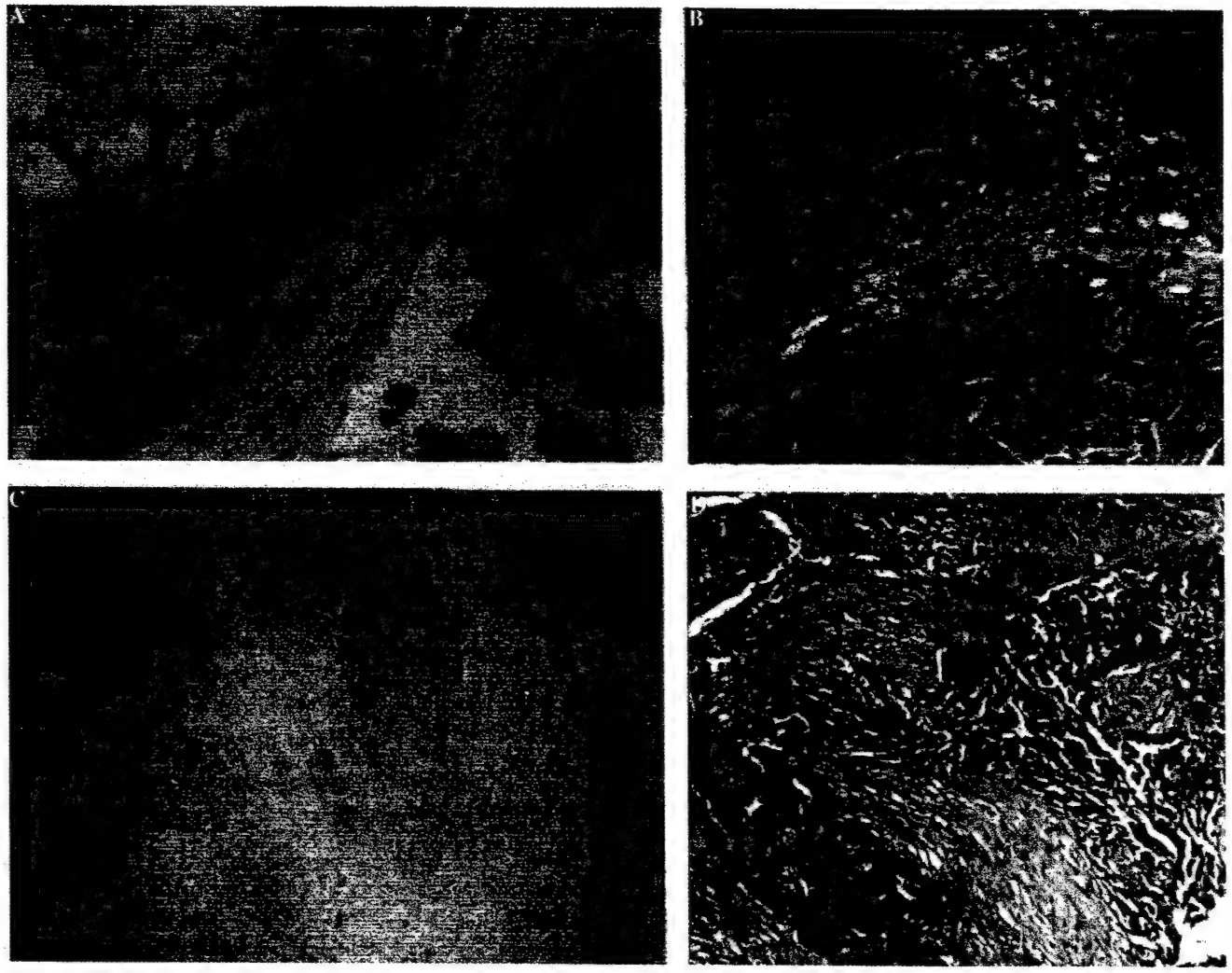

Figure 4 Analysis of tumor biopsies after i.p. SCH 58500. *In situ* PCR measurement of viral DNA. **Panel A:** Biopsy from a patient before SCH 58500 (×400). **Panel B:** Biopsy from a patient after three cycles of SCH 58500 (×200). **Panel C:** 5-μm section from the same sample as **(4-B)** but a negative control based on omission of Taq polymerase from the PCR reaction (×40). **Panel D:** An H and E section from the same sample (×200).

exit. Three tumors, all in group 1, were CA125 negative (<35 U/dL) at the time of enrollment. Although all three had biopsy-proven recurrence of disease, none had CT-measurable disease either. Six other individuals with elevated CA125 levels did not have CT-measurable disease at study entry. Two individuals without CT-measurable disease were treated in both group 1 and group 2. There were no CR or PRs documented by CT scan. On the contrary, the best CT responses were four cases of SD, three from group 1 and one from group 2. The most striking feature of the follow up CT scans was the frequency that disease progression was called on the basis of the development of new lesions — documented in 18 treatment regimens. For nine of these cases, apparent disease progression was accompanied by at least a 26% decrease in CA125 from baseline. In several of these cases, apparent CT progression was found at laparoscopy to represent a pocket of inflammatory cells. Five of nine patients treated in groups 2 and 3 with purported CT disease progression demonstrated at least a 50% CA125 response. In contrast, for six of nine group 1 patients, the development of new CT lesions was accompanied by at least a 25% increase in CA125 disease. Together these observations are consistent with the hypothesis that the new CT lesions often occurred due to SCH 58500–induced inflammatory changes rather than disease progression. This conclusion prompted us to carry out a more detailed analysis of the response to SCH 58500 on the basis of the associated CA125 change from baseline.

Serum CA125 levels were measured immediately before dosing with SCH 58500 and following each treatment cycle. Two of the three patients with baseline CA125s <35 U/dL more than doubled their CA125 during study. CA125 could thus be considered a valid response parameter for all but a single patient. In addition, it is clear that the inflammatory response initiated by SCH 58500 did not uniformly give rise to an increase in CA125 by itself. The percent change in CA125 was then calculated for each individual for each treatment cycle, and overall at 28 days after study

Table 4 Relationship of CT-based response to CA125 response

Treatment regimen	Best response	Cases	CA125 change			
			>+25%	+24% to −25%	−26% to −74%	>−75%
Single-dose SCH 58500	SD	3	–	1	2	–
	PD	3	3	–	–	–
	PD^n	9	6	1	1	1
	NM	2	1	1	–	–
Multiple-dose SCH 58500	SD	1	–	1	–	–
	PD	9	3	4	1	1
	PD^n	9	2	–	3	4
	NM	5	2	1	–	2

SD=stable disease; PD=progressive disease by enlargement of response lesion; PD^n=progressive disease by virtue of new lesions; NM=no measurable disease.

completion. Comparison of CA125 levels following treatment with SCH 58500 alone at $\leq 2.5\times10^{11}$ particles/dose to treatment at $\geq 2.5\times10^{12}$ particles/dose demonstrated a mean increase in serum CA125 of 94% versus a mean decrease of 8.5% at the higher dose (P=.07, 2-tailed, unequal variances). Thus, SCH 58500 alone at higher doses provides a favorable change in CA125 not seen at lower doses of vector. Figure 5 summarizes the CA125 response data. Dosing with SCH 58500 alone resulted in a mean decrease in CA125 of 33.6% for the 16 of 41 women whose CA125 levels declined during the 28 days following dosing. These declines ranged from 4% to 77%. One additional patient's CA125 was unchanged at 46 U/mL. In contrast, with the addition of chemotherapy for cycle 2, 15 of 18 women demonstrated a mean decrement of 47.7% in their pre-cycle 2 CA125 levels. This result indicates enhanced CA125 response over treatment with SCH 58500 alone. For cycle 3, 11 of 16 of treated women showed a mean decline in CA125 levels of 36.6% compared to cycle 2 day 28 CA125. Thus, a continued response was seen in excess of that seen with SCH 58500 alone. Overall, 2 of 14 women demonstrated a 50% or greater decline in CA125 following a single dose of SCH 58500. For the 16 women who completed all three multiple-dose cycles, 8 registered a CA125 decline ≥54% from study entry. Among all responders, the average decline in CA125 was 60.1% (P=.06 vs SCH 58500 alone). Favorable changes in CA125 levels were independent of the time interval from initial diagnosis to SCH 58500 dosing. Likewise, the number of prior treatment cycles and regimens did not preclude a CA125 response and there was no apparent relationship between transgene expression and CA125 response.

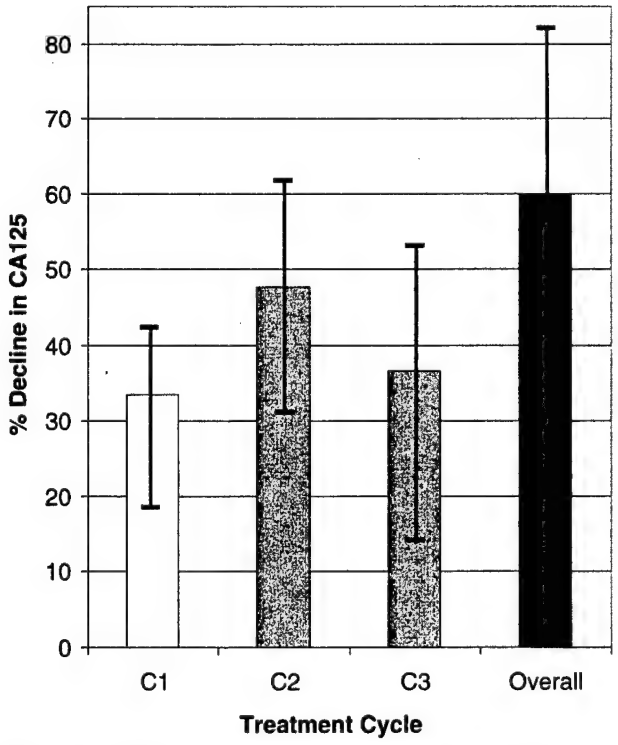

Figure 5 CA125 responses following treatment with SCH 58500. In cycle 1 (C1: □) all patients received SCH 58500 alone. Cycles 2 and 3 (C2, C3: ■) includes all patients who received chemotherapy in addition to SCH 58500. The mean decline in serum CA125 was calculated for responders only. Overall (▨) is the average percent decline at the end of the study for individuals who responded relative to their screening CA125 level. In each case, CA125 is measured over a 28-day interval or at the beginning of the subsequent treatment cycle. The error bars are 95% confidence limits of the mean.

Discussion

Because p53 tumor suppressor gene dysfunction is seen in 50–60% of all human malignancies,[9,10] this gene has become a leading candidate for clinical studies involving gene transfer technology for the treatment of cancer. Preclinical studies utilizing a variety of cell lines have shown efficient transduction, cell cycle arrest, apoptosis, and enhanced cell death following treatment with adenoviral constructs containing wild-type *p53* gene sequence alone and in combination with cytotoxic chemotherapy.[22-31] Although some evidence suggests that this effect may not be solely dependent on the presence of mutant p53, others have found greater efficacy when the endogenous p53 is mutant.[31,44] Results from *in vitro* xenograft models of several malignancies, including ovarian cancer, suggest

promise for the strategy of *p53* gene replacement as a novel cancer therapeutic approach.[25,30,31,45] There is no apparent effect of wild-type p53 overexpression on normal tissue such as fibroblasts.[46] Of particular relevance is the preclinical observation that the effects of *p53* gene replacement are synergistic with both cisplatin and paclitaxel, the two mainstays of ovarian cancer chemotherapy.[22,23,30] Most clinical data to date with *p53* gene replacement are limited to intratumoral injections,[32-36] in contrast to the body cavity exposure of the large surface area of the peritoneal cavity exposed to SCH 58500 in the present study. Finally, although carcinogenesis clearly involves multiple gene defects, data support a therapeutic approach that corrects only a single, critical gene defect.[47,48]

Intraperitoneal therapy of ovarian cancer was initially reported in 1955 by Weisberger et al.[49] In the past 5–10 years encouraging results from the i.p. delivery of a variety of chemotherapeutics and biologics have been reported both for primary therapy and for small-volume recurrent or persistent disease.[19,50-55] These studies have suggested the importance of treating small-volume disease and have established safety and symptom data to which one can then compare results of i.p. gene therapy. Indeed, encouraged by these data, phase I trials of the herpes simplex thymidine kinase/ganciclovir system,[56-58] and adenoviral E1a gene therapy,[59] have been initiated for recurrent ovarian cancer. Early results of phase I/II retroviral and adenoviral *BRCA1* i.p. gene replacement have also been published.[60,61]

Several potential limiting factors associated with i.p. drug delivery of gene therapy *per se* have been identified. For example, the uniformity of drug distribution is always of concern. For the present study, all patients were required to have widespread i.p. distribution verified by a pretreatment radiologic study before initial dosing. The fraction of the cancer cells that needs to be transduced in order for a clinical effect to be measured is unknown. It is clear that not all tumor target cells will be transduced, especially with a single administration of vector because the depth of penetration into tumor appears limited.[62] Furthermore, there is concern that the accumulation of adhesions and the host immune response may prevent effective gene transfer with repetitive dosing of a viral vector. In the present study, multiple laparoscopies on the same patient provided the opportunity to demonstrate that individual inflammatory response was highly variable and that peritoneal distribution can clearly change over time.

The present study was designed to determine the safety of the SCH 58500 adenoviral vector delivered into the peritoneal cavity of women with refractory ovarian cancer. No maximum tolerated dose (MTD) was established as the protocol-defined DLT was not met. The doses delivered ranged from 7.5×10^{10} to 7.5×10^{13} particles per i.p. infusion. The highest dose tested was limited by practical considerations including the i.p. delivery volume for multiple-day dosing regimens. Tolerance to SCH 58500 was excellent with manageable toxicity. Aside from fever, the toxicity profile, even with multiple cycles was similar to that reported for i.p. chemotherapy in general.[19,50,51] Overall, 82.2% of the planned doses were delivered and this included 219 of 270 (81%) doses on the multiple-dose/multiple-cycle regimens. By way of comparison, 84% of the planned i.p. chemotherapy was delivered in a similarly sized study by Morgan et al[51] whereas 76.8% of the planned i.p. cisplatin doses were delivered in the large cooperative group study reported by Alberts et al.[19] Progression of disease was the most common reason for incomplete dosing rather than side effects in the present study.

Vector-specific gene transfer and mRNA expression of SCH 58500 was seen at doses as low as 7.5×10^{10} particles/single dose and was frequently detected in patients that received 7.5×10^{11} particles/dose. It seemed desirable to increase the dose level and number of doses to a maximum based on the theoretical tumor burden within the peritoneal cavity and the need to maximize exposure of tumor cells to SCH 58500. Preclinical modeling indicated that multiple fractionated doses of SCH 58500 had greater efficacy than a single bolus injection.[22]

Early concerns that the presence of serum neutralizing antibodies to the adenovirus might limit its effectiveness, particularly with repetitive exposure are not borne out by our results.[63] Preclinical work with immunized rodents treated with intratumoral injection of an adenoviral vector expressing IL-12 demonstrated minimal reduction in transfer efficiency.[25] Despite the generation of increased antiadenoviral antibody titers to SCH 58500 in all treated patients, we were also able to demonstrate transgene expression after multiple cycles of dosing. There was no obvious enhanced transgene expression in the two individuals who were treated at level 1 because of no demonstrable adenoviral immunity. Not all patients underwent sampling with each cycle of treatment, due to the invasive nature of laparoscopy. Nonetheless, our data clearly show the presence of transgene expression in RNA isolated from both ascitic fluid and tumor biopsies. The alternative explanation of persistent, stable expression of SCH 58500 over time is inconsistent with *in vitro* and *in vivo* preclinical observations.

For a single case, *in situ* PCR data confirmed gene transfer in tumor cells obtained at laparoscopic biopsy. It is not possible to determine the percent of tumor cells transduced because of variability in the size of the biopsies obtained and the variation in the depth of SCH 58500 penetration. For example, in the case of a 3-mm biopsy with 1 mm of penetration and 100% transduction to the level of penetration, one might infer 33% transduction efficiency. However, because the size of the lesion is unknown, the true transduction efficiency cannot be calculated. Similarly, a smaller (2 mm) biopsy from the same site would provide a different estimate of transduction efficiency. This important parameter cannot be estimated nearly as well in human clinical trials as it can be in cell culture, or in orthotopic animal models with smaller and more uniform lesions. Further *in situ* PCR studies are ongoing and will be the subject of a separate report (S Wen et al, in preparation).

Several investigators have postulated that adenoviral transfection efficiency is determined by the presence of coxsackie viral receptor (CAR) on the surface of epithelial cells.[64,65] We did not have sufficient samples to test this hypothesis as an explanation for the failure to achieve transfection in all samples collected or the differential

expression of transgene, which varied between barely detectable to 89,000 copies/per copy of β-actin. Variations in CAR receptor levels, however, may explain differences in transfection efficiency between ovarian cancer cell lines transduced with SCH 58500 *in vitro*.[66]

The inclusion of a subset of patients who received multiple courses of SCH 58500, both alone and in combination with chemotherapy, provided the opportunity not only to compare cumulative toxicity but also to gain preliminary data relevant to clinical response. As we have demonstrated, the combination of SCH 58500 with conventional chemotherapy for ovarian cancer added little to the toxicity of SCH 58500 alone. The frequent appearance of new CT-measurable lesions during the course of treatment with SCH 58500 accompanied by concomitant dramatic decreases in CA125 suggests that for gene replacement studies utilizing adenoviral vectors, CT scans are not a valid means to assess response. Also supporting this conclusion is the observation of mixed clinical responses observed in the same individual with objective responses of some lesions accompanied by the simultaneous development of new lesions in the same individual. Fortunately, other studies have demonstrated that CA125 responses to ovarian cancer treatment correlate very well with CT responses when CT is a valid measure of response.[41,42] Because CA125 responses also correlate well with overall survival,[67-70] they should not be dismissed out of hand. Indeed, because inflammatory changes in the peritoneal cavity may effect modest elevations of CA125 independent of ovarian cancer,[71-74] the interpretation of the overall responses in this study solely on the basis of CA125 response in the face of extensive inflammation, may actually serve to underestimate true response rates. The number of CA125 responders and the degree of response observed in groups 2 and 3 is remarkable based on the heavily pretreated nature of these patients. These data suggest that SCH 58500 has no negative impact on clinical outcome expected from standard chemotherapy treatments. Finally, it should also be noted that our multiple-dose cohort contained bulky tumor deposits, not the most optimal group to study i.p. regimens of any type.[75] We conclude that SCH 58500 is safe, well tolerated, and in combination with platinum-based chemotherapy provides response data to justify its further clinical testing for efficacy in the newly initiated phase III trial for front-line treatment of minimal residual ovarian cancer after primary surgical cytoreduction.

Acknowledgments

The following individuals contributed significantly to the development, monitoring, and/or execution of this trial: from Iowa — Barrie Anderson MD, Joel Sorosky, MD, Anil Sood MD, Teresa Benda, RN, Karen Powliss, RN, Linda Sanders, BS, Melanie Hatterman, BS; from UCLA — Natalie Uhorne, Lenore Gordon, Lisa Yanemoto, Malgarzata Beryt; from SPRI — Michelle Kerin, Mary Ann Fritz, PhD, L Nielsen PhD, Shu FenWen, PhD; from Ulm — Dres T Hawighorst, S Regele, K Maidel, Ms T Kohler, Dres E Stickeler, T Einzmann, and Ms L Walz.

References

1. Greenlee RT, Hill-Harman MB, Murray T, Thun M. Cancer statistics, 2001. *Ca-Cancer J Clin.* 2001;51:15–36.
2. International Federation of Gynecology and Obstetrics Annual Report on the Results of Treatment in Gynecological Cancer. Stockholm: FIGO1994:24.
3. Geisler J, Geisler H. Brain metastases in epithelial ovarian carcinoma. *Gynecol Oncol.* 1995;57:246–249.
4. Sood AK, Sorosky J, Dolan M, et al. Distant metastases in ovarian cancer: why do they occur? *Clin Cancer Res.* 1999;5:2485–2490.
5. Griffiths CT. Surgical resection of tumor bulk in the primary treatment of ovarian carcinoma. *Natl Cancer Inst Monogr.* 1975;42:101–104.
6. Hoskins WJ, McGuire WP, Brady MF, et al. The effect of diameter of largest residual disease on survival after primary cytoreductive surgery in patients with suboptimal residual epithelial ovarian carcinoma. *Am J of Obstet Gynecol.* 1994;170:974–979.
7. Podratz KC, Schray MF, Wieand HS, et al. Evaluation of treatment and survival after positive second-look laparotomy. *Gynecol Oncol.* 1988;31:9–24.
8. Hoskins WJ, Rubin SC, Dulaney E, et al. Influence of secondary cytoreduction at the time of second-look laparotomy on the survival of patients with epithelial ovarian carcinoma. *Gynecol Oncol.* 1989;34:365–372.
9. Levine AJ, Momand J, Finlay CA. The p53 tumour suppressor gene. *Nature.* 1991;351:453–456.
10. Harris CC. Structure and function of the p53 tumor suppressor gene: clues for rational cancer therapeutic strategies. *J Natl Cancer Inst.* 1996;88:1442–1455.
11. Lee JM, Bernstein A. Apoptosis, cancer and the p53 tumour suppressor gene. *Cancer Metastasis Rev.* 1995;14:149–161.
12. Hawkins DS, Demers GW, Galloway DA. Inactivation of p53 enhances sensitivity to multiple chemotherapeutic agents. *Cancer Res.* 1996;56:892–898.
13. Kirsch DG, Kastan MB. Tumor-suppressor p53: implications for tumor development and prognosis. *J Clin Oncol.* 1998;16:3158–3168 (Review).
14. Blandino G, Levine AJ, Oren M. Mutant p53 gain of function: differential effects of different p53 mutants on resistance of cultured cells to chemotherapy. *Oncogene.* 1999; 18:477–485.
15. Wen W, Reles A, Runnebaum IB, et al. P53 mutations and expression in ovarian cancers: correlation with overall survival. *Int J Gynecol Pathol.* 1999;18:29–41.
16. Skilling JS, Sood AK, Niemann T, et al. An abundance of p53 null mutations in ovarian carcinoma. *Oncogene.* 1996;13: 117–123.
17. Shahin M, Sood AK, Hughes JH, et al. The prognostic significance of p53 tumor suppressor gene alterations in ovarian cancer. *Cancer.* 2000;89:2006–2017.
18. Dedrick RL. Theoretical and experimental bases of intraperitoneal chemotherapy. *Semin Oncol.* 1986;12:1–6.
19. Alberts DS, Liu PY, Hannigan EV, et al. Intraperitoneal cisplatin plus intravenous cyclophosphamide versus intravenous cisplatin plus intravenous cyclophosphamide for stage III ovarian cancer. *N Engl J Med.* 1996;335:1950–1955.
20. Gomez-Navarro J, Siegal GP, Alvarez RD, et al. Gene therapy: ovarian carcinoma as the paradigm. *Am J Clin Pathol.* 1998;109:444–467.
21. Baselga J. New horizons: gene therapy for cancer. *Anti-Cancer Drugs.* 1999;10:39–42.
22. Nielsen LL, Gumani M, Syed J, et al. Recombinant E1-deleted adenovirus-mediated gene therapy for cancer: efficacy

studies with p53 tumor suppressor gene and liver histology in mouse tumor xenograft models. *Hum Gene Ther.* 1998;9: 681–94.
23. Nielsen LL, Lipari P, Dell J, et al. Adenovirus-mediated p53 gene therapy and paclitaxel have synergistic efficacy in models of human head and neck, ovarian, prostate, and breast cancer. *Clin Cancer Res.* 1998;4:835–846.
24. Nielsen LL, Dell J, Maxwell E, et al. Efficacy of p53 adenovirus-mediated gene therapy against human breast cancer xenografts. *Cancer Gene Ther.* 1997;4:129–138.
25. Bramson JL, Hitt M, Gauldie J, et al. Pre-existing immunity to adenovirus does not prevent tumor regression following intratumoral administration of a vector expressing IL-12 but inhibits virus dissemination. *Gene Ther.* 1997;4:1069–1076.
26. von Gruenigen VE, Santoso JT, Coleman RL, et al. *In vivo* studies of adenovirus-based p53 gene therapy for ovarian cancer. *Gynecol Oncol.* 1998;69:197–204.
27. Kim J, Hwang ES, Kim JS, et al. Intraperitoneal gene therapy with adenoviral-mediated p53 tumor suppressor gene for ovarian cancer model in nude mouse. *Cancer Gene Ther.* 1999; 6:172–178.
28. Anderson SC, Johnson DE, Harris MP, et al. P53 gene therapy in a rat model for hepatocellular carcinoma: intra-arterial delivery of a recombinant adenovirus. *Clin Cancer Res.* 1998;4:1649–1659.
29. Gurnani M, Lipari P, Dell J, et al. Adenovirus-mediated p53 gene therapy has greater efficacy when combined with chemotherapy against human head and neck, ovarian, prostate, and breast cancer. *Cancer Chemother Pharmacol.* 1999;44: 143–151.
30. Fujiwara T, Grimm EA, Mukhopadhyay T, et al. Induction of chemosensitivity in human lung cancer cells *in vivo* by adenovirus-mediated transfer of the wild-type p53 gene. *Cancer Res.* 1994;54:2287–2291.
31. Zhang W-W, Fang X, Mazur W, et al. High-efficiency gene transfer and high-level expression of wild-type p53 in human lung cancer cells mediated by recombinant adenovirus. *Cancer Gene Ther.* 1994;1:5–13.
32. Roth JA, Nguyen D, Lawrence DD, et al. Retrovirus-mediated wild-type gene transfer to tumors of patients with lung cancer. *Nat Med.* 1996;2:985–991.
33. Nemunaitis J, Swisher SG, Timmons T, et al. Adenovirus-mediated p53 gene transfer in sequence with cisplatin to tumors of patients with non-small-cell lung cancer. *J Clin Oncol.* 2000;18:609–622.
34. Clayman GL, El-Naggar AK, Lippman SM, et al. Adenovirus-mediated p53 gene transfer in patients with advanced recurrent head and neck squamous cell carcinoma. *J Clin Oncol.* 1998;16:2221–2232.
35. Swisher, SG, Roth JA, Nemunaitis J, et al. Adenovirus-mediated p53 gene transfer in advanced non-small-cell lung cancer. *J Natl Cancer Inst.* 1999;91:763–771.
36. Cusack JC, Spitz FR, Nguyen D, et al. High levels of gene transduction in human lung tumors following intralesional injection of recombinant adenovirus. *Cancer Gene Ther.* 1996;3:245–249.
37. Nielsen LL, Maneval DC. P53 tumor suppressor gene therapy for cancer. *Cancer Gene Ther.* 1998;5:52–63.
38. Buller RE, Pegram M, Runnebaum I, et al. A phase I/II trial of recombinant adenoviral human p53 (SCH 58500) intraperitoneal (IP) gene therapy in recurrent ovarian cancer. *Gynecol Oncol.* 1999;72:452–453.
39. Wills KN, Maneval DC, Menzel P, et al. Development and characterization of recombinant adenoviruses encoding human p53 for gene therapy of cancer. *Hum Gen Ther.* 1994; 5:1079–1088.
40. Cockcroft DW, Gault, MH. Prediction of creatinine clearance from serum creatinine. *Nephron.* 1976;16:31–41.
41. Rustin GJ, Nelstrop AE, McClean P, et al. Defining response of ovarian carcinoma to initial chemotherapy according to serum CA 125. *J Clin Oncol.* 1996;14:1545–1551.
42. Rustin GJ, Nelstrop AE, Bentzen SM, et al. Use of tumour markers in monitoring the course of ovarian cancer. *Ann Oncol.* 1999;10:S21–S27.
43. Musco ML, Cui S, Small D, et al. A comparison of flow cytometry and laser scanning cytometry for the intracellular evaluation of adenoviral infectivity and p53 protein expression in gene therapy. *Cytometry.* 1998;33:290–296.
44. Wolf JK, Mills G, Bazzet L, et al. Adenovirus-mediated p53 growth inhibition of ovarian cancer cells is independent of endogenous p53 status. *Gynecol Oncol.* 1999;75:261–266.
45. Mujoo K, Maneval DC, Anderson SC, et al. Adenoviral-mediated p53 tumor suppressor gene therapy of human ovarian carcinoma. *Oncogene.* 1996;12:1617–1623.
46. Liu T-J, el-Naggar AK, McDonnell TJ, et al. Apoptosis induction mediated by wild-type p53 adenoviral gene transfer in squamous cell carcinoma of the head and neck. *Cancer Res.* 1995;55:3117–3122.
47. Chen P-L, Chen Y, Bookstein R, et al. Genetic mechanisms of tumor suppression by the human p53 gene. *Science.* 1990;250:1576–1580.
48. Fujiwara T, Grimm EA, Roth JA. Gene therapeutics and gene therapy for cancer. *Curr Opin Oncol.* 1994;6:96–105.
49. Weisberger AS, Levine B, Storaasli JP. Use of nitrogen mustard in treatment of serous effusions of neoplastic origin. *J Am Med Assoc.* 1955;159:1704–1707.
50. Berek JS, Markman M, Stonebraker B, et al. Intraperitoneal interferon-α in residual ovarian carcinoma: a phase II gynecologic oncology group study. *Gynecol Oncol.* 1999;75: 10–14.
51. Morgan RJ Jr, Braly P, Cecchi G, et al. Phase II trial of intraperitoneal cisplatin with intravenous doxorubicin and cyclophosphamide in previously untreated patients with advanced ovarian cancer — long-term follow-up. *Gynecol Oncol.* 1999;75:419–426.
52. Barakat RR, Almadrones L, Venkatraman ES, et al. A phase II trial of intraperitoneal cisplatin and etoposide as consolidation therapy in patients with stage II–IV epithelial ovarian cancer following negative surgical assessment. *Gynecol Oncol.* 1998;69:17–22.
53. Muggia FM, Liu PY, Alberts DS, et al. Intraperitoneal mitoxantrone or floxuridine: effects on time-to-failure and survival in patients with minimal residual ovarian cancer after second-look laparotomy — a randomized phase II study by the Southwest Oncology Group. *Gynecol Oncol.* 1996;61: 395–402.
54. Markman M, Reichman B, Hakes T, et al. Impact on survival of surgically defined favorable responses to salvage intraperitoneal chemotherapy in small-volume residual ovarian cancer. *J Clin Oncol.* 1992;10:1479–1484.
55. Markman M, Brady MF, Spirtos NM, et al. Phase II trial of intraperitoneal paclitaxel in carcinoma of the ovary, tube, and peritoneum: a Gynecologic Oncology Group Study. *J Clin Oncol.* 1998;16:2620–2624.
56. Link CJ Jr, Moorman D, Seregina T, et al. A phase I trial of *in vivo* gene therapy with the herpes simplex thymidine kinase/ganciclovir system for the treatment of refractory or recurrent ovarian cancer. *Hum Gene Ther.* 1996;7:1161–1179.
57. Alvarez RD, Curiel DT. A phase I study of recombinant adenovirus vector–mediated intraperitoneal delivery of herpes simplex virus thymidine kinase (HSV-TK) gene and

intravenous ganciclovir for previously treated ovarian and extraovarian cancer patients. *Hum Gene Ther.* 1997;8:597–613.
58. Hasenburg A, Tong XW, Rojas-Martinez A, et al. Thymidine kinase (TK) gene therapy of solid tumors: valacyclovir facilitates outpatient treatment. *Anticancer Res.* 1999;19: 2163–2165.
59. Hortobagyi, GN, Hung MC, Lopez-Berestein G. A phase I multicenter study of E1A gene therapy for patients with metastatic breast cancer and epithelial ovarian cancer that overexpresses HER-2/neu or epithelial ovarian cancer. *Hum Gene Ther.* 1998;9:1775–1798.
60. Tait DL, Obermiller PS, Redlin-Frazier S, et al. A phase I trial of retroviral BRCA1sv gene therapy in ovarian cancer. *Clin Cancer Res.* 1997;3:1959–1968.
61. Tait DL, Obermiller PS, Hatmaker AR, et al. Ovarian cancer BRCA1 gene therapy: phase I and II trial differences in immune response and vector stability. *Clin Cancer Res.* 1999; 5:1708–1714.
62. Grace MJ, Xie L, Musco ML, et al. The use of laser scanning cytometry to assess depth of penetration of adenovirus p53 gene therapy in human xenograft biopsies. *Am J Pathol.* 1999; 155:1869–1878.
63. Hitt M, Addison CL, Graham FL. Human adenovirus vectors for gene transfer into mammalian cells. *Adv Pharmacol.* 1997;40:137–206.
64. Bergelson JM, Cunningham, JA, Droguett G, et al. Isolation of a common receptor for Coxsackie B viruses and adenoviruses 2 and 5. *Science.* 1997;275:1320–1323.
65. Yingming L, Pong R-C, Bergelson JM, et al. Loss of adenoviral receptor expression in human bladder cancer cells: a potential impact on the efficacy of gene therapy. *Cancer Res.* 1999;59:325–330.
66. Pegram M, Tseng Y, Baldwin RL, et al. Expression of coxsackie and adenovirus receptor (CAR) correlates with efficiency of adenovirus transduction of human ovarian carcinoma cells. *Gynecol Oncol.* 1999;72:452.
67. Buller RE, Berman ML, Bloss JD, et al. CA 125 regression: a model for epithelial ovarian cancer response. *Am J Obstet Gynecol.* 1991;165:360–367.
68. Buller RE, Vasilev S, DiSaia PJ. CA125 kinetics: a cost effective clinical tool to evaluate clinical trial outcomes in the 1990s. *Am J Obstet Gynecol.* 1996;174:1241–1254.
69. van der Burg MEL, Lammes FB, van Putten WLJ, et al. Ovarian cancer: the prognostic value of the serum half-life of CA125 during induction chemotherapy. *Gynecol Oncol.* 1988; 30:307–312.
70. Rustin GJS, Gennings JN, Nelstrop AE, et al. Use of CA-125 to predict survival of patients with ovarian carcinoma. *J Clin Oncol.* 1989;7:1667–1671.
71. Yedema CA, Kenemans P, Thomas CM, et al. CA125 serum levels in the early post-operative period do not reflect tumour reduction obtained by cytoreductive surgery. *Eur J Cancer.* 1993;29A:966–971.
72. Van Der Zee AG, Duk JM, Aalders JG, et al. The effect of abdominal surgery on the serum concentration of the tumour-associated antigen CA 125. *Br J Obstet Gynaecol.* 1990;97: 934–938.
73. Talbot RW, Jacobsen DJ, Nagorney DM, et al. Temporary elevation of CA 125 after abdominal surgical treatment for benign disease and cancer. *Surg Gynecol Obstet.* 1989;168: 407–412.
74. Zeimet AG, Offner FA, Marth C, et al. Modulation of CA-125 release by inflammatory cytokines in human peritoneal mesothelial and ovarian cancer cells. *Anticancer Res.* 1997; 17:3129–3131.
75. Howell SB, Zimm S, Markman M, et al. Long-term survival of advanced refractory ovarian carcinoma patients with small-volume disease treated with intraperitoneal chemotherapy. *J Clin Oncol.* 1987;5:1607–1612.